Coherent Optical OFDM Modem Employing Artificial Neural Networks for Dispersion and Nonlinearity Compensation in a Long-Haul Transmission System

Mutsam Abdel-karim Jarajreh

PhD

2012

Coherent Optical OFDM Modem Employing Artificial Neural Networks for Dispersion and Nonlinearity Compensation in a Long-Haul Transmission System

Mutsam Abdel-karim Jarajreh

A thesis submitted in partial fulfilment
of the requirements of the
University of Northumbria at Newcastle
for the degree of
Doctor of Philosophy

Research undertaken in the
School of Computing, Engineering and Information Sciences

July 2012

Abstract:

In order to satisfy the ever increasing demand for the bandwidth requirement in broadband services the optical orthogonal frequency division multiplexing (OOFDM) scheme is being considered as a promising technique for future high-capacity optical networks. The aim of this thesis is to investigate, theoretically, the feasibility of implementing the coherent optical OFDM (CO-OOFDM) technique in long haul transmission networks. For CO-OOFDM and Fast-OFDM systems a set of modulation formats dependent analogue to digital converter (ADC) clipping ratio and the quantization bit have been identified, moreover, CO-OOFDM is more resilient to the chromatic dispersion (CD) when compared to the bandwidth efficient Fast-OFDM scheme. For CO-OOFDM systems numerical simulations are undertaken to investigate the effect of the number of sub-carriers, the cyclic prefix (CP), and ADC associated parameters such as the sampling speed, the clipping ratio, and the quantisation bit on the system performance over single mode fibre (SMF) links for data rates up to 80 Gb/s. The use of a large number of sub-carriers is more effective in combating the fibre CD compared to employing a long CP. Moreover, in the presence of fibre non-linearities identifying the optimum number of sub-carriers is a crucial factor in determining the modem performance. For a range of signal data rates up to 40 Gb/s, a set of data rate and transmission distance-dependent optimum ADC parameters are identified in this work. These parameters give rise to a negligible clipping and quantisation noise, moreover, ADC sampling speed can increase the dispersion tolerance while transmitting over SMF links. In addition, simulation results show that the use of adaptive modulation schemes improves the spectrum usage efficiency, thus resulting in higher tolerance to the CD when compared to the case where identical modulation formats are adopted across all sub-carriers. For a given transmission distance utilizing an artificial neural networks (ANN) equalizer improves the system bit error rate (BER) performance by a factor of 50% and 70%, respectively when considering SMF

firstly CD and secondly nonlinear effects with CD. Moreover, for a fixed BER of 10^{-3} utilizing ANN increases the transmission distance by 1.87 times and 2 times, respectively while considering SMF CD and nonlinear effects. The proposed ANN equalizer performs more efficiently in combating SMF non-linearities than the previously published Kerr non-linearity electrical compensation technique by a factor of 7.

Table of Contents

List of Figures

Abbreviations

ADC	Analogue to Digital Convertor
ACP	Adaptive Cyclic Prefix
ADSL	Asymmetric Digital Subscriber Loop
AM	Amplitude Modulation
ANN	Artificial Neural Networks
AWGN	Additive White Gaussian Noise
BP	Back Propagation
BER	Bit Error Rate
BPSK	Binary Phase Shift Keying
C-band	Conventional Band
CCI	Co-Channel Interference
CD	Chromatic Dispersion
CIR	Channel Impulse Response
CO-OOFDM	Coherent Optical OFDM
CP	Cyclic Prefix
CPR	Common Phase Rotation

DAC	Digital to Analogue Convertor
DA	Data-Aided
DCT	Discrete Cosine Transform
DFT	Discrete Fourier Transform
DQPSK	Differential Quadrature Phase Shift Keying
DP-QPSK	Dual Polarized Quadrature Phase Shift Keying
DSP	Digital Signal Processing
DWDM	Dense Wavelength-Division Multiplexed
EDFA	Erbium Doped Fibre Amplifier
EDC	Electronic Dispersion Compensation
E/O	Electrical-to-Optical
EPD	Electrical Pre-Distortion
F-OFDM	Fast-OFDM
FDM	Frequency Division Multiplexing
FEC	Forward Error Correction
FIR	Finite Impulse Response
FFT	Fast Fourier Transform

FM	Frequency Modulation
FSK	Frequency Shift Keying
FWM	Four Wave-Mixing
ICI	Inter-Carrier Interference
IDCT	Inverse Discrete Cosine Transform
IDFT	Inverse Discrete Fourier Transform
IF	Intermediate Frequency
IFFT	Inverse Fast Fourier Transform
IM-DD	Intensity Modulation and Direct Detection
IP	Internet Protocol
IPVT	Internet Protocol Video Television
I/Q	Imaginary/Quadrature
ISI	Inter-Symbol Interference
ISD	Information Spectral Density
EKF	Kalman Filter
LAN	Local Area Networks
LO	Local Oscillators

LPF	Low-pass Filter
LTE	Long-Term Evolution
LMS	Least Mean Square
MAN	Metropolitan Area Network
MAP	Maximum A-Posterior
MIMO	Multi-Input Multi-Output
MLP	Multilayer Perceptrons
MLSE	Maximum Likelihood Sequence Estimator
MMF	Multi-Mode Fibre
MZM	Mach-Zehnder Modulator
NG	Natural Gradient
OADM	Optical Add/Drop Multiplexers
OFDM	Orthogonal Frequency Division Multiplexing
OSNR	Optical Signal-to-Noise Ratio
OSS	One Step Secant
OSSB	Optical Single Side Band
PAPR	Peak-to-Average Power Ratio

PA	Pilot Aided
PMD	Polarization Mode Dispersion
QAM	Quadrature Amplitude Modulation
QPSK	Quadrature PSK
RB	Rayleigh Backscattering
RBF	Radial Base Function
RF	Radio Frequency
ROF	Radio over Fibre
RP	Riedmiller's Resilient Back Propagation Algorithm
RLS	Recursive Least Square
RNN	Recurrent Neural Network
S/P	Serial-to-Parallel
SPM	Self-phase Modulation
SRS	Stimulated Raman Scattering
SSB	Single Sideband
SMF	Single-Mode Fibre
SNR	Signal-to-Noise Ratio

VoD	Video-on-Demand
WDM	Wavelength Division Multiplexing
XPM	Cross-phase Modulation
ZFE	Zero Forcing Equalizer

Acknowledgment

Above all, I would like to express my deep and sincere gratitude to my supervisor, Prof. Zabih Ghassemlooy from Northumbria University, for his guidance, patience, advice, and support during my PhD research. His kindness and wealth of knowledge have been of great values for the completion of the current PhD Thesis. He was always accessible and willing to help all of his students with their research. As a result, research life in Northumbria University became smooth and rewarding for me.

I also would like to thank my second supervisor Dr. Wai-Pang Ng who was supportive and provided me with fruitful guidance. I would like to thank Dr. Sujan Rajbhandari for his support and a very useful comments; I would also like to thank Prof. Jianming Tang from Bangor University for a useful discussion at the start of this project.

I would like to deeply thank the Sir Robert William Engineering scholarship, Cast Technium Company at Wales, and the Leach Trust Foundation for funding me throughout this project.

Special thanks go to the colleagues in OCRG at Northumbria University for the good times we spent together, also I would like to thank my friends Dr. Elias Giacoumidis from Telecom-Paris Tech, Paris, France, Dr. Jinlong Wei, from Cambridge University, for their friend ship and support during this PhD, I wish to thank my family for supporting me all these years specially my father, and my brothers Yousef , Dr.Ahmad, Alaa, Gaith, and my sister Doaa.

Lastly, and most importantly, I wish to thank my mother for her love, help, and support and for giving me a second life after donating her kidney to me. To her I dedicate this Thesis.

Declaration

I declare that the work contained in this thesis is entirely mine and that no portion of it has been submitted in support of an application for another degree or qualification in this, or any other university, or institute of learning, or industrial organisation.

Mutsam Jarajreh

July -2012

Chapter 1. Introduction

1.1 Introduction

Nowadays, satisfying the needs of the end users for communication speed and bandwidth as well as offering better and secure quality of services is the real motivation behind the rapid increase in the internet protocol (IP) traffic and newly emerging applications such as IP television (IPTV), video-on-demand (VoD) and video surveillance. This adds more pressure on the networks infrastructure at every scale, which explains the real motive behind all optical communications research. Moreover, in modern communication systems, the cost efficiency, flexibility and the high transmission performance of digital signal processing (DSP) techniques have shifted to become a potential candidate for photonic networks [1, 2]. As a successful example of the practical implementation of DSP, the orthogonal frequency division multiplexing (OFDM) scheme has been rapidly adopted in wireless communications systems to combat the multi-path fading and multipath induced inter symbol interference (ISI) effects [3, 4]. As a multi-carrier modulation scheme, OFDM splits a high-speed data stream into a number of low-speed data streams transmitted simultaneously over a number of harmonically related narrowband sub-carriers [3]. By introducing OFDM in the optical domain, optical OFDM (OOFDM) was proposed in 2005 [5]. Over the last a few years, two main variants of OOFDM have been extensively investigated, including the incoherent OOFDM such as the intensity modulation and direct detection (IM-DD) OOFDM scheme [6] and the coherent OOFDM (CO-OOFDM) technique [7, 8].

IM-DD OOFDM has demonstrated great potential for practical implementation in cost-sensitive applications such as local area networks (LANs) and metropolitan area networks (MANs) [6, 9]. Whilst CO-OOFDM has been regarded as a promising candidate for future long-haul high capacity transmission systems [7], its practical application has been mainly

determined by its tolerance to the optical fibre chromatic dispersion (CD) and susceptibility to the fibre nonlinearity particularly at high data rates and high optical power levels. Cyclic prefix (CP) is introduced to the CO-OOFDM symbols in order to combat CD as well as the second order polarization mode dispersion (PMD) as outlined in [10]. In [11] a careful management of these effects has lead to a successful experimental demonstration of 20Gb/s CO-OOFDM signal transmission over 4160 km of single mode fibre using the sub carriers multiplexing technique.

In 2007 the first experimental set up of a CO-OOFDM system at 8 Gb/s over 1000 km SMF fibre was reported in [12]. In [13] and [7] the first CO-OOFDM with the polarization-diversity with a record PMD tolerance has been realized as a 128 OFDM subcarriers with a nominal data-rate of 8 Gbit/s are successfully processed and recovered after 1000 km transmission through SMF.

Currently research in coherent transmissions is moving toward increasing the system capacity by using: (i) wavelength division multiplexing (WDM) and optical add/drop multiplexers (OADM) [8], and (ii) sub-carriers modulation with dual polarized quadrature phase shift keying (DP-QPSK) in multi-input multi-output (MIMO) configurations to achieve to high data rates up to 40 Gb/s [14]. In sub-carrier based schemes, the phase noise results in a common phase rotation (CPR) of all the subcarriers within a symbol and the inter-carrier interference (ICI). Therefore, phase estimation is necessary to mitigate the phase noise. Data-aided (DA) and pilot-aided (PA) methods have been proposed, and compared for CO-OOFDM systems at 8Gb/s over 1000 km of SMF [12-15].

In 2009 an experimental demonstration of 100 Pbit/s-km CO-OOFDM link, which is equivalent to 400 DVDs per second, over 7000 km transoceanic cable has been carried out by the Alcatel-Lucent Bell Labs [16]. Tb/s CO-OOFDM systems using the optical frequency combs at both the transmitter and receiver was realized in [17]. A multi-band CO-OOFDM systems have been used in generating high data rate signals from 100 Gb/s, [18, 19] up to 10 Tb/s [20].

The main challenges for the optical communication systems are the CD and fibre non-linearity. To address these technical challenges in particular for the CO-OOFDM modems and to increase CO-OOFDM system tolerance to CD and fibre non-linearities, a number of methods has been proposed including: (i) including low-cost DSP techniques such as electronic dispersion compensation (EDC) that provides a simpler solution to compensated for the fibre CD [21]-[22], and optical single side band (OSSB) for CD compensation at the receiver [23], and (ii) electrical pre-distortion (EPD) at the transmitter [24] as well as non-linear electrical post-compensation at the receiver [25]. In 2012 a 101.7 Tb/s, was demonstrated using 370 dense wavelength-division multiplexed (DWDM) channels of CO-OOFDM signal modulated with the polarization-division-multiplexing (PDM) 128-ary quadrature amplitude modulation (QAM) at each modulated subcarrier. This experiment was enabled using the DSP pre-equalization of transmitter impairments, all Raman amplification, heterodyne coherent detection, and DSP post equalization of the channel and receiver impairments, including the pilot-based phase noise compensation [26].

CD compensation in the optical domain by utilizing dispersion compensation fibre (DCF), optical resonators and fibre Bragg gratings, offer a number of advantages compared to EDC in particular for WDM systems where different wavelength can be compensated without the

need for a different EDC circuit for each wavelength. However, both schemes require either the use of additional circuitries or longer length of fibres, which requires a further signal amplification. The adaptive cyclic prefix (ACP) [10], and the modem parameter such as the number of subcarriers, sampling speed for transmitting over multimode fibre MMF links for the IM-DD OOFDM scheme have been investigated [6]. However, the effects of CO-OOFDM modem parameters (i.e. number of subcarriers, cyclic prefix length, modulation format, analogue to digital converter / digital to analogue converter (ADC/DAC) quantization bits and clipping ratio on CO-OOFDM transmission performance over SMF links has not been investigated by the researchers.

Considering the physical nature of CP, it is clear that, if a CP time duration is smaller than the CD associated with a SMF link, the imperfectly compensated dispersion effect limits considerably the maximum achievable transmission performance of the CO-OOFDM signals. In addition, a small CP may also affect the sub-carrier orthogonality, thus resulting in a significant increase in the minimum required optical signal-to-noise ratio (OSNR) [3]. On the other hand, if the CP is longer than the CD of the SMF link, for a fixed signal sampling speed, the CP wastes a large percentage of the transmitted signal power, thus giving rise to a degraded effective signal OSNR. Moreover, for a given ADC, a large number of sub-carriers within one CO-OOFDM symbol increase the time duration of the CO-OOFDM symbol and thus the time duration of the CP, consequently this give rise to an enhanced dispersion tolerance and improved transmission performance. However, a large number of sub-carriers also decrease the frequency spacing between adjacent sub-carriers. Therefore, the fibre nonlinear may affect the orthogonality between sub-carriers, leading to transmission performance degradation. It is expected that there exists an optimum number of sub-carriers for a specific application scenario.

It is widely known that ADCs have a wide range of sampling speeds, as utilizing lower sampling rate can increase the symbol period, thus CD tolerance. However considering fibre nonlinear effects, the sampling speed can affect the spacing between adjacent CO-OOFDM sub-carriers; therefore, this may affect sub-carriers orthogonality. Given the fact that CO-OOFDM signals suffers from large a peak-to-average-power-ratio (PAPRs), which makes CO-OOFDM modems more sensitive to the fibre nonlinearity. Similar to IM-DD OOFDM cases [10], it is therefore expected that signal clipping and quantization associated with an ADC (DAC) are also crucial for determining the maximum achievable transmission performance of the modems.

OOFDM multiplexes different optical subcarriers while maintaining the orthogonality between the subcarriers. This allows subcarriers to overlap without introducing interference consequently effectively utilizing the available bandwidth, where different users are supported by allocating a specific part of the spectrum [27]. Moreover, in comparison with TDM, OFDM offers a higher performance either in terms of the capacity or the time required and the overall throughput. It is important for the communication system to have the ability to utilize the given bandwidth efficiently, therefore recently the discrete cosine transform (DCT) based OFDM (Fast-OFDM) has been proposed [28], which is used within the coherent domain [29]. This new technique can save half of the given bandwidth if compared with the conventional CO-OOFDM [30]. Therefore, it is important to investigate the performance of Fast-OFDM when transmitting over SMF link that includes only CD, thereafter compare the results with CO-OOFDM.

For OFDM systems, the orthogonality of the consecutive OFDM symbols is maintained by appending a CP at the start of each symbol. For each OFDM symbol to be independent and

to avoid any ISI or ICI, the length of the channel impulse response (CIR) should be less than CP+1 samples [31]. Therefore, at the receiver after the extraction of the modulated data and the FFT process a frequency domain equalizer is applied. However a time domain equalizer can also be applied in order to reduce the effect of the inter-channel interference [32] .

The artificial neural network (ANN) is an attractive alternative for compensating the optical fibre linear and non-linear distortions. ANN based equalizers have been used in the receiver for distortion compensation induced by the fibre, optical and radio frequency (RF) wireless channels, where it can offer similar or better performance compared to the traditional finite impulse response filter equalizers [33].

Nonlinear equalizers have been used to compensate for all three types of distortion. In the literature it has been shown that the nonlinear feed-forward equalizers based on the multilayer perceptron (MLP) can outperform linear equalizers [34]. This research also proposed an intelligent compensation scheme for CD and fibre non-linearities. A new design of ANN equalizer based on the feed forward MLP networks with reduced complexity is proposed in order to compensate for CD and fibre no-linearity for CO-OOFDM.

1.2 Research Aims

- To propose a design of CO-OOFDM modem, thereafter optimize the proposed modem parameters in order to attain a basic base rate of 156.25 Mb/s up to 1.25 Gb/s if 256-QAM modulation format is used.
- To propose an artificial intelligent based compensation schemes and investigate its performance in terms of the fibre dispersion and non-linearity. To study the effect of

the bandwidth efficient Fast-OFDM in comparison with the CO-OOFDM system, while transmitting over SMF, which includes only CD.

1.3 Methodology

In this thesis all the presented results are theoretical results, based on the numerical simulation approach. Matlab software is used to model the CO-OOFDM modem and the ANN equalizer. The communication link, which is a SMF, is modelled using C++, in line with published work [35-37]. Where necessary results are compared with the published data.

1.4 The Thesis Structure

This section gives a brief description all the chapters constructing this thesis:

Chapter 1: Introduction

This chapter provides a brief introduction of the research work, original contribution and thesis objectives, research aims, and thesis structure.

Chapter 2: Principles of OFDM

To gain a better understanding of OOFDM, this chapter deals with the principles of OFDM and OOFDM. The history of OFDM and the fundamentals of key components involved in a general OFDM system are described. SMF together with its linear and nonlinear effects is

also presented followed by discussions on two main variants of OOFDM including CO-OOFDM and IM-DD OOFDM, whose advantages and drawbacks are also discussed.

Chapter 3: Introduction to ANN

This chapter introduces the basic concepts of the ANN, moreover discusses the need for equalization, particularly the ANN equalization concepts. Furthermore describes the operating principle of ANN MLP.

Chapter 4: Theoretical Analysis of the CO-OOFDM and Fast-OFDM Systems in AWGN

This chapter provide a basic study of the CO-OOFDM modem over the additive white Gaussian noise (AWGN) channel. It includes channel modelling, bit error rate analysis, and the link model when using modulation formats of differential binary phase shift keying (DBPSK), differential quadrature phase shift keying (DQPSK) 16 to256-QAM. In addition, the effect of ADC parameters such as clipping and quantization are investigated to see how they influence the system performance over the same channel.

The second part of the chapter presents the performance results of the coherent Fast-OFDM in AWGN for different amplitude shift keying (ASK) modulation formats including 4-ASK, 8-ASK, and 16-ASK. Moreover, in order to optimize the ADC parameter for a given system, the quantization and clipping ratio effects on the link performance is also carried. The last part of this chapter gives a comparison between the transmission performance of Fast-OFDM

and CO-OOFDM when used over SMF links in the presence of the chromatic dispersion only.

Chapter 5: Investigation of the Effects of CO-OOFDM Parameters on the System Performance over SMF Links

This chapter provides a detailed study of the CO-OOFDM modem key parameter the data rate versus transmission distance while transmitting over SMF links. This study includes investigation of the optical launch power, number of subcarriers and the cyclic prefix on the CO-OOFDM dispersion tolerance, as well as the fibre non-linear impairments. The chapter also addresses the effect of ADC key parameters such as the clipping, quantization, and sampling speed on transmission link performance.

The last part of the chapter investigates the CO-AMOOFDM data rate versus distance performance, as AMOOFDM support higher signal capacity and significantly improves the tolerance to the fibre modal dispersion in the LAN networks [6]. For CO-OOFDM adaptivity in signal transmission in the presence of fibre chromatic dispersion and non-linearities is also investigated.

Chapter 6: Artificial Neural Network Equalizer for CO-OOFDM Modems

This chapter focuses on the design and implementation of an artificial neural networks equalizer to compensation for SMF CD and non-linearities impairments. Moreover, chapter five study the effect of ANN different learning algorithms on the transmission performance

over SMF links in the presence of dispersion only and together with nonlinearity impairments.

1.5 Original Contribution and Thesis Objectives

The contributions to knowledge are as follow:

- Design of the CO-OOFDM modem and adaptation of modulation schemes such as DBPSK, DQPSK, and multi-level-QAM (M-QAM), which have been used in RF, in order to increase the system data rate without utilizing WDM based technologies, the results are shown in Chapters 4 and 5.
- Investigation the effect of ADC key parameters on the performance of the modem over the AWGN channel, see Chapter 4.
- Theoretical investigation of the performance of a coherent Fast-OFDM modem, while using different ASK modulation formats, over the AWGN channel and optimize the ADC parameters such as the clipping ratio and the quantization bits, see Chapter 4.
- Investigation of the use of Fast-OFDM for the coherent transmissions and comparison of its performance with CO-OOFDM in the presence of the chromatic dispersion only, Chapter 4.
- Optimization of the CO-OOFDM modem parameter, which includes investigating the CO-OOFDM modem parameters such as CP, number of subcarriers, responsible ADC key parameters such as clipping, quantization and sampling speed on the performance over SMF links, see Chapter 5.
- Theoretically investigation of the effect of adaptively modulated CO-OOFDM (AM-CO-OOFDM) on the data rate versus the transmission distance performance in the presence of SMF non-linearities as well as the dispersion, see Chapter 5.

- Theoretically investigation of the effect of adopting ANN based equalizer in compensating for channel linear and non-linear effect for CO-OOFDM signals, see Chapter 6.

1.6 Published Papers

1. M. A. Jarajreh, J. L. Wei, J. M. Tang, Z. Ghassemlooy, W. P. Ng, 'Effect of number of sub-carriers, cyclic prefix and analogue to digital converter parameters on coherent optical orthogonal frequency division multiplexing modem's transmission performance', Communications, IET. 01/2010; 4: pp.213-222.
2. M.A. Jarajreh, Z. Ghassemlooy, W.P. Ng, 'Improving the chromatic dispersion tolerance in long-haul fibre links using the coherent optical orthogonal frequency division multiplexing', Microwaves, Antennas & Propagation, IET. 06/2010; pp.651-658
3. M.A. Jarajreh, Z. Ghassemlooy, W. P. Ng, 'Improving the chromatic dispersion tolerance in long-haul fibre links using the coherent OOFDM', Mosharaka International Conference on Communications, Propagation and Electronics (MIC-CPE 2009); 01/2009, pp. 74-78
4. M A Jarajreh and J M Tang, 'Improved Transmission Performance of Coherent Optical OFDM Signals by Increasing The Number of Sub-Carriers', Semiconductor & Integrated Optoelectronics (IEE/SIOE), Cardiff, Wales, April 2008.
5. M. A. Jarajreh, E. Giacoumidis, and J. M. Tang, 'Quantization and Clipping Effects on the Transmission Performance of Coherent Optical OFDM Signals over AWGN Channels', Semiconductor & Integrated Optoelectronics (IEE/SIOE), Cardiff, Wales, UK, April 2007.

6. E. Giacoumidis, M. A. Jarajreh, and J. M. Tang, ‘Effect of Analogue-to-Digital Conversion on the Performance of Optical OFDM Modems in Coherent and IM-DD Transmission Links’, Semiconductor & Integrated Optoelectronics (IEE/SIOE), Cardiff, Wales, April 2007.

1.7 Conclusions

This chapter has explored the main milestones in the CO-OOFDM research, as well as stating the original contributions, the aims and methodology adopted in carrying out the work. The thesis structure and published papers from the work carried out were also outlined

Chapter 2. Principles of Optical OFDM

2.1 Introduction

This chapter introduces the basic concepts of OFDM and OOFDM, which is the foundation of the work presented in the rest of this thesis. OFDM has been intensively used in radio frequency wireless communications for the thirty years. However, its appearance in the optical communications system occurred relatively late. The chapter starts with a brief historical review of the major OFDM systems research its applications milestones and thereafter detailed discussions are made of the principles of each individual building block that forms a representative OFDM system. An understanding of OFDM in optical fibre communications requires a good knowledge of the fibre channel characteristics. Thus, both linear and nonlinear fibre effects are also discussed in this chapter. Finally an intensive discussion of the two major option of OOFDM transmissions which are CO-OOFDM and IM-DD-OOFDM is presented, after which there strengths and drawbacks are addressed.

2.2 OFDM

The year 1966 witnessed the birth of a new concept which revolutionized the communication engineering industry; this new idea developed at the Bell Lab is known as OFDM, which came as a an alternative to the existing FDM technique [38]. Latter in 1971, Weinstein and Ebert proposed a modified version of the OFDM system [39] in which a bank of sinusoidal modulators were replaced by the discrete Fourier transform (DFT). This modification significantly reduced the implementation complexity of the design while maintaining the subcarriers orthogonality.

To further improve the effectiveness of mitigating inter symbol interference (ISI), the use of CP or the cyclic extension was first introduced by Peled and Ruiz in 1980 [40]. Her the conventional null guard band was replaced by a cyclic extension, which is a copy of the last fraction of each OFDM symbol that is added to the front of each symbol to maintain the orthognality and further reduce the effect of ISI. In order to suppress both ISI and ICI that may have resulted from a channel distortion, synchronization error, or phase error, a new equalization algorithm was proposed in 1980[41].

The pilot tone technique was introduced by Cimini in 1985 for the purpose of compensating for channel induced interference and noise [42]. In the nineties, OFDM systems have been exploited for high data rate communications. OFDM considered as part of the IEEE 802.11 standard, where the carrier frequency as high as 2.4 GHz or 5 GHz is recommended. In 1995, Telatar reported bandwidth and transmitted power efficient MIMO OFDM systems [43], which further pushed the OFDM research cycle even further to include the use of OFDM for the optical wireless communications in 2001.

Since the foundation of OFDM we have seen a significant mile stone in system improvement until it is considered in many of today's wireless communications standards including wireless LANs (WiFi; IEEE 802.11a/g), wireless metropolitan area networks MANs (WiMAX; 802.16e), and long-term evolution (LTE) - the 4G mobile communication technology [44].

Application wise OFDM was only utilized for RF communication systems until it was finally introduced in the optical domain in 2005. Thereafter we have seen a growing interest in simulations and experimental demonstrations of OOFDM in radio over fibre (RoF) [45, 46],

for access networks and for MANs using single mode fibre (SMF) and multimode mode fibre (MMF) [47, 48], as well as long-haul coherent transmission systems [7, 8, 37, 49].

As OFDM is considered as a evolutional form of the traditional FDM technique, where different users data are transmitted simultaneously over a number of frequency carriers [50] as shown in Fig. 2.1(a).

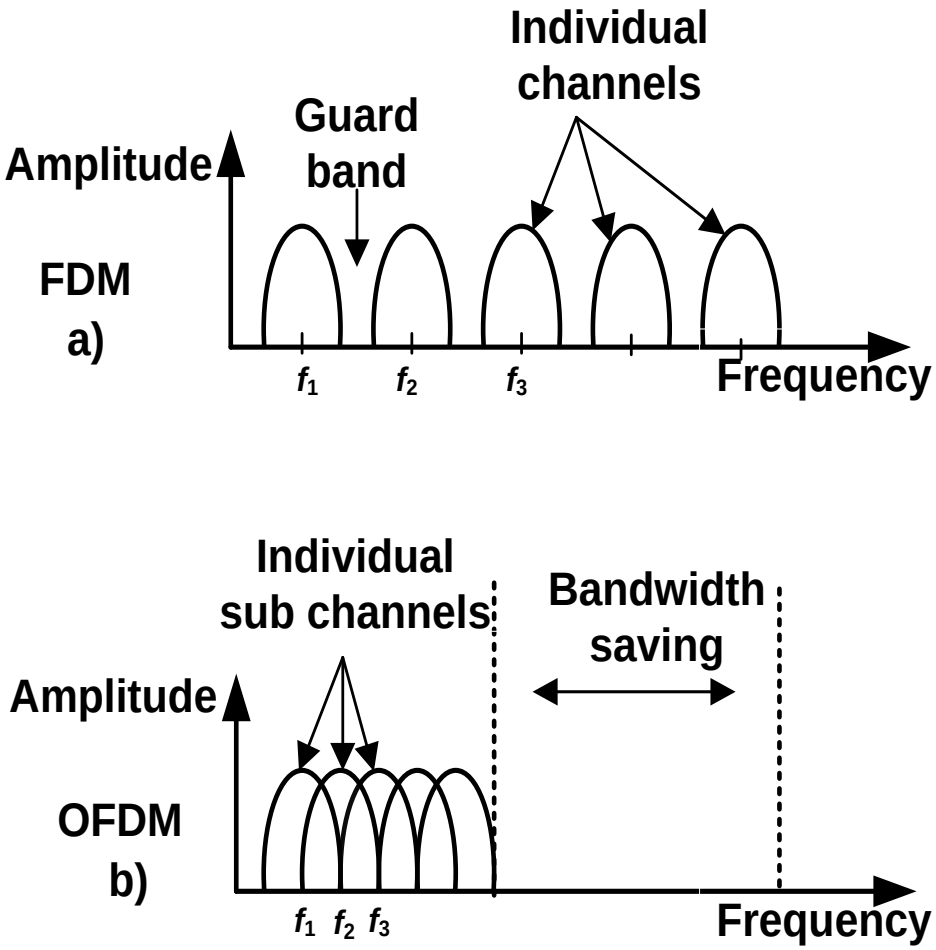

Figure 2.1: Compression between: (a) FDM, and (b) the OFDM spectral.

At the FDM transmitter, each subcarrier signal is modulated by a data signal and with a guard band between the adjacent subcarriers in order to prevent carriers overlapping and therefore

reduce ISI and ICI. However, inclusion of the wide guard band leads to spectral inefficiency in early FDM systems. This is due to the lack of digital filtering which made it possible to closely pack subcarrier channels. At the receiver side, the received signals are demodulated using oscillator bank arrays and band-pass filters.

Although both FDM and OFDM see Fig. 2.1(b) are multicarrier transmission schemes, OFDM has the advantage of using IFFT and FFT instead of oscillator banks. Consequently, carefully selecting subcarrier signals and with the demodulation of one subcarrier being independent of others even if there are spectral overlaps between subcarriers.

The OFDM modem consists of a transmitter and a receiver as illustrated in Fig. 2.2.

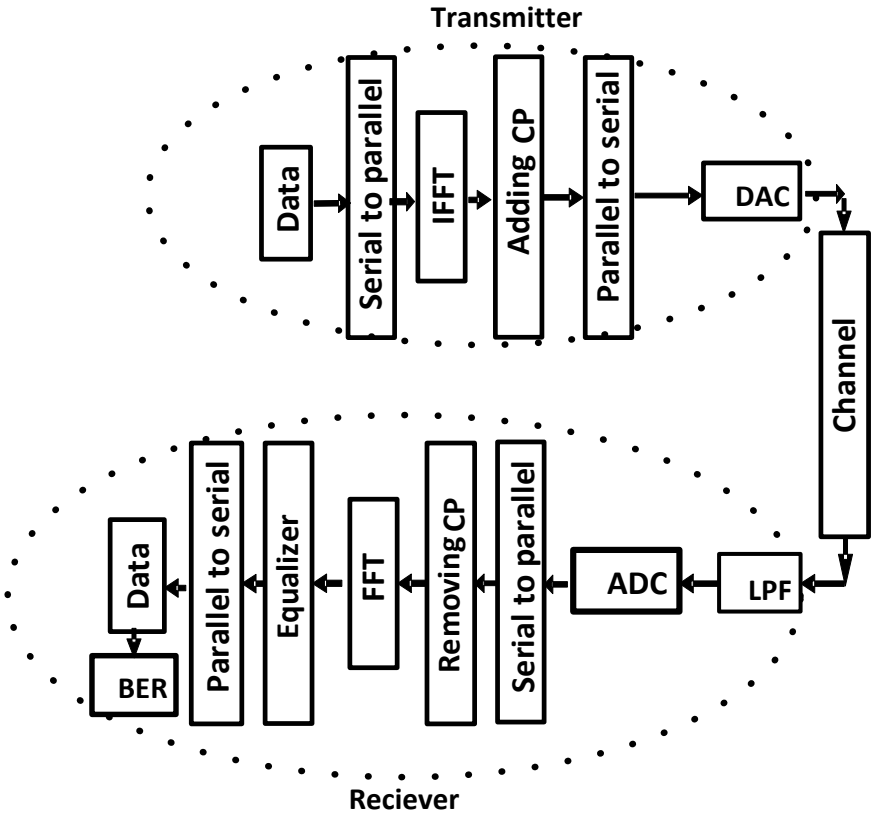

Figure 2.2: OFDM system block diagram.

2.2.2 OFDM Transmitter

The transmitter is composed of a number of modules as outlined below.

Data: The incoming serial data is first converted into parallel streams followed by the M-ary modulation as illustrated in Fig. 2.3. Each of the encoded parallel outputs corresponds to a separate subcarrier signal.

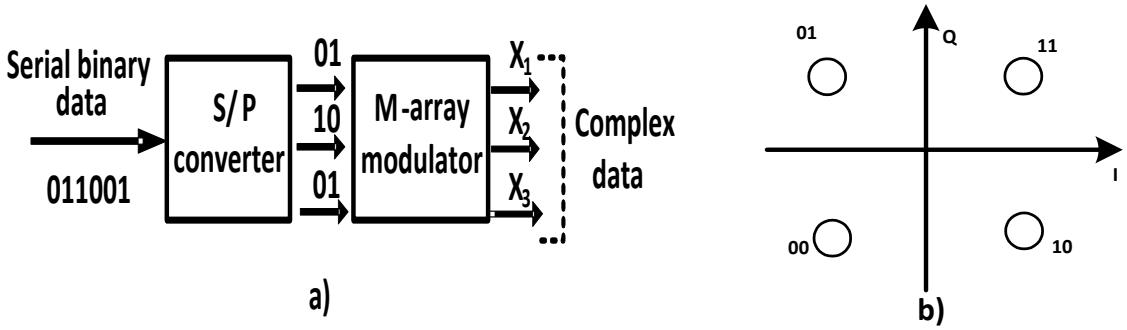

Figure 2.3: (a) Bit encoder, and (b) QPSK constellation diagram.

Figure 2.3(b) shows examples of multi-level modulation format namely quadrature phase shift keying (QPSK). In QPSK the signal phase is keyed between four possible phase values (45°, 135°, 225° and 315°) to represent the four possible variations of a two-bit set. In the other hand, for other multilevel modulation formats such as the 16-QAM both the signal amplitude and phase are keyed to represent the 16 possible stats of a 4-bit combination. Using higher modulation formats on different subcarriers can be different, which improves the OFDM system scalability and flexibility of the system [51], in the next section the discussion is taken a bit further in order to discuss some popular QAM modulation formats.

Inverse fast Fourier transform (IFFT): OFDM has the advantage of using the digital inverse fast Fourier transform IFFT, which is an efficient and accurate method for frequency up converting and multiplexing the bit encoded complex subcarriers. On the other hand de-modulation and de-multiplexing at the receiver side is achieved using the FFT process, consequently the digital process of IFFT/FFT is considered as the core component in the transmitter/receiver to perform the functionalities of modulation demodulation and multiplexing de-multiplexing. The IFFT is defined by [3]:

$$x(l) = \frac{1}{\sqrt{N}} \sum_{k=0}^{N-1} X(k) e^{j2\pi k \frac{l}{N}}, \tag{2.1}$$

$$X(k) = A_{k,n} e^{2j\theta_{k,n}}, \tag{2.2}$$

Where $X(k)$ represents users bit encoded data of the *k*-th subcarrier and *N*-th symbol, and $A_{k,n}$, $\theta_{k,n}$ are respectively the amplitude and phase of the signal constellation points. The *k*-th subcarrier waveform can be modulated independently with data. The *k*-th subcarrier time domain waveform within the *n*-th symbol period can be expressed as:

$$x_{k,n}(t) = X_{k,n} \Psi(t - nT_s)\, e^{j2\pi f_k(t)}, \qquad k=0, 1, 2,\ldots,N_s, \tag{2.3}$$

$$\Psi(t) = \begin{cases} 1, t \in [0, T_s] \\ 0, t \notin [0, T_s] \end{cases}, \tag{2.4}$$

Where N_s is the number of subcarriers, f_k is the frequency of the *k*-th subcarrier, T_s is the OFDM symbol period, and $\Psi(t)$ has a rectangular pulse shape of unity magnitude over the time duration of T_s therefore, as a result this will give rise to *sinc* form spectrum for each subcarrier see Fig. 2.4.

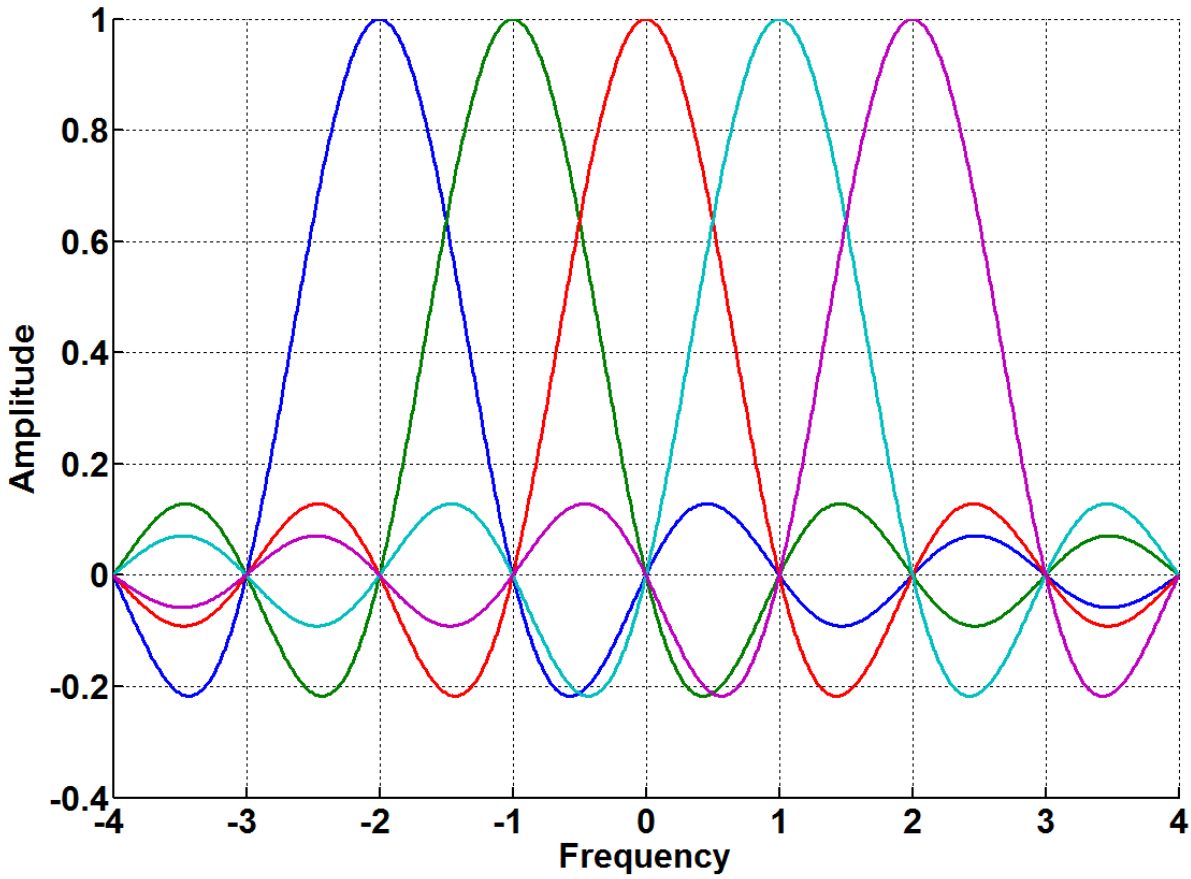

Figure 2.4: OFDM subcarriers waveform.

The correlation between any two subcarriers in the n-th symbol period is given by [51]:

$$\frac{1}{T_S}\int_{(n-1)T_S}^{nT_S} x_{k,n}(t)x^*_{l,n}(t)\,dt = e^{j2\pi(f_k-f_l)}\frac{sin(\pi(f_k-f_l)T_s)}{\pi(f_k-f_l)T_s}, \tag{2.5}$$

The above equation is considered when $X_{k,n}$ is treated as a unit for simplicity.

Subcarrier frequency spacing can be expressed as:

$$\Delta f = (f_k - f_{k-1}) = \frac{1}{T_s}, \quad k=1,2,\ldots,N_s-1. \tag{2.6}$$

Signals are normally orthogonal if the integral value is zero over the interval $[(n-1)T_s, nT_s]$. Since the carriers are orthogonal to each other the nulls of one carrier coincides with the peak of another sub carrier. As a result, it is possible to extract the sub carrier of interest

$$\frac{1}{T_S}\int_{(n-1)T_s}^{nT_s} x_{k,n}(t)\, x^*{}_{l,n}(t)\, dt = e^{\frac{j2\pi(k-l)}{T_s}} \frac{sin(\pi(k-l))}{\pi(k-l)} \begin{cases} 1, k = l \\ 0, k \neq l \end{cases} \quad (2.7)$$

The equation 2.7 shows that the mutual orthogonality between subcarriers is only achieved, when the subcarrier frequency spacing and the symbol period satisfies the equation 2.6. By combining equations 2.3, 2.4 and 2.6, the expression for the OFDM signal associated with the *k*-th subcarrier within the time duration of is given by:

$$x_{k,n}(t) = X_{k,n} e^{j2\pi \frac{k}{T_s} t} \quad (2.8)$$

It is shown in equation (2.8) that each subcarrier waveform has an integer number of cycles within a single OFDM symbol period, moreover it can be noticed that, the number of cycles grows as the subcarrier index increases.

The orthogonality of subcarriers can be viewed in either the time domain as well as the frequency domain. For time domain perception, each subcarrier is a sinusoid with an integer number of cycles contained in one FFT interval. From the frequency domain perspective, this corresponds to each subcarrier having the maximum value at its own centre frequency and zero at the centre frequency of each of the other subcarriers.

Signal $y(t)$ is the result of propagating subcarriers $x(t)$ through a channel with an impulse response $h(t)$ and with a noise variant $w(t)$, consequently the signal will be of this format:

$$y(t) = x(t) \otimes h(t) + w(t). \quad (2.9)$$

Upon reception, the signal $y(t)$ will be applied to the FFT digital processor this is in order to get the signal back to the frequency domain and calculate the bit error rate (BER) afterward, the FFT processor is given by (2.10):

$$Y_{k,n}(f) = \sum_{k=0}^{N-1} y_{l,n}(t) e^{-j2\pi k \frac{l}{N_s}} , \qquad l = 0,1,2..N_s - 1 \tag{2.10}$$

In a multi-path environment, transmitted symbol normally takes different paths propagation paths and thus times to reach the receiver. From the receiver‘s point of view, the transmission channel introduces time dispersion in which, the duration of the received symbol is extended. Stretching the symbol duration causes the current received symbol to overlap previous received symbols and results in ISI.

In OFDM, ISI usually refers to interference of two adjacent OFDM symbols. However, for OFDM the system bandwidth is broken up into *N* subcarriers, which reduces the symbol rate by a factor of *N* times lower than the single carrier transmission. This low symbol rate makes OFDM naturally resistant to effects of ISI caused by multipath propagation environment; Interference caused by data symbols on adjacent sub-carriers is referred to ICI. Similar to the wireless domain case, ICI occurs when the multipath channel varies over one OFDM symbol time. When this happens, the Doppler shift on each multipath component causes frequency offset on the subcarriers, resulting in the loss of orthogonality among them [51]. This situation can be viewed from the time domain side, in which the integer number of cycles for each subcarrier within the FFT interval of the current symbol is no longer maintained due to the phase transition introduced by the previous symbol. Finally, any offset between the subcarrier frequencies of the transmitter and receiver also introduces ICI to an OFDM symbol [51].

Cyclic prefix (CP): The solution adopted from the introduction of the CP in 1980 [52] in order to reduce the ICI impact and improve the performance robustness to the multipath propagation problem. CP which is a copy of the last fraction of each OFDM symbol added to the front of the symbol, the concept of this technique is illustrated in Fig. 2.5.

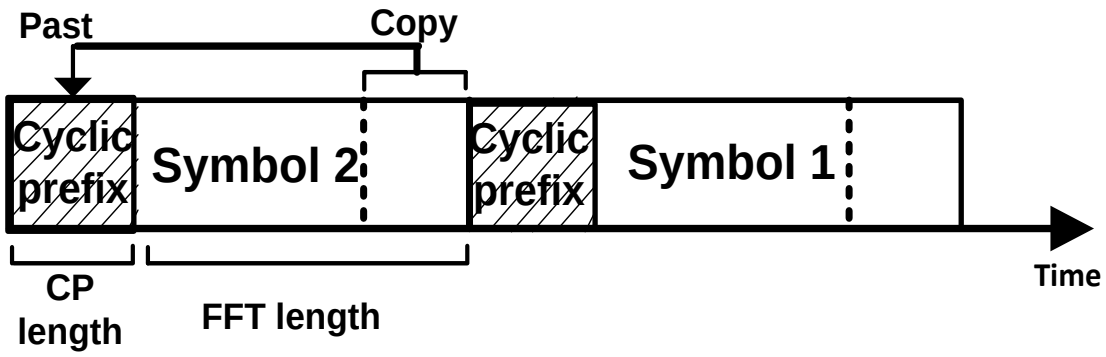

Figure 2.5: OFDM cyclic prefix.

It should be pointed out that the CP data is a redundant data, which means that it reduces the system throughput and data rate, consequently the choice of CP length should be selected carefully corresponding to the amount of delay and CD in the channel. The CP operator is generally defined according to:

$$\eta = \frac{T_P}{T_s - T_P}, \tag{2.11}$$

Where T_p is the CP length and T_s is the new symbol length i.e after the addition of the CP, T_s - T_p equals to the FFT length.

As maintained earlier OFDM symbol has an integer number of cycles, consequently placing copies of the symbol end-to-end results in a continuous signal, with no discontinuities at the

joins. Thus by copying the end of a symbol and appending this to the start results in a longer symbol time. More importantly, if the CP is longer than the expected largest time delay, the dispersion effect is localized within the CP region only which mean the signal will suffer from a zero ICI and ISI, however in this case the CP wastes a large portion of the transmitted signal power, resulting in an effective degradation of the signal SNR [53]. Moreover, this may also prevents the system from making full use of the available link bandwidth.

Parallel to serial converter: Before transmitting the OFDM signal they should be applied to a digital analogue converter (DAC) consequently beforehand the signals have to pass through a serializer which converts the a number of low-speed parallel subcarrier signals into a high-speed serial signal.

Digital to analogue converters (DAC): One major drawback of the OFDM signals is their large peak to average power ratio PAPR. The high PAPR limits the system transmission capacity due to the distortion caused by the nonlinear fibre and other associate component such as the fibre amplifier. Moreover, this increases the demand of having a more complex digital to analogue converters.

The nonlinear effects on the OFDM signals can vary from spectral spreading, inter-modulation, in-band and out-of-band interference to signals [54], this kind of distortion causes spectral spreading and introduce changes to the signal constellation thus increasing the BER. Therefore, reducing the PAPR is of practical interest. Since the large peaks occur with low probability, consequently clipping signal that exceed the DAC maximum amplitude limit could be an effective technique for the reduction of PAPR. DAC is key system component

limiting the maximum transmission capability of the OFDM signals due to its signal clipping and quantization effects.

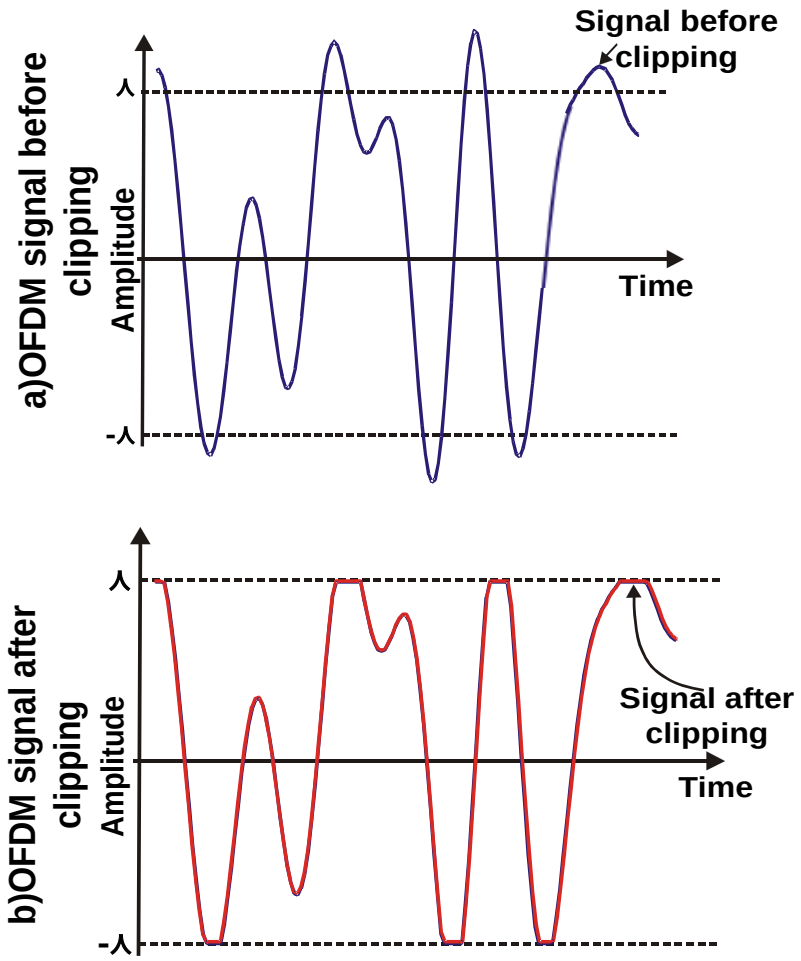

Figure 2.6: Comparison between (a) OFDM waveform before clipping, and (b) OFDM waveform after clipping.

Since the effect of signal clipping and quantization in DAC are similar as that of ADC, consequently DAC and ADC in the following discussion are, therefore, referred to by ADC only. As ADCs have limited amplitude ranges, signal clipping is closely related to the operating point of the automatic-gain-control unit that precedes the analogue-to-digital stage. For a clipping level ξ which is referred to as clipping ratio throughout this document, clipped signals can be defined as [55]:

$$A_{clip}(t) = \begin{cases} A(t), & |A(t)| \leq \lambda \\ \lambda\, e^{jarg[A(t)]}, & |A(t)| > \lambda \end{cases}. \quad (2.12)$$

The signal amplitude threshold λ is defined as $\lambda = \sqrt{\xi P_{av}}$ where P_{av} is the average power of the OFDM signal. Figure 2.6 illustrates further the process of signal clipping.

The clipped OFDM signal is sampled in ADC resulting in a discrete signal with continuous-valued amplitudes. At the receiver ADC linear quantizer digitizes the sampled OFDM signals into discrete amplitudes, which span the entire dynamic range of' [-λ, λ]. The quantization process can be expressed according as a generic symmetric-staircase functions [56, 57]:

$$Q(A_s) = \sum_{k=-\left(\frac{L}{2}\right)+1}^{\frac{L}{2}} \frac{\hat{A}_k + \hat{A}_{k-1}}{2}\, g(A_s, \hat{A}_k, \hat{A}_{k-1}), \quad (2.13)$$

Where $\hat{A}_k$ and $\hat{A}_{k-1}$ are the k-th and the $(k-1)$-th quantization threshold values. L is the quantization levels depicted $L = 2^b$ with a number of quantization bits of b, and g is the rectangular function defined as [55]:

$$g(A_s, \hat{A}_k, \hat{A}_{k-1}) = \begin{cases} 1, & \hat{A}_k \leq A_s < \hat{A}_{k-1} \\ 0, & else \end{cases}. \quad (2.14)$$

2.2.3 OFDM Receiver

For OFDM system, the receiver is a mirror image of the transmitter. Once the received signal is passed through an ADC then the CP extension is removed. Thereafter de-modulation and de-multiplexing is carried out using the FFT process, where the signals are converted back into the frequency domain. The distortion applied to the signal can be further

compensated using a technique called the pilot tone, which is discussed in the following section.

Pilot-tone channel equalization: In OFDM system, channel estimation is achieved by padding the transmitted signals with pilot frequency domain signals. Whilst at the receiver side, the channel frequency response is estimated by extracting the pilot signals from the received signals, which will be used afterward for the channel equalization purpose, therefore, the effect of the channel frequency response effect will be reversed and then possibly totally removed, consequently the signal will be restored before bit decoding [58]. Since the equalization is a frequency domain process, therefore, the time channel convolution equation 2.9 can be expressed as a multiplication process in the frequency domain; therefore, the signal after the FFT will be as the following:

$$Y_k = X_k . H_k + W_k, \tag{2.15}$$

Where Y_k is the FFT output of the k-th subcarrier and X_k is the k-th subcarriers frequency domain user data, H_k is the channel frequency response, W_k is the channel noise that which is applied to the k-th subcarrier. The frequency response of the channel is can be estimated at the receiver side according to [3]:

$$H_{k,p} = \frac{Y_{k,p}}{X_{k,p}}, \tag{2.16}$$

As $Y_{k,p}$, $X_{k,p}$ are the corresponding received and sent pilot samples for the k-th subcarrier. Afterward at the receiver, the received signals will be multiplied with the inverse of the channel estimation impulse response of the k-th subcarrier [59], and the expression is given by:

$$\hat{X}_k = Y_k * H_k^{-1} = X_k + \frac{W_k}{H_k}. \quad (2.17)$$

This method has some disadvantages such as that in order to further reduce the signal distortion a high number of pilot signals are required which in turn will reduce the data rate. The equalized signal is applied to the bit decoder in order to decode the transmitted signal.

Data (Received): The data decoder often employs a maximum-likelihood detector for recovery of the digital symbols from the noisy signals. The implementation of the digital baseband maximum likelihood detector based upon comparing the received signal samples, $y(n)$, with every each of the constellation points. thereafter the constellation point that is corresponding to the smallest distance, between the sample and that point, is selected as the most likely digital symbol, which can then be rearranged as a bit value.

A schematic diagram of the maximum-likelihood detector for QPSK is shown in Fig. 2.7. In this figure, the distances of the actual received value from each point on the QPSK constellation is found to be a_1, a_2, a_3 and a_4. In this case, the shortest distance is a_1, indicating that symbol S1, representing bits 01, is the most likely symbol sent.

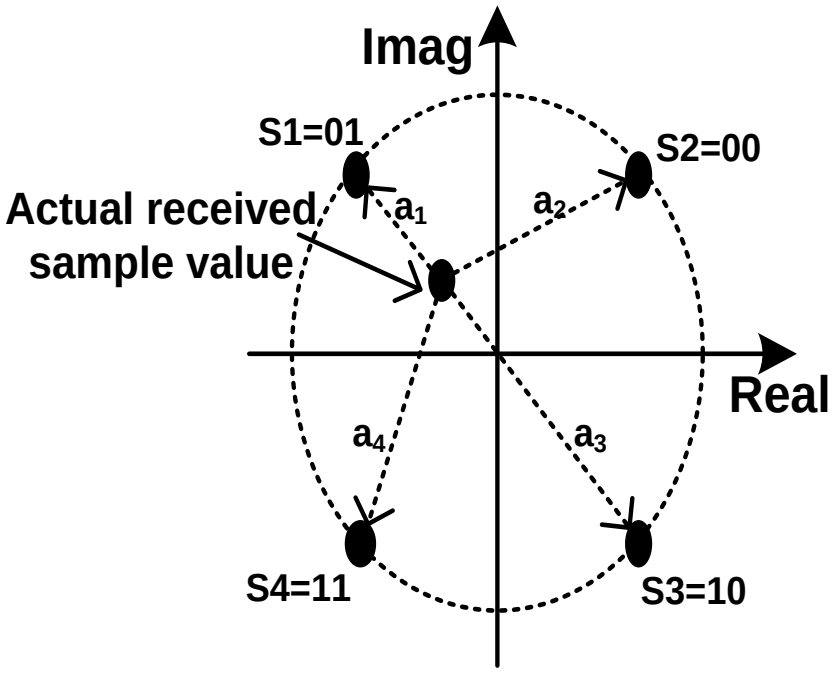

Figure 2.7: Maximum-likelihood detector for QPSK.

After discussing common modulation formats used in the modern communication systems in particular the OFDM system, the next section introduces the principles of the optical OFDM principles.

2.3 Optical OFDM Principles

Having discussed the general building blocks of the OFDM system, the next section investigates optical OFDM systems, as it is not valid to compare the RF domain OFDM with the optical version of the OFDM (OOFDM). This is mainly due to OOFDM signals being up-converted to higher optical frequencies using electro-optic convertors, which thereafter introduces nonlinear effects to modulated OOFDM signals when transmitted through the optical fibre channel.

Optical fibres can be divided in to two subcategories: (i) SMF which has a small core diameter and light propagates only in the single mode; and (ii) MMF with a larger core diameters and light propagating in multiple modes. The use of MMF results in a mode delay as signals propagate in different modes thus arriving at different times; consequently, this kind of fibre is not preferred for the long haul transmission and only used as a legacy fibre in local area networks. On the other hand SMFs are used in MAN as well as the long haul transmission offering very low dispersion (thus higher data rates) and very low attenuation SMF impairments can be further sub-categorised into two fibres with the linear regime such as CD and PMD, and the non-linear regime such as Kerr, four wave mixing (FWM), self phase modulation (SPM), and cross phase modulation (XPM).

2.3.1 Linear Fibre Impairments

Fibre loss: This is also known as the attenuation, which is the reduction in intensity of the light signal with respect to distance travelled through the fibre channel. The attenuation coefficient is usually expressed in dB/km is defined as [60]:

$$\alpha = -\frac{10}{z} log_{10} \frac{P_{in}}{P_z}, \tag{2.18}$$

Where P_{in} is the power of the optical signal launched in to the fibre and P_z is the optical power at z distance. It is shown at the figure below the loss spectrum of silica fibre. It can be seen that for the long wavelength range, optical scattering is due to lattice vibrations, which is considered to be the main factor for fibre loss. The attenuation peak around 1.38 μm shown in Fig. 2.8 is due to absorption by hydroxide (OH) impurities formed during manufacturing process.

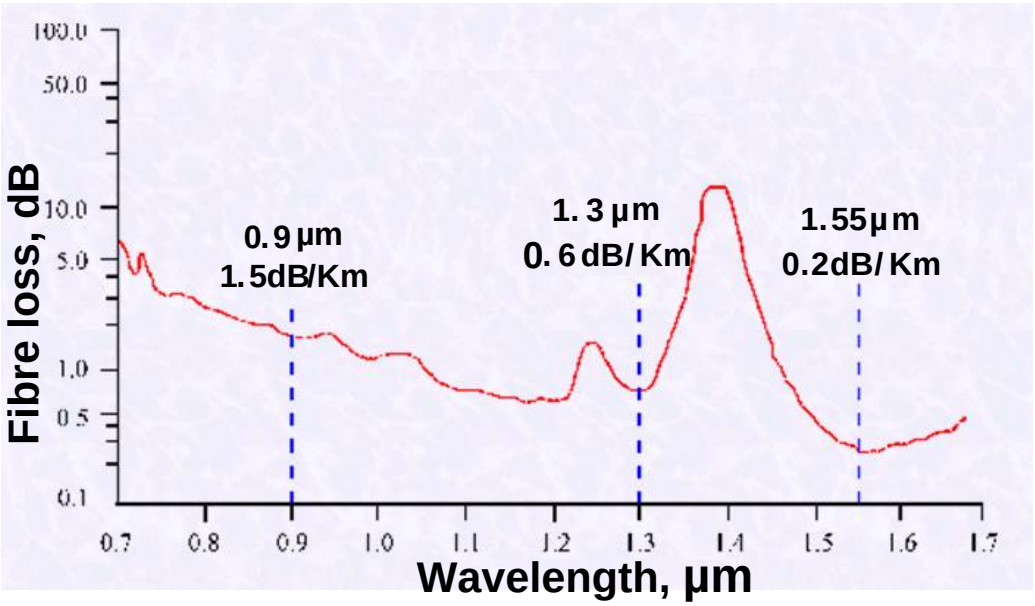

Figure 2.8: Wavelength versus fibre loss [60].

The lowest fibre loss occurs at 1.55 µm, the effect of lose can be overcome by utilizing optical amplifier such the erbium doped fibre amplifier (EDFA), consequently 1.55 µm is a favourite transmission wavelength window, which is located in the conventional band (C-band). For lower wavelengths, the loss is mainly due to the Relay scattering, which is discussed in the following section.

Rayleigh scattering: Rayleigh scattering is a form of elastic scattering in which, the kinetic energy of the incident light is conserved, only their direction of propagation is modified by interaction with other particles, consequently it is considered as a very important component of the scattering of optical signals in fibres. Generally, in fibre links, Rayleigh scattering occurs because of the imperfection in manufacturing of the silica core as the core density varies, on a microscopic scale, this density fluctuation result in energy loss due to the elastic scattered of light and backward propagation of a portion of the scattered light which is

referred to as rayleigh backscattering (RB). Figure 2.9 shows the effect of the loss induced due to rayleigh scattering in silica fibre noted by the dashed line.

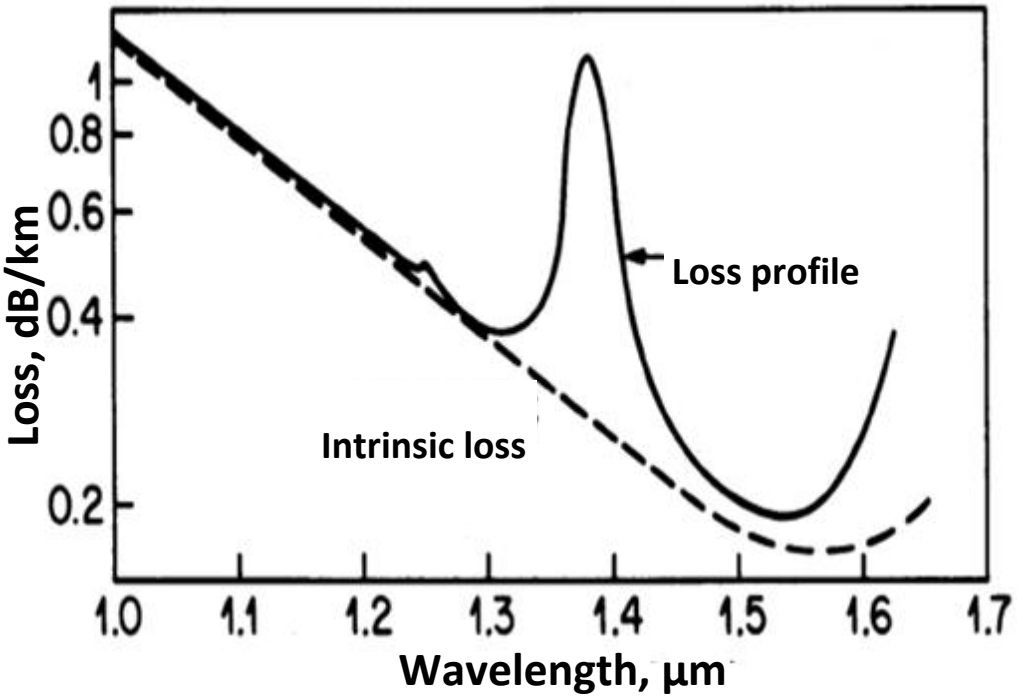

Figure 2.9: Measured loss spectrum of a single-mode silica fibre. Dashed curve shows the contribution resulting from Rayleigh scattering [60].

RB introduces noise fluctuations at the input surface of the optical fibre. The optical signal power P_{in} launched into a SMF generates RB noise propagating at the opposite direction. The RB noise power P_{RB} is given by [61]:

$$P_{RB} = P_{in}\xi, \tag{2.19}$$

Where ξ is the back scattering power normalized to the fibre launch power, which generally converges to a constant value for long fibre length. ξ is deified as:

$$\xi = B(1 - e^{-2\mu z}), \tag{2.20}$$

Where $B = S\alpha_s/2\mu$, α_s is the fibre scattering coefficient, S is the fibre recapture coefficient, and μ is the SMF attenuation coefficient which is defined as $\mu = \frac{20}{\ln 10}\alpha$, where α is the fibre loss defined in the previously at the equation 2.18 and z is the fibre length. The next linear fibre impairment is the CD, which is descried next.

Chromatic dispersion: Chromatic dispersion (CD) is an optical phenomenon, at which, light frequencies propagates in the fibre with different speeds. This effect depends upon the refractive index of the fibre core material and the frequency components of the optical signal. As signals occupy a finite frequency spans, CD leads to pulses broadening while propagating along the optical fibre, thus giving rise to ISI, which ultimately limits the maximum data rate. For an electromagnetic waveform propagating through fibre links, the optical signal field at a distance z_o can be expressed as follow:

$$E(z_o, \omega) = E(0, \omega).\, e^{[j\beta(\omega)z_o]}, \tag{2.21}$$

Where ω is the angular frequency and $\beta(\omega)$ represents the propagation constent. Fibre CD effects is represented mathematically by expanding the mode-propagation constant in a Taylor Series with respect to the central frequency (ω_0) [60] [51].

$$\beta(\omega) = n(\omega)\frac{\omega}{c}, \tag{2.22}$$

$$\beta(\omega) = \beta_0 + (\omega - \omega_0)\beta_1 + \frac{1}{2}(\omega - \omega_0)^2\beta_2 + \frac{1}{6}(\omega - \omega_0)^3\beta_3 + \cdots, \tag{2.23}$$

Where

$$\beta_m = \left(\frac{d^m \beta}{d\omega^m}\right)_{\omega=\omega_0} for\ m = 0,1,2,3, \ldots. \tag{2.24}$$

The group velocity β_1 equals $\frac{c}{n}$, where c is the speed of light and n is normal arpiture of the SMF link, β_2 is the group velocity delay (GVD), β_3 is the third order dispersion parameter [60].

Generally, the dispersion is represented by the dispersion parameter that is defined as

$$D = -\frac{2\pi c}{\lambda^2}\beta_2. \tag{2.25}$$

From (2.25) it can be seen that CD parameter is wavelength dependent. Standard SMF has zero dispersion at around the 1.3 µm region, and 17 ps/nm/km at 1.55 µm. The later is the preferred wavelength adopted for optical networks as well as being compatible with the conventional EDFA.

Polarization mode dispersion (PMD): This is a kind of modal dispersion, where signals with two different polarization modes in a waveguide, which normally travel at the same speed, travel at different speeds due to the random manufacturing imperfections and asymmetries in the refractive index of the fibre core and birefringes, causing random spreading of the optical pulses. Unless it is compensated, which is difficult, this ultimately limits the maximum data rate can be transmitted over the fibre. Figure 2.10 shows the PMD on a dual polarized signal for a SMF.

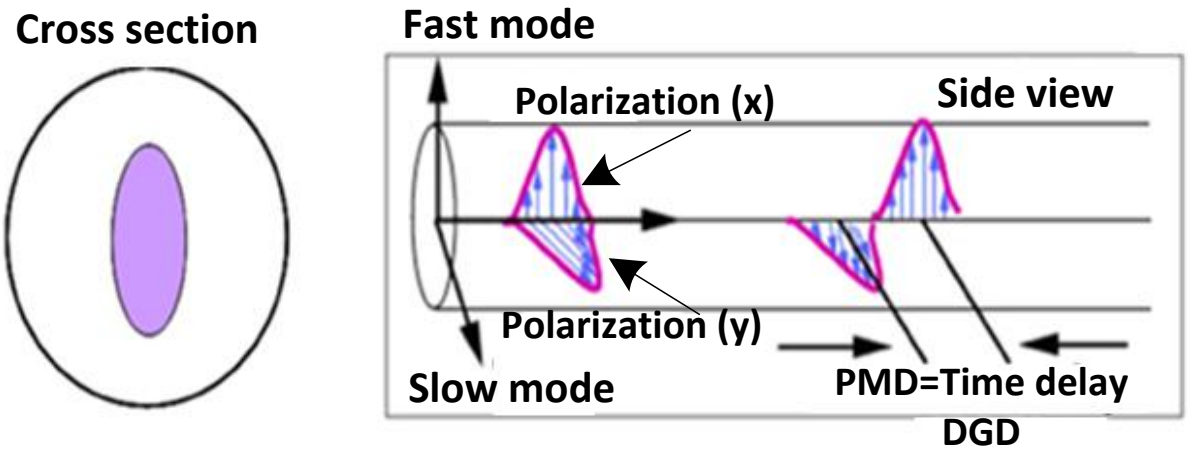

Figure 2.10: the polarization mode dispersion effect introduced by the asymmetric profile of the optical fibre core [62].

As a consequence of the PMD, the orthogonality between the polarization or the modes do not hold, which cases the signals to disperse and spread, therefore, arrive at the different times.

The PMD induced time delay between two polarizations can be expressed as:

$$\Delta\partial = D_{PMD}\sqrt{z}, \tag{2.26}$$

Where D_{PMD} is the PMD parameters in $(\mathrm{ps}/\sqrt{\mathrm{km}})$, in practical fibre normally the value of D_{PMD} varies between 0.1 to 1 $\mathrm{ps}/\sqrt{\mathrm{km}}$ [60]. Having discussed the linear impairments of the optical fibre link the next section is about the non-linear fibre impartment that limits the data transmission through SMF links.

2.3.2 Fibre Non-linearities

Not only the fibre dispersion affects the propagating optical signal phase and power but the signal can be subject to the fibre non-linearities. The first type of nonlinear effects is called the Kerr nonlinearity, which arises from the dependence of refractive index on intensity of the propagating signal. It is defined as: $n(\omega, |E|^2) = n(\omega) + n_2|E|^2$, where n_2 is the nonlinear-index coefficient, which is also called the Kerr coefficient, ω is the angular frequency. Moreover, the most important nonlinear effects in this category are SPM, XPM, and FWM [60]. The second type of fibre nonlinearities that exhibits energy transfer from the optical field to the medium via a stimulated elastic scattering process are known as the stimulated Brillouin scattering (SBS) and the stimulated Raman scattering (SRS).

Self-phase modulation (SPM): this is a refractive index dependence nonlinear optical effect. It mainly occurs during the propagation of an ultra short pulse of light through SMF, which will induce a varying refractive index of the medium due to the optical Kerr effect. This refractive index variation will produce a phase shift in the pulse, leading to a change of the pulse's frequency spectrum. The nonlinear phase shift ϕ_{NL} imposed on the optical field is proportional to the optical intensity, is expressed as follow:

$$\phi_{NL}(l,T) = n_2 k_0 l \mid E(l,T)|^2, \tag{2.27}$$

Where n_2 is the non-linear refractive coefficient (Kerr coefficient), l is the fibre length, $E(l,T)$ is the electrical field at a distance l, and $k_0 = {}^{2\pi}/_{\lambda_0}$, λ_0 is the signal wavelength. The SPM broadens the spectrum of optical pulses without changing the pulse shape. In optical fibre spectral broadening generates frequency chirp, which adds new frequency components to the optical pulse.

Cross-phase modulation (XPM): XPM exhibit the same behaviour as the SPM, but it mainly occur when two optical pulses or more affect the phase and intensity of each other's when broadening. When two optical fields E_1 and E_2 at frequencies $\boldsymbol{\omega_1}$, and $\boldsymbol{\omega_2}$, respectively, co-propagate in the fibre, the nonlinear phase shift for the field at $\boldsymbol{\omega}$, is represented as:

$$\phi_{NL}(l,T) = n_2 k_0 l(|E_1|^2 + |E_2|^2). \quad (2.28)$$

Similar to SPM, XPM also causes a greater sequential broadening as signal propagates along the fibre due to the effect of CD.

Four-wave mixing (FWM): FWM is an intermediation process for the optical pulses while propagating through SMF. This phenomenon takes place when 3 wavelengths are interfering with each other, thus resulting in refractive index gratings. Such gratings interact with signals and produce new frequencies at the 4th wavelength [53].

Stimulated Raman scattering (SRS): SRS is a phenomenon occurs when light particles travels through a SMF link it causes vibration and excitation of the molecules. This in turn causes scattering of light particles travelling through that medium, which is known as SRS that can occur either in the forward or backward directions.

Stimulated Brillouin scattering (SBS): SBS also occurs at high optical input power in optical fibres but much lower than those needed for SRS. Moreover, SBS generates a beam that propagates in the backward direction only. In practice, the effect of SBS is negligible at lower launched power levels. However, the effect becomes significant when the input power is high [60]

2.4 Optical OFDM

The OFDM technique, together with the fibre linear and non-linear impairments was briefly discussed in the previous sections. In 2005 OFDM was introduced into the optical domain and since then two main OOFDM variants have been developed that are classified according to the detection scheme. The first technique is known as IM-DD- OOFDM [63], and the second scheme is the CO-OOFDM [37]. Moreover, a comparison between these two techniques in terms of advantages and disadvantages are discussed latter in this chapter.

2.4.1 IM-DD OOFDM

Figure 2.11 shows a block diagram of a typical IM-DD-OOFDM system. At the transmitter side, the electrical OFDM signal are produced by an OFDM transmitter and then up-converted into the optical domain by using an electrical-to-optical (E/O) up-converter. Signals are then transmitted through the optical channel and an EDFA. At the receiver side, an optical -to- electrical (O/E) down-converter is utilized to convert the signal back into its electrical domain for processing by the OFDM receiver.

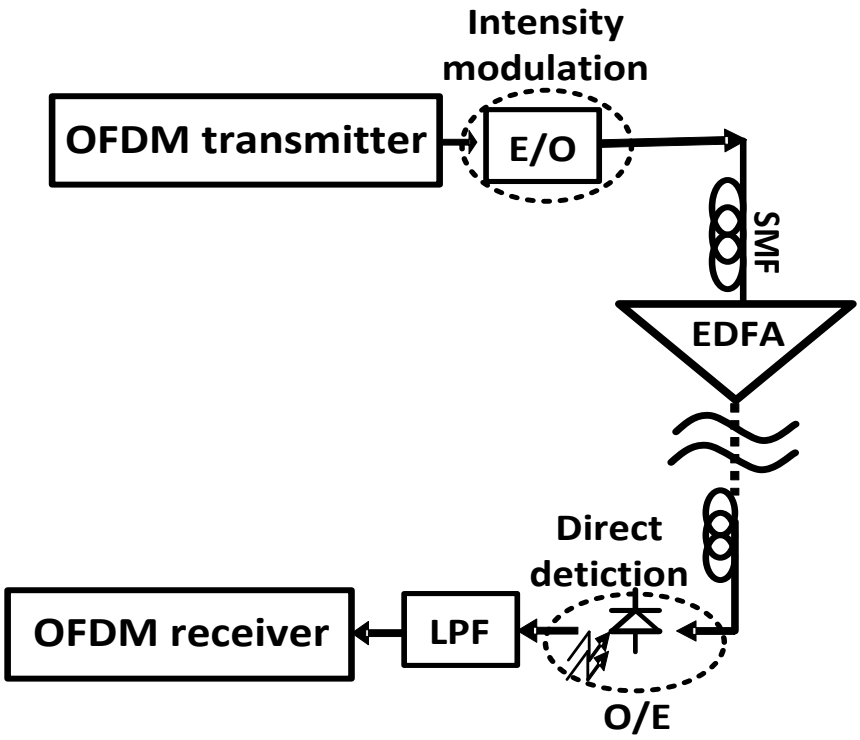

Figure 2.11: IM-DD-OOFDM system block diagram.

The E/O conversion requires the OFDM signal to have only real values in order to operate the DFB laser source. Therefore, two main methods had been employed in order to produce a real OFDM signal; the first method is to arrange IFFT inputs to have a Hermitian symmetry. Therefore, the IFFT inputs can be expressed as in [51]:

$$\bar{X}_{k,n} = \begin{cases} 0\,, & k = 0 \\ X_{k,n}, & k = 1,2,\ldots\frac{N_s}{2} - 1 \\ 0, & k = \frac{N_s}{2} \\ X^*_{N_s,-k,n}, & k = \frac{N_s}{2} + 1, \ldots., N_s - 1 \end{cases}, \tag{2.29}$$

Where $X_{k,n}$ represents the encoded complex data of the equation (2.2) and $X^*_{k,n}$ is the signal conjugate. The above expression can be explained as the OFDM transmitter is modified by creating the truncated original complex parallel data in the positive frequency bins i.e.

bins 1 to $\frac{N_S}{2} - 1$ and the complex conjugate of the data in the negative frequency bins i.e bins $\frac{N_S}{2} + 1$ to $N_S - 1$, with the first positive and negative bins carrying no user data i.e zeros [51]. As it can be understood the IM-DD system wastes half of the spectra as it carrys no user data.

Based on the IM-DD system diagram, it can be seen that after inserting the CP to each symbol of OFDM, the real value OFDM symbols are then serialized before being applied to DAC. Subsequently a real value analogue OFDM signal can be E/O up-converted during by means of IM. Thereafter, the up converted OOFDM signal is launched into the optical fibre [59].

At the receiver side, the O/E down-converter is used to recover the electrical version of the OFDM signal using a square-law photodiode. The received electrical signal $A_e(t)$ is given by:

$$A_e(t) = |A_0(t)|^2 \otimes h_e(t) + w(t), \tag{2.30}$$

Where $A_0(t)$ is the OOFDM signal, $h_e(t)$ is the link impulse response in the electrical domain and $w(t)$ is the system noise.

After the OE down conversion process, the signal is passed through a LPF and an ADC, subsequently the sampled electrical signal is decoded into the original data sequence by the receiver, which is an inverse design of the transmitter. In IM-DD based schemes, no local oscillators are required; generally speaking, IM-DD system simplifies the system complexity as compared with the CO-OOFDM that is normally used in long haul transmission.

2.4.2 Coherent Optical OFDM (CO-OOFDM)

Having discussed the basic concept of the IM-DD OOFDM system, this section focuses on the OOFDM variant that is known as CO-OOFDM, as shown in Fig. 2.12.

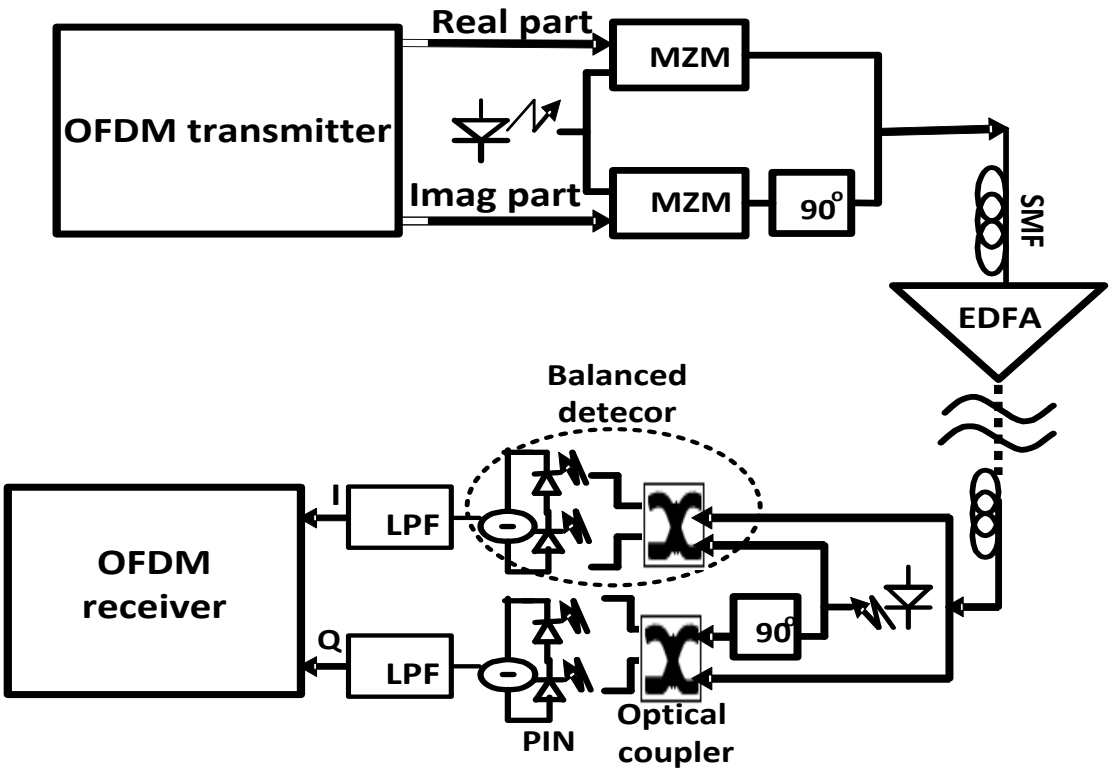

Figure 2.12: CO-OOFDM system block diagram.

In an optical coherent system, an optical local oscillator is utilized to generate optical signals at a certain wavelength [64]. According to whether the frequency of the local oscillator matches that of the incoming information signal the coherent detection can be classified into two main categories.

The first one is the heterodyne detection, where the frequency of the local oscillator does not match the frequency of the incoming signal. Therefore, when the two incoming signals are

mixed on the surface of the photo detector a new frequency is intermediate frequency (IF) is generated which is the difference between the two frequencies [65]. This method gives rise to a reduced thermal and shot noise induced currents, consequently this means an improved signal-to-noise ratio (SNR) performance. However, the frequency of an optical source is known to drift over time. Therefore, the IF frequency needs to be continually monitored at the input of the electrical detector and the local oscillator frequency must be varied accordingly to keep the IF centre frequency constant.

The second coherent detection scheme is called the homodyne detection, which is adopted in this research. This is similar to the heterodyne detection scheme except that the local oscillator has the same frequency as the received optical carrier [64]. The resultant photocurrent thus contains the information signal at the baseband region. As it can be seen from Fig. 2.12, that the CO-OOFDM system is similar to the basic OFDM system, except for additional optical components including the real / imaginary (I/Q) modulator and an optical fibre cable.

In order to convert the I and Q components of the digital signal into analogue signal two separate DACs are used at the transmitter, the optical I/Q modulator comprising of two Mach-Zehnder modulators (MZM) up-converts the real/imaginary components of the complex OFDM signal from the electrical domain to the optical domain. It is well know that by biasing the MZM module at the null point (a bias voltage equal to the half-wave switching voltage of MZM), a linear conversion from the transmitted OFDM electrical signal to the optical field signal can be achieved [7, 58]. Consequently, the corresponding modulated signal can be represented as:

$$E(t) = x(t)exp(jw_{LD1}t + \emptyset_{LD1}), \tag{2.31}$$

Where $x(t)$ is the transmitter electrical signal after the DAC, w is the angular frequency and $\emptyset$ is the phase of the laser diode at the transmitter. At the receiver side, the signal can be expressed as:

$$E_r(t) = E(t) \otimes h_e(t) + w(t), \tag{2.32}$$

Where $h(t)$ and $\omega(t)$ represent the channel impulse response and channel noise, respectively. Upon the reception, the signal will be detected by a two pairs of balanced detectors and an optical 90° hybrid to perform the I/Q detection. the four output ports of the 90° optical hybrid can be expressed as [51]:

$$E_1 = \frac{1}{\sqrt{2}}[E_r + E_{LD2}], \tag{2.33}$$

$$E_2 = \frac{1}{\sqrt{2}}[E_r - E_{LD2}], \tag{2.34}$$

$$E_3 = \frac{1}{\sqrt{2}}[E_r - jE_{LD2}], \tag{2.35}$$

$$E_4 = \frac{1}{\sqrt{2}}[E_r + jE_{LD2}], \tag{2.36}$$

Where E_{LD2} corresponds to the electrical signal from the LD at the receiver. Moreover, as shown at the receiver side two photodiodes (PD_1 and PD_2) are used in order to recover the corresponding I component (photocurrent), which can be expressed as follow:

$$I_1 = |E_1|^2 = \frac{1}{2}[|E_r|^2 + |E_{LD2}|^2 + 2Re(E_r {E_{LD2}}^*)], \tag{2.37}$$

$$I_2 = |E_2|^2 = \frac{1}{2}[|E_r|^2 + |E_{LD2}|^2 - 2Re(E_r {E_{LD2}}^*)], \quad (2.38)$$

Where Re represents the real component of the signal. Because of the balanced detection, the photocurrent that represents the real part of the complex signal can be expressed as [51]:

$$I_I(t) = I_1 - I_2 = 2Re(E_r {E_{LD2}}^*). \quad (2.39)$$

It should be pointed out that the noise component $w(t)$ is suppressed upon the balanced detection and this is one of the main advantages of coherent detection.

Similarly, the photocurrent that carries the Q component of the complex signal is mathematically represented as:

$$I_Q(t) = I_3 - I_4 = 2Im(E_r {E_{LD2}}^*), \quad (2.40)$$

Where *Im* represents the imaginary component of the signal. As a result the total complex photo current $I(t)$ is the summation of both the photo-current of both I and Q components, thus this can be represented as:

$$I(t) = I_I - jI_Q = E_r {E_{LD2}}^*. \quad (2.41)$$

By combining the above equations, the detected electrical OFDM signal can be represented as:

$$y(t) = I(t) = x(t)\exp(j\Delta\omega t + \Delta\emptyset) \otimes h(t) + w(t), \quad (2.42)$$

Where $\Delta\omega$ and $\Delta\emptyset$ are the angular frequency and phase difference between the transmitter laser diode LD_1 and the receiver laser diode LD_2 can be represented as:

$$\Delta\omega = \omega_{LD1} - \omega_{LD2}, \qquad \Delta\emptyset = \emptyset_{LD1} - \emptyset_{LD2}. \tag{2.43}$$

After the optical detection process, the received signals is sampled by ADC and passed through OFDM building blocks as was explained previously.

2.4.3 Comparison between CO-OOFDM and IM-DD OOFDM

In comparison with IM-DD, CO-OOFDM provides superiority when it comes to robustness to CD and PMD, as CD and PMD induced phase shifts can be well preserved [49]. This is owned to linear coherent detection technique, which further provides extra receiver sensitivity when used for the CO-OOFDM modem. As a result, CO-OOFDM, in theory, is capable of providing virtually unlimited dispersion tolerance. On the contrary, the tolerance to CD and PMD for IM-DD OOFDM, is limited due to less sensitive nonlinear direct detection process [59].

On the other hand, CO-OOFDM requires frequency offset compensation [53]. This is due to the use of a local laser at the coherent detection process, which further complicates the receiver synchronization compared to IM-DD OOFDM where there is no frequency offset. Secondly, the application of CO-OOFDM is limited to long-haul transmission systems, as coherent modem requires expensive and bulky equipments for E/O and O/E conversions, where IM-DD-OOFDM offers better solutions for cost sensitive applications including LAN, access networks, and MANs.

2.5 Conclusions

OOFDM enables excellent robustness against the optical fibre linear impairments such as CD and PMD. According to the data detection mechanism OFDM can be classified in to two main variants, the IM-DD-OOFDM and the CO-OOFDM, which is mainly utilised for in long-haul transmission systems due to its high performance and sensitivity. The IM-DD-OOFDM uses simple and less expensive IM-DD scheme. Thus outperforming CO-OOFDM on cost-sensitive application scenarios such as access networks. In the meantime, CO-OOFDM also brings about important challenges including the PAPR, dispersion and nonlinearity compensation, addressing these challenges forms the main task of this thesis.

Chapter 3. Introduction to Artificial Neural Network

3.1 Introduction

The advent of high-speed global communication is considered as one of the most important development milestones in human civilization from the second half of twentieth century to until this day. Nowadays there is a need for high speed and efficient data transmission over the communication channel. It is a challenging task for the communication engineers and researchers to deliver a trustworthy communication service by utilizing the available resources effectively in-spite of many impairments that distort the quality of the signal.

The main task of the digital communication system is to transmit data streams with minimum number of errors, which are generated because transmitted signals are distorted along the transmission path. Distortion generally can be categorized into two main types. First is the linear distortion, which includes the ISI, the co-channel interference (CCI) and the additive noise [66, 67]. Second is the nonlinear distortions, which are due to the subsystem modules such as amplifiers, modulator and demodulator as well as the transmission medium. Compensating all the channel distortion calls for the use of channel equalization techniques at the receiver side to ensure quality link performance.

Generally, equalizer performs like an inverse filter, which is placed in the receiving side of the communication link. Its transfer function is the inverse of the associated channel transfer function [68], and is able to reduce the errors between the desired and estimated signals. The traditional equalization techniques based on the finite impulse response (FIR) filter are well studied and provide a significant performance improvement for a different number of communication channels [69].

Adaptive channel equalizers are significant in now days digital communication systems [69]. More recently, the adaptive equalization has been defined as a classification problem, thus opening new gates for utilization of classification tools like the artificial neural network (ANN) for equalizations [68, 70]. ANN equalizer has a number of advantages when used for a time-varying environment, including the adaptability, a nonlinear decision boundary and parallel processing capabilities.

The main aim of this chapter is to describe the ANN main concepts, where Section 5.2 discusses the need for the equalization and the ANN equalization. Section5.3 describes the ANN and its concepts, whereas in Section 5.4 the operating principle of MLP is outlined. Section 5.5 talks about the adaptive equalization, and finally the chapter is concluded in Section 5.6.

3.2 Channel ANN Equalizer

In communication systems, compensation for all distortions induced to the transmitted signals while propagating through a communication channel can be carried out using channel equalization schemes, which is mainly a technique performed at the receiver for the purpose of correctly reconstructing the transmitted symbols.

The research work on equalization mainly started at around 1960 with the development of the zero forcing equalizers (ZFE). Moreover, the adaptive filter design and research on the equalization benefited from the work on the least mean square (LMS) algorithm proposed by Widrow and Hoff in 1960 [71], which was followed by the first adaptive equalization technique in 1965 [72]. LMS has a good performance in estimating the channel distortion,

however, in spite of the best training its tolerance to the dispersion was not acceptable, therefore, this led to the investigation of new techniques such as the maximum likelihood sequence estimator equalization (MLSE) [73] and its Viterbi implementation schemes [74] in 1970's.

The seventies and eighties witnessed the developments of fast convergence algorithms with low computational complexity, linear equalizers and linear filters with the transversal or lattice structure and adaptative algorithms such as the recursive least square (RLS), fast RLS, square-root RLS, and the gradient RLS [75, 76]. Nevertheless, the linear equalization techniques do not give accurate channel estimation when used for channels with deep spectral nulls. This is because of the nonlinear decision boundary problem [77, 78]. This problem can be solved using ANN, as ANNs are capable of forming the arbitrarily nonlinear decision boundaries to take up complex classification tasks [75, 79, 80].

ANN concept was first reported by MacCulloch and Pitts in 1943 [81]. However, the extensive theoretical studies on ANN were not reported by the growing community of researchers research until the early eighties [82, 83]. The original model of the present neural network was proposed by Rosenblatt in 1958 and was called the Perceptron. However, it was mimetically proven that the Perceptron does not have the have the capability to solve linearly non-separable problems, which requires identifying multi-dimensional data that are mutually unified [83-85].

In 1986, Rumelhart has proposed a learning algorithm called the back-propagation (BP), which was applied to the multilayer feed-forward neural network; this combination has the

ability to solve linearly the non-separable problems that could not be solved by the perceptron [67].

Hopfield network was introduced in 1984 as a connected recurrent neural network [67], at which input signals can pass through the network not only in the forward direction but also in the opposite direction. In 1995 Kohonen showed that a large amount of data can be automatically classified using neural network, where the neurons on the input and output layers are weighted with the weight parameters [84].

Neural networks have proven abilities and have been applied to various fields such as telecommunications, robotics, bioinformatics, image processing, and speech recognition, in which complex numbers (2 dimensions) are often used with the Fourier transformation [86, 87]. This indicates that complex-valued neural networks, whose parameters (weights and threshold values) are all complex numbers, are useful and necessary [88].

In 1971, in the former Soviet Union, Aizenberg proposed the first complex-valued neuron model, prior to this; most researchers outside Russia had assumed that the first complex-valued neuron model presented in 1975 by Widrow. Introduction of the complex neural networks has fuelled a growing research interest especially in the communication field. Since 1990's various types of neural network models have been proposed for communication systems [89, 90].

For standard equalization techniques, the process of equalization generally starts with modelling of the communication channel as an adaptive filter with a specific transfer function. This is followed by estimating the channel transfer function, thereafter attempts to

undo the effects of time-varying channel distortion [91]. The introduction of the ANN provided new forms of equalisers that are efficient compared to the existing techniques such as the MLSE conventional equalisers and adaptive filters. However, ANN equalizers had some drawbacks such as a slow convergence rate, which is a number of nodes and layers dependent process [91]. Therefore, Bayesian equalizers, which are based on the principle of the maximum a-posterior probability (MAP) were proposed [81] [92].

In the mid nineties researchers were working on producing a single layer, more efficient nonlinear ANN channel equalizers including the Chebyshev ANN [93], and the Functional link ANN [94, 95].

In modern communications, transmitting the signal phase and amplitudes are necessary, consequently high data rates are transmitted using high modulation formats such as QAM. In order to compensate for the channel impairments a complex ANN equalizer for QAM signals have been proposed [96]. Researchers have designed a complex MLP and extended the BP algorithm in the complex domain [97, 98].

Two approaches for the development of the complex ANN are discussed in [99]. The first one uses fully complex activation functions, which can satisfy a conflicting relationship between the boundedness and the differentiability of a complex function [99]. The second approach, which is adopted in this research, employs what is called the "split" complex activation functions, where two conventional real-valued activation functions process the in-phase and quadrature components.

A complex version of the resilient propagation (RPROP) has also been presented that is used for realistic mobile systems [88], and been applied in the GSM mobile channel. Performance comparisons made in terms of the bit error rates (BER) and the computational complexity has shown that the MLP network trained with the complex RPROP algorithm almost have the same BER performance as that of the MLP network trained with complex BP, but with the smaller computational load [88].

Research also have focused on producing learning algorithms with faster convergence, such as the Kalman filter (EKF), the unscented Kalman filter (UKF), and the natural gradient (NG) descent algorithms. Ibnkahla and Yuan [100] have utilized the NG descent algorithm for nonlinear satellite mobile channels moreover, have proved its superiority to the conventional BP algorithm.

Genetic algorithms and wavelet transforms can also be incorporated in the receiver before applying ANN in order to solve the local minimum problems associated with ANN and feature extraction tools [101]. Moreover, radial base function (RBF) has been applied to ANN in order to improve the non-linear classification associated with MLP. This is mainly achieved by replacing the sigmoid function of the ordinary MLP with a RBF. Nevertheless RBF based NN suffered from problems associated with the blind equalization, consequently; many techniques have been proposed for tackling this problem using RBF [102, 103].

More improved equalizer designs are available in the literature as unsupervised nonlinear blind equalization based on the fuzzy structure [104, 105]. Following the discussion on the need for ANN equalization, the next section outlines the ANN basic building block types and operating principles.

3.3 ANN Concepts

ANN is a mathematical model of massively connected parallel-distributed processors, made up of simple building blocks called neurons, which are based on the concept and behaviour of the biological neural networks. Behaviour wise ANN resembles the brain in two aspects which are as follow, firstly the neural network obtains information from the environment through a process called learning, secondly the acquired knowledge are stored by the synaptic weights which represents the inter-neuron connection strengths [69]. The technique which is used to perform the learning procedure is called a learning algorithm, which is also the function that is responsible of updating the synaptic weights of the network in a systematic manner in order to obtain a required design objective.

The ANN information learning capabilities made it suitable for solving complex problems and application such as nonlinear system identification, motor control, and pattern recognition. Furthermore, due to the large parallel interconnection between different layers and the nonlinear processing characteristics, adaptive ANN has the capability of performing nonlinear mapping between a set of inputs and an output space, therefore, the ANN is now predominantly used for equalization [106-109], finance [110], control system [111] , statistical modelling [112], and engineering applications [113] .

3.3.1 The Neuron

An artificial neuron, is built of a computing elements which perform summation of the input signal multiplied with the connecting weight, the weighted sum is thereafter is added with a

threshold called bias, the resultant signal is afterward is processed through a nonlinear activation function.

Each neuron is associated with three adjustable parameters during the learning process. These free parameters are the connecting weights, the bias and the slope of the nonlinear function. The neuron has N inputs $[x_i: i = 1, \dots, N]$, a weight w_i associated with each inputs and an output y. And a parameter known as the bias which can be considered as weight component associated with an input x_0, which is always fixed to a value of one. The neuron block diagram is shown in Fig. 3.1.

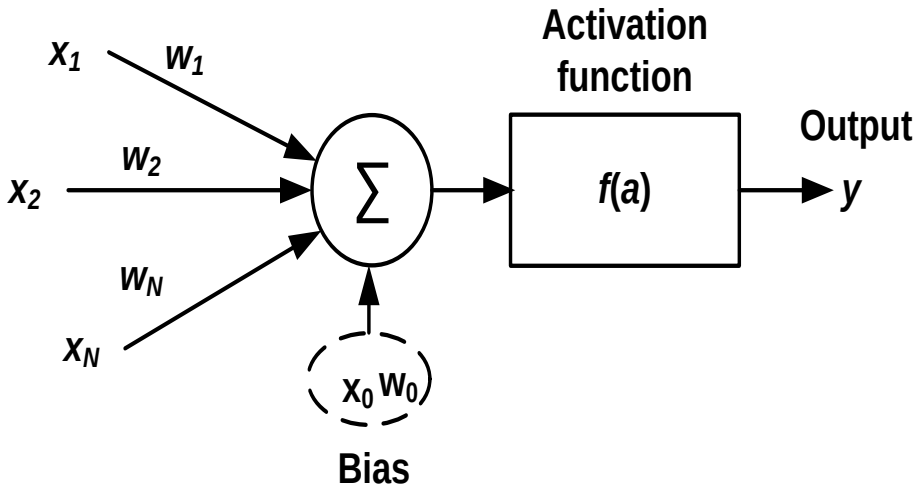

Figure 3.1: Artificial neural network neuron.

The output 'a' can mathematically be expressed as:

$$a = \sum_{i=1}^{n} x_i w_i. \tag{3.1}$$

Afterward the output y, which is a function of a, is given by:

$$y = f(a). \tag{3.2}$$

The activation or transfer function *f*(.) is application dependent and it is mostly required to be a differentiable function. Some popular activation functions are described below.

- **Linear function:** Defined as $y = ma$. For $m = 1$, the function is known as an identity function as the output is the exact copy of input.
- **Binary threshold function:** such as Hardlim: limits the activation to 1 or 0 depending on the net input relative to the some threshold function. Considering a threshold level of ζ, the output is given by:

$$y = \begin{cases} 1, & n \geq 0 \\ 0, & n < 0 \end{cases}. \tag{3.3}$$

The Hardlim function plot is shown in Fig. 3.2.

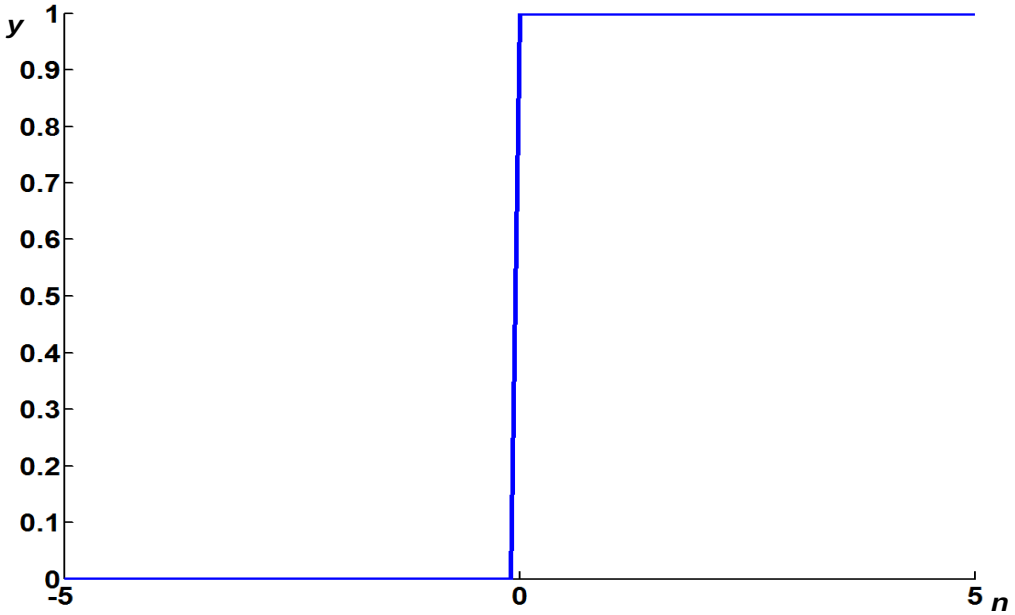

Figure 3.2: Hardlim function.

- **Sigmoid function *(logistic and tanh)*:** are some of the most widely used activation functions for pattern classification and nonlinear processing. The output of the log-sigmoid function is a continuous function in the range of 0 to 1 defined as:

$$y = \frac{1}{1 + e^{-n}} \tag{3.4}$$

Figure 3.3 represents a sigmoid function plot

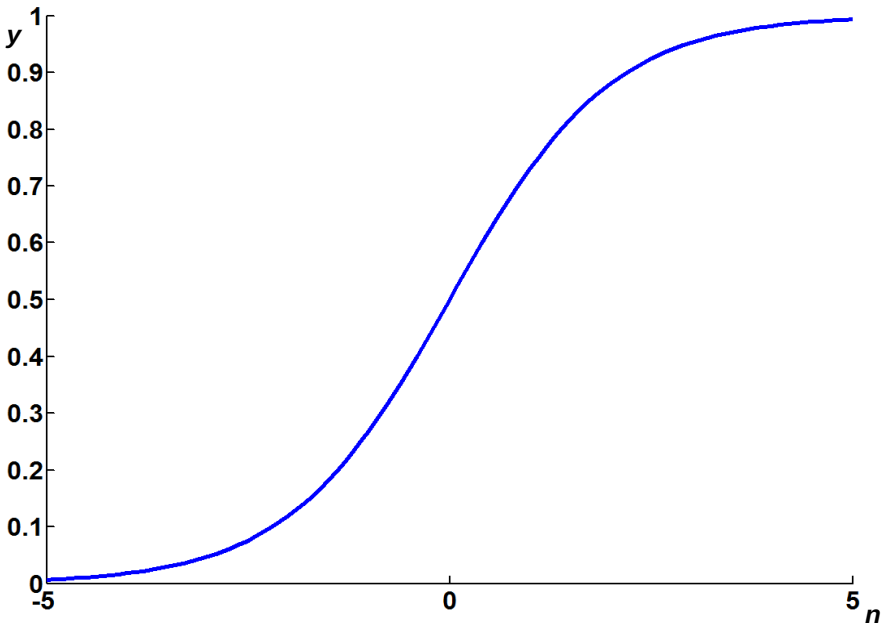

Figure 3.3: Sigmoid function.

The tan-sigmoid function is a variation of the log-sigmoid function as output ranges from -1 to +1, given by:

$$y = tan(n). \tag{3.5}$$

A neuron is limited to functionality of classifying only linearly separable classes [114]. However, ANN with many neurons can perform a complicated task like pattern classification,

nonlinear mapping. In fact, ANN's with sufficient number of neurons are universal approximators [115].

3.3.2 ANN Architectures

The neurons can be interconnected in different and complex forms, the manner is to arrange neurons in a single layer [34]. There are other topologies; the most common are described below briefly.

i. **Single layer feed forward network:** It contains only one output layer connected to single input layer (Fig. 3.4), where the neurons number at every layer is dependent upon the application number of inputs and outputs, but the network is strictly feed-forward, where the signal flows from the input layer to the output layer only. On the other hand, single layer networks have limited capacity, this is as this network has the classification capability only when the classes are linearly separable [114].

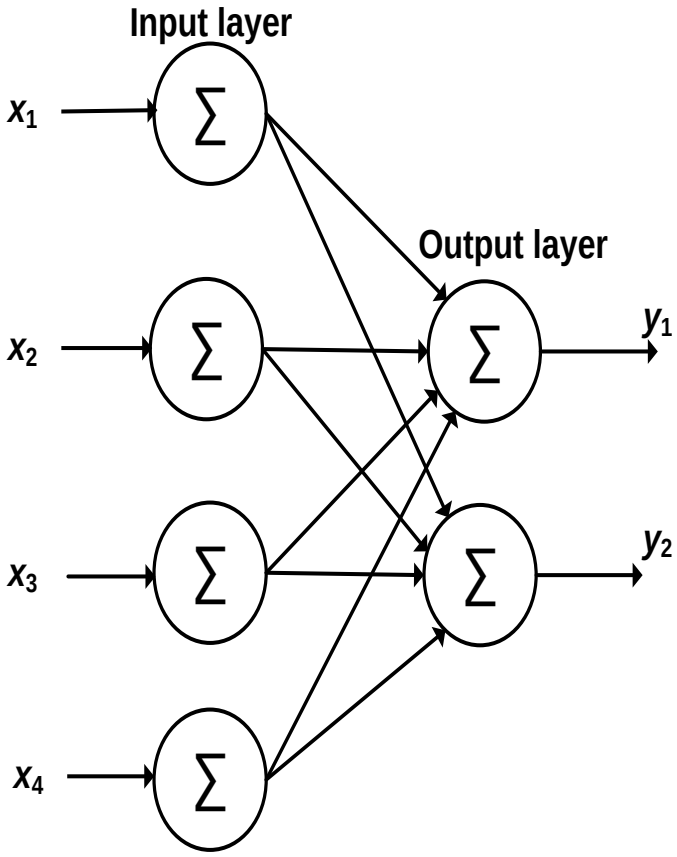

Figure 3.4: A single layer feed-forward network with 2 output neurons.

For application scenarios which requires a complex decision making, a single layer feed-forward network cannot achieve the designated tasks [115], consequently more than a single layer of a feed forward network, and more number of neurons is required to extract the higher order statistics of data [116]. Provided there are a sufficient number of neurons a two-layer ANN can be used as a universal approximator mapping any input-output data set [115].

ii. **Multilayer feed forward network:** Figure 3.5 shows a fully connected two-layer network. Every multilayer network consists of (i) an input layer with no processing taking place, thus not counted as part of a network layers, (ii) a hidden layer and (iii) an output layer.

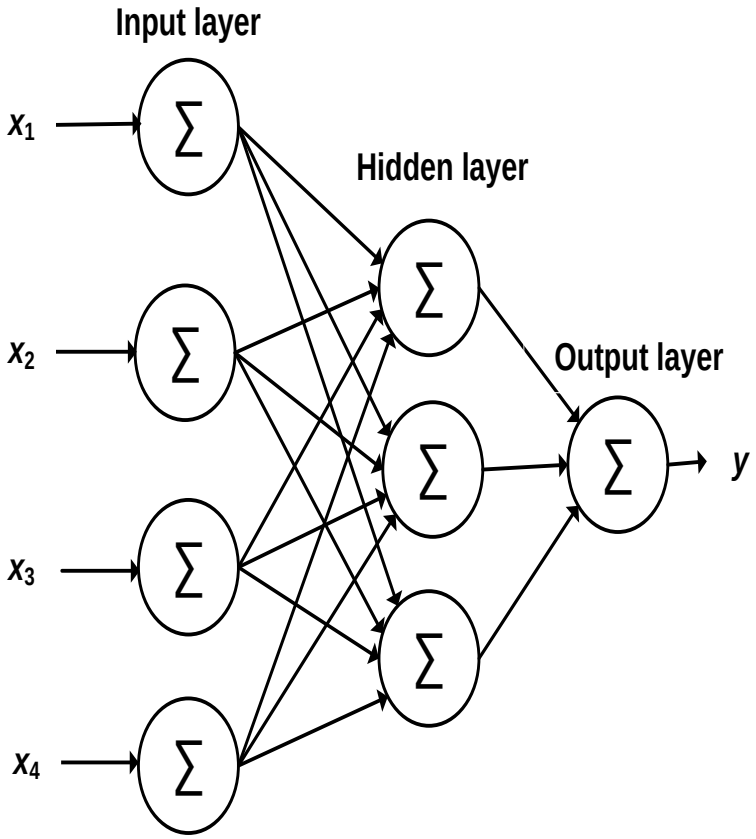

Figure 3.5: Fully connected feed-forward multilayer network.

iii. **Recurrent neural network (RNN):** Unlike multilayer network, the *RNN* output is feedback to the input layer as shown in Fig. 3.6. The network is mainly used in time-series prediction. Here network training is more complicated because of its chaotic behaviour [117]. Elman and the Hopfield networks are considered as common recurrent network architecture [117].

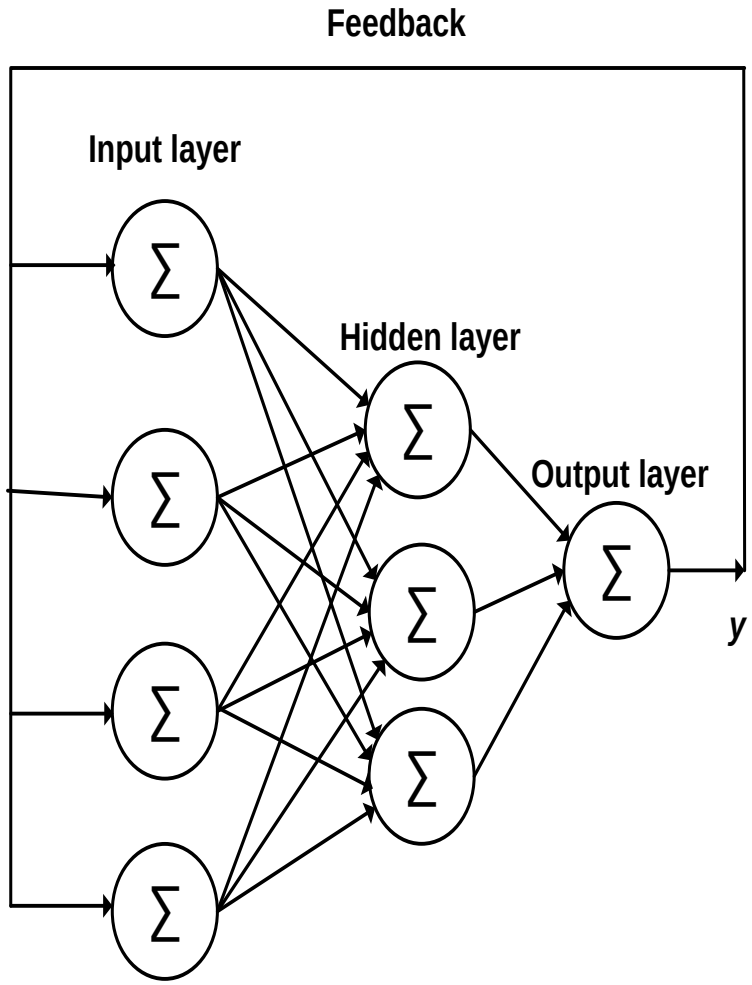

Figure 3.6: Neural network with feedback connection.

3.3.3 Training the Network

The ANN training process is performed by providing the network with the input data and the desired output data sets, thereafter the ANN can adjust its parameters such as the weights and bias based upon the input and the desired output, this is in order to minimize the difference between the training set and actual response of the network which is the instantaneous output. ANN training procedure depends on two main aspects, firstly the training data set, which should be representative of the task to be taught, as a poorly selected training set may increase the learning time. The second aspect is the training algorithm which is required to

minimize the cost function, which is the difference between the training set and actual response of the network. The convergence of cost function to the local minima instead of the global minimum has been a dilemma in ANN design, therefore, algorithms based on the adaptive learning can improve the learning rate as well as a convergence to the global minimum [118, 119].

The learning process can be categorized into two main methods, the first one is the supervised learning, at which the network is provided with the input and the output sets, so the ANN can adjust the weight and bias parameters until the cost function is minimized. The second learning method is the unsupervised learning or self-organization, which at the training set is not supplied and the network is trained to respond to clusters of pattern within the input, consequently, in the unsupervised learning paradigm, the ANN is assumed to discover statistically salient features of the input set [120].

For simplicity, in this research a multilayer feed-forward ANN with supervised learning algorithm is used as a SMF channel equalizer. The supervised learning is more suitable for the equalizer applications, this is because training sequence can be used to approximate channel more accurately [34]. A BP training algorithm, which is descriped below, is a popular example of a supervised training algorithm.

3.3.4 Back-propagation Learning

It was shown that a two layer feed-forward network can overcome some of the restrictions associated with the single layer network, however, did not solve the problem of adjusting the the ANN weights from input to hidden units. A solution to this problem was presented in

1985 by Parker, and by Rumelhart in 1986 [84]. The solution is based on the concept that the hidden layer units errors are determined by back-propagating the errors of the units of the output layer. This is reason why this method is often called back-propagation learning rule [84]. One of the advantages of the BP algorithm is that its hardware circuit can be easily realized [84].

The BP supervised learning algorithm is considered as the most popular training algorithm used for multilayer networks [84], where it adjusts the weight of the ANN to minimize the cost function $E(n)$:

$$E(n) = \|d(n) - y(n)\|^2. \tag{3.6}$$

In the BP algorithm, the weights are updated by applying gradient descent on the cost function; this is in order to reach a minimum. The weights are updated according to:

$$w_{ij}(n+1) = w_{ij}(n) - \eta \frac{\partial E(n)}{\partial w_{ij}(n)}, \tag{3.7}$$

Where w_{ij} is the weight from the hidden node i to the node j, and η is the learning rate parameter. When η is very small, the algorithm will take long time to converge, in contrast when is η very large; the system may oscillate causing instability [116].

The BP algorithm procedures can be summarized as [116]:

Step 1: Initialize the weights and thresholds to small random numbers.

Step 2: Present the input vectors, $x(n)$ and desired output $d(n)$.

Step 3: Calculate the actual output $y(n)$ from the input vector sets and calculate .

Step 4: Adapt weight based on (3.7).

Step 5: Go to step 2.

3.3.5 Multilayer Perceptron Network

Perceptron was practically demonstrated for the first time in 1958, that perceptron is a single level connection of McCulloch-Pitts neurons is called as single-layer feed forward networks [69], which has the ability of linearly classify input vectors into pattern of classes by a hyper plane. However, this type of network has problems in solving difficult tasks; therefore, this gave rise to the introduction of multilayer perceptron network (MLP), which is a network of connections between many perceptrons connected in layers; the input signal data propagates through the MLP layers in the forward direction, on a layer-by-layer basis. This network has been applied successfully to solve diverse problems.

Figure 3.7 shows a four layers MLP, in the figure s represent the inputs $[s_1, s_2, \dots, s_n]$ to the network input layer, and y_k represents the output of the final layer. The layers connection weights between the input to the first hidden layer is w_i, first to second hidden layer is w_{ji} and the second hidden layer to the output layer is w_{kj}. Therefore, the output signal at the final output layer of the MLP can be expressed as:

$$y_k = \varphi_k \left[\sum_{k=1}^{P_1} w_{k,j}\, \varphi_j \left(\sum_{j=1}^{P_2} w_{j,i}\, \varphi_i \left\{ \sum_{i=1}^{P_n} w_i\, s_i + b_i \right\} + b_j \right) + b_k \right], \tag{3.8}$$

Where P_1, P_2, P_n are the number of neurons in the MLP layers, b_i, b_j, b_k is the threshold to the neurons of each specific layer, and $\varphi(.)$ is the nonlinear activation function which is application dependent. The most popular activation functions are sigmoid and the hyperbolic tangent since there are differentiable functions.

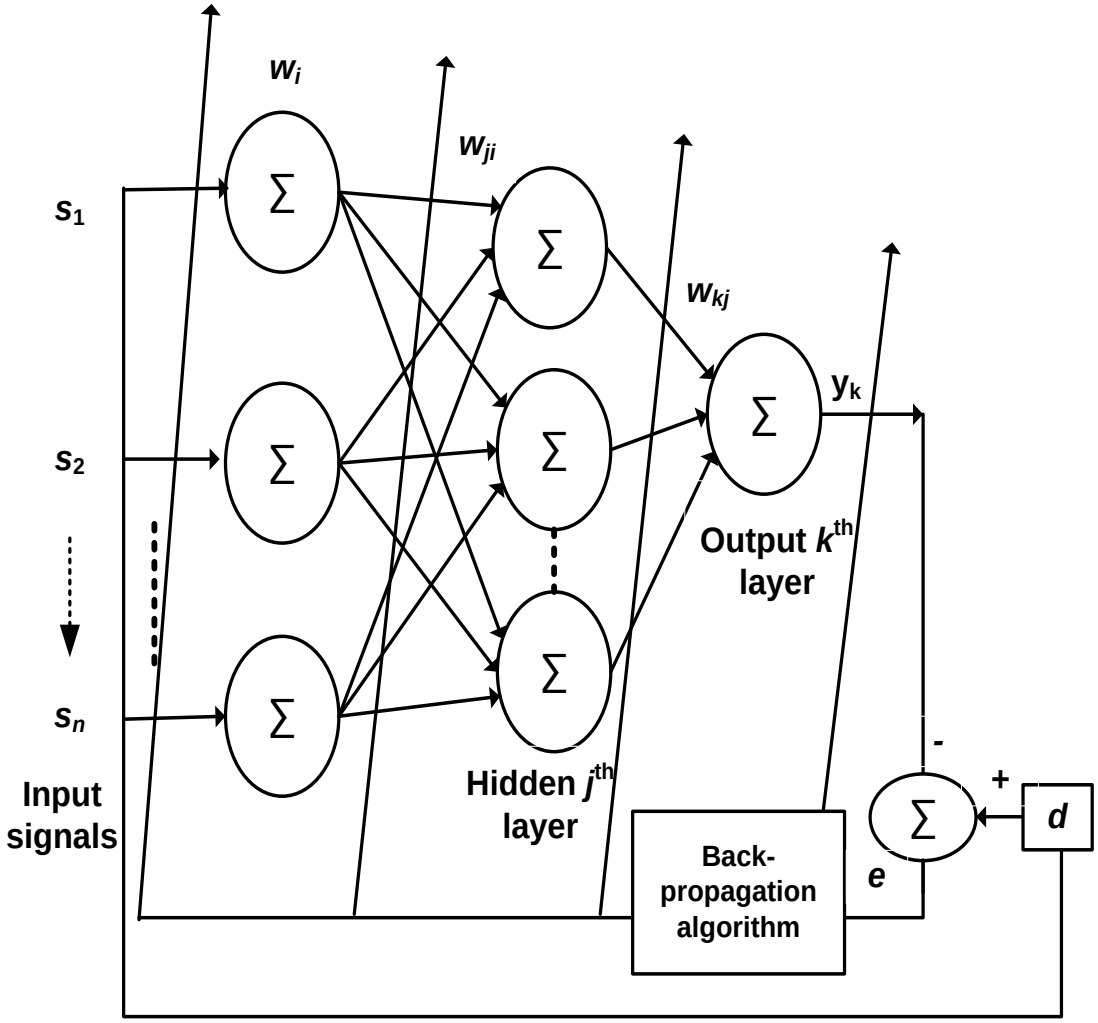

Figure 3.7: MLP network [69].

As a continuous learning process, the output signal of the output layer (y_k) is compared with the desired output (d) and the resulting error signal (e) is therefore obtained.

$$e_t = d(t) - y_k(t). \tag{3.9}$$

The instantaneous value of the total error energy, which is used to update the weights of the hidden layers and output layer, is obtained by summing all error signals over all neurons in the output layer, that is:

$$\xi(t) = \frac{1}{2}\sum_{k=1}^{P_3} e^2(t). \tag{3.10}$$

The updated weights therefore are:

$$w_{kj}(t+I) = w_{kj}(t) + \Delta w_{kj}(t), \tag{3.11}$$

$$w_{ji}(t+I) = w_{ji}(t) + \Delta w_{ji}(t), \tag{3.12}$$

$$w_i(t+I) = w_i(t) + \Delta w_i(t), \tag{3.13}$$

Where Δw is the change in the weights of each individual hidden layer, moreover the thresholds of each layer can also be updated similarly,

$$b_k(t+I) = b_k(t) + \Delta b_k(t). \tag{3.14}$$

$$b_j(t+I) = b_j(t) + \Delta b_j(t). \tag{3.15}$$

$$b_i(t+I) = b_i(t) + \Delta b_i(t). \tag{3.16}$$

Δb is the changes in thresholds of the hidden and input layers.

3.4 Adaptive Equalization

In communication channels, the transmission channel parameters are not known in advance and because of its time varying physical nature, it is very difficult for estimating both the

channel distortion and energy using the conventional equalization techniques. Thus, it is important to use an equalization process that is adaptive, in this scenario a training sequence is transmitted to approximate channel characteristics, means the equalizer needs to change its parameters such as weights and bias during the supervised training process according to the nonlinear changing environment and this is what is called adaptive equalization.

3.5 Conclusions

In this chapter, the history and main milestones in the ANN and ANN equalizers research have been reviewed, where the drawbacks of the traditional equalization techniques were highlighted. Due to its high performance when compared with the traditional equalizers, ANN equalizers have been utilized widely in the communication industry and in particular for the optical communication transmission compensation; Therefore in this chapter the concepts of ANN were discussed together with ANN different architectures, this includes the neuron architecture, and the most popular activation functions. Followed by a review of the ANN training processes and algorithms and MLP network which will be used as an equalizer in this thesis.

Chapter 4. Performance Comparison of CO-OOFDM and Fast-OFDM over AWGN Channel

4.1 Introduction

OFDM is a signal modulation technique that splits a high-speed data stream into a number of low-speed data streams transmitting simultaneously over a number of harmonically related narrowband sub-carriers [3]. OOFDM was proposed in 2005 [5], and since then significant advances have been made by utilizing adaptive modulation schemes [54, 56, 57, 63]. It has been shown that OOFDM is a promising scheme for providing a cost-effective and a high-speed solution with an excellent flexibility and robustness for practical implementation in access and local area networks. For such applications the IM-DD scheme has widely been adopted in practice for reducing the transmission link cost. For future high-capacity long-haul networks, a coherent optical transmission is an alternative option that could be employed. CO-OOFDM have been utilized for combating dispersion [121] and PMD [122] in long haul optical fibre communications.

A Tb/s data transmission over fibre has been realized using low speed electronics and optoelectronics through parallel processing of coherent optical frequency combs at both the transmitter and the receiver [17]. More over DCT based OFDM which is referred to as fast-OFDM (Fast-OFDM) schemes, which have been used to reduce the bandwidth requirement by the half when compared to the traditional OFDM system [30]. However, in published literatures very little, if at all, information is given on the optimum design for CO-OOFDM and Fast-OFDM modems.

Quantization and clipping effects of an ADC, one of the key components in OOFDM modems, which significantly limit the maximum achievable performance of coherent and IM-DD based OOFDM systems [57]. Very little work has been published on the design

optimization of coherent OOFDM/ coherent Fast-OFDM modems namely ADC quantization bits and the clipping ratio. In this chapter, the impact of the clipping and quantization effects on the performance of CO-OOFDM and coherent Fast-OFDM modems is investigated theoretically. To obtain generic design criteria the additive white Gaussian noise (AWGN) channel is considered here. The optimum design criteria in the presence of fibre nonlinearities will be reported in the next chapter. The rest of the chapter is organized as follow.

Section 2, is describing the principles of Fast-OFDM, Section 3 explores the Coherent Fast-OFDM modem design. Section 4 outlines results and analysis for of Coherent Fast-OFDM/CO-OOFDM performance in AWGN channel, which includes transmission, effect of clipping and equalization on the modem's performance. Performance comparison between CO-OOFDM and coherent Fast-OFDM is illustrated in Section 5, and finally the chapter is concluded in the Section 6.

4.2 Principle of Fast-OFDM

As mentioned previously, in OFDM multiple subcarriers with equal frequency spacing are used to form parallel data transmission [63]. Reducing the spacing between subcarriers in OFDM system, results in improved bandwidth efficiency. For this purpose, Rodrigues and Darwazeh have proposed the IDCT based OFDM (Fast-OFDM) [123]. In contrast to the conventional OFDM, Fast-OFDM uses half of the subcarrier spacing, which will result in an increase in the inter-symbol interference (ISI) between adjacent narrowband Fast-OFDM subcarriers [123]. Thus it is necessary to utilize single-dimensional signal modulation

formats such as m-array amplitude shifted keying (M-ASK), in order to reduce this effect [123].

Recently, Fast-OFDM has been effectively implemented experimentally for long haul optical fibre communications, where DCT is used for double-side band (DSB) signals [124]. Whereas for single-side band (SSB) signals the real-to-Hermitian symmetric property of fast Fourier transform (FFT)/inverse FFT (IFFT) is the preferred option [125, 126].

Fast-OFDM has also been used for upgrading already installed MMF communication links and the Ethernet backbone [127]. This is due to Fast-OFDM being cost effective and a high-speed solution requiring half the bandwidth compared with the conventional OFDM system with single-quadrature modulation formats using IM-DD. Moreover, ADCs are considered as one of the key devices in conventional OFDM systems that limits the maximum achievable data rate versus the distance performance [17]. It is also playing a crucial role in Fast-OFDM systems.

4.2.1 Definition of Fast-OFDM

Fast-OFDM is based on the OFDM principle with the advantage of having twice the bandwidth efficiency when compared with OFDM, where the frequency separation of the sub-carriers is $(1/2T)$ Hz, and T is the subcarriers time interval. This means that Fast-OFDM system will produce the same data rate as that of an OFDM, meanwhile requiring half of the bandwidth only. The complex envelope of a Fast-OFDM signal is given by:

$$S_{tx} = \sum_{k=-\infty}^{\infty} \sum_{n=0}^{N-1} a_{n,k} g_n(t - KT), \tag{4.1}$$

Where $a_{n,k}$ is the complex symbole transmitted on the n^{th} subcarrier, N is the number of subcarriers and g_n is the complex subcarrier which is expressed as:

$$g_n(t) = \frac{1}{\sqrt{T}} e^{j\frac{2\pi nt}{2T}}, \qquad t \,\epsilon [0, T]. \tag{4.2}$$

However, if phases of the subcarriers can be controlled, the minimum frequency spacing to achieve the orthogonality can be reduced to $1/(2T)$ [63]. Reducing subcarriers spacing to half means that, the information spectral density (ISD) is doubled, while keeping the same symbol rate per carrier.

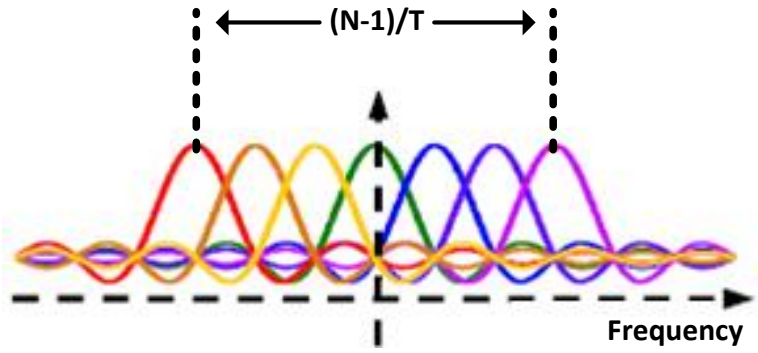

(a)

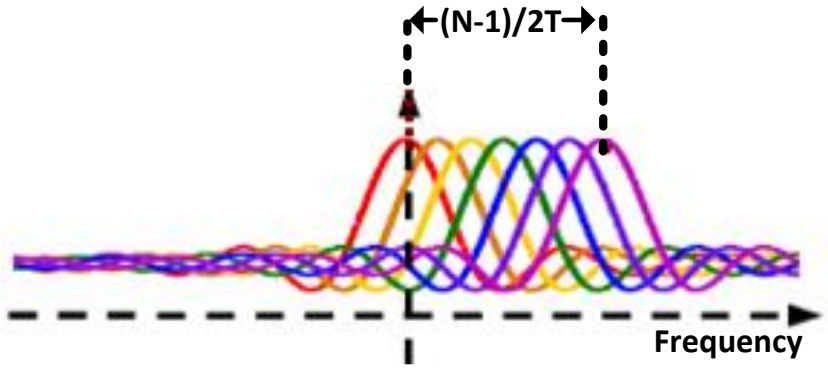

(b)

Figure 4.1: Frequency spectrum: (a) OFDM and (b) Fast-OFDM.

Figure 4.1 represents the frequency spectrum of the conventional OFDM and the Fast-OFDM. Notice how subcarriers are closely packed together in Fig. 4.1(b). Fast-OFDM mainly can deal with single dimensional modulation schemes such binary phase shift keying (BPSK) and M-ASK. This is because subcarriers orthogonality is only maintained for the real part of the Fast-OFDM signal but not for the imaginary part when the spacing is 1/(2*T*). This can be explained as follows [128]:

Consider two signals $s_1(t) = e^{j2\pi.f_1 t}$, and $s_2(t) = e^{j2\pi.f_2 t}$. Both signals have the signal duration *T* and their correlation coefficient ξ is defined as:

$$\xi = \frac{1}{T}\int_0^T s_1(t)\, s_2(t)^* dt = \frac{1}{T}\int_0^T e^{j2\pi.f_1 t}\, e^{-j2\pi.f_2 t} dt, \tag{4.3}$$

$$\xi = sinc[(f_1 - f_2)T].\, e^{j\pi(f_1 - f_2)T}, \tag{4.4}$$

Where,

$$sinc(x) = \frac{sin\,(\pi.x)}{\pi.x}. \tag{4.5}$$

Consequently, the real and imaginary parts of ρ are represented as:

$$\xi_r = Re(\rho\,) = sinc[(f_1 - f_2)T].\, cos\pi(f_1 - f_2)T = \frac{sin\,(2\pi(f_1 - f_2)T)}{2\pi(f_1 - f_2)T}. \tag{4.6}$$

$$\xi_i = imag(\rho\,) = sinc[(f_1 - f_2)T].\, sin\pi(f_1 - f_2)T = \frac{sin^2\,(2\pi(f_1 - f_2)T)}{\pi(f_1 - f_2)T}. \tag{4.7}$$

It can be understood from the (4.6) that ξ_r is zero when the$(f_1 - f_2) = N\frac{1}{2T}$, where N is an integer number, which means that the orthogonality is preserved for the real part as long as the frequency separation is 1/(2*T*). However, form equation 4.7 it can be seen that the orthogonality is only maintained for frequency spacing 1/*T*, which is only valid for OFDM but not Fast-OFDM [128].

4.3 CO-OOFDM and Fast-OFDM Modem Design

Figure 4.2 shows a system block diagram of a CO-OOFDM modem. As explained previously in Chapter 2, the encoded data is first mapped onto various OFDM sub-carriers, which are then converted into time domain symbols by using IFFT. After adding a prefix to each of these symbols, the generated new symbols are then serialized to form a long digital complex sequence. The real (I) and imaginary (Q) parts of such sequence are separated and subsequently applied to two DACs. The outputs are modulated using two MZMs biased at the null biasing point and a 90-degree phase shifter.

Finally, coherent optical signals are generated and coupled into an AWGN channel. The receiver is just a reverse of the transmitter. Based on such a diagram, numerical simulations for the CO-OOFDM are undertaken.

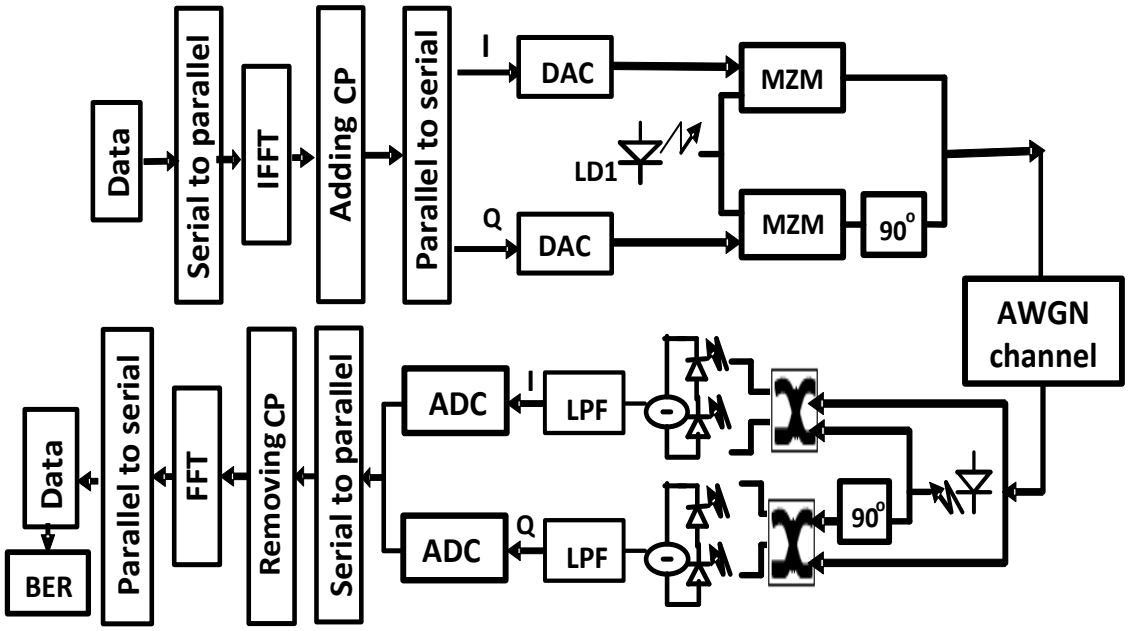

Figure 4.2: Coherent OOFDM modem system diagram.

For the second part of this chapter Fast-OFDM modem is used where the inverse discrete cosine transform (IDCT/DCT) is used instead of IFFT/FFT units. It should be noted that the input and output of DCT are real numbers, which will reduce the cost and design complexity of the system. Hence, only one DAC and two MZM units are required at the transmitter side. The rest of components used are the same as in the CO-OOFDM system, see Fig. 4.3 for the Fast-OFDM modem.

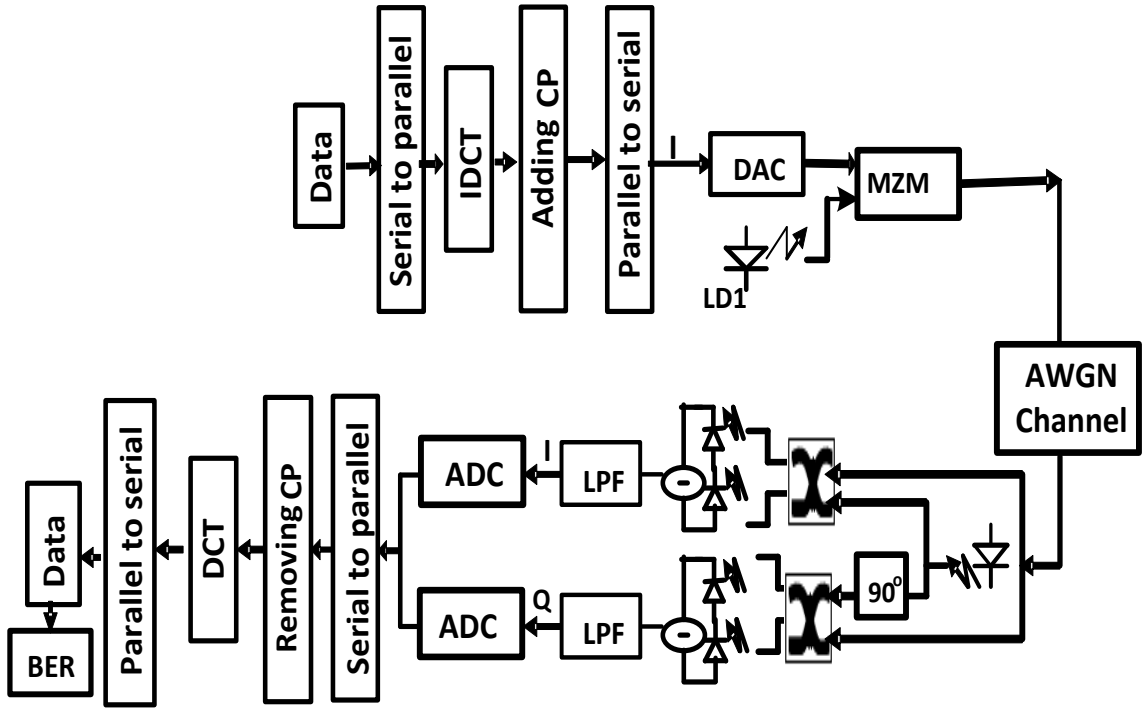

Figure 4.3: Coherent Fast-OFDM modem diagram.

4.4 Results and Analysis

In simulations, 64 sub-carriers are used, with identical modulation formats adopted from DBPSK, DQPSK and 16-QAM to 256-QAM for the CO-OOFDM modem, moreover for the coherent Fast-OFDM modem simulation a single dimensional modulation format such as the 4-ASK, 8-ASK, and 16-ASK are utilized [129]. The modem contains ADCs with a fixed sampling rate of 12.5 GS/s, and a variable quantization bits and clipping ratios.

The parameters mentioned above (the number of subcarriers and ADC sampling speed) give a sub-carrier bandwidth of 12.5 GHz/64 ≈195 MHz, a total symbol length of 7 ns, of which a 1.6 ns is occupied by the cyclic prefix, for the giving sampling rate signal bit rate of 10 Gb/s, 20 Gb/s, 40 Gb/s, 50 Gb/s, 60 Gb/s, 70 Gb/s, and 80 Gb/s, for the DBPSK, DQPSK, 16-

QAM, 32-QAM, 64-QAM, 128-QAM, and 256-QAM, respectively. And 20 Gb/s, 30 Gb/s, 40 Gb/s for 4-ASK, 8-ASK, and 16-ASK while using Fast-OFDM.

4.4.1 CO-OOFDM Performance in AWGN Links

4.4.1 Performance of CO-OOFDM in AWGN Links

Figure 4.4 shows the back-to-back performance of a CO-OOFDM modem subject to AWGN without considering the quantization and clipping effects. It can be seen that higher order modulation format requires higher optical SNR at 0.1 nm to achieve a specific BER performance. The OSNR required for achieving a BER of 10^{-3} when using the 16-QAM modulation format is 10 dB and it is 22 dB when 256-QAM are used for the same BER value. The simulated performance agrees with the analytical results in [3], confirming the validity of the proposed model.

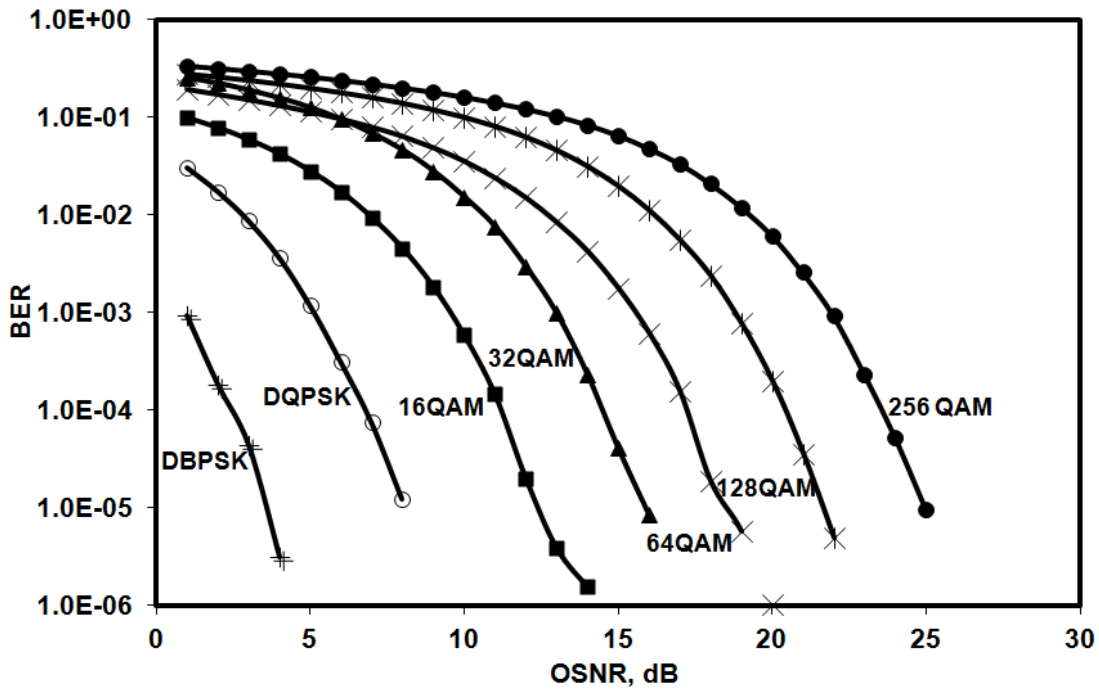

Figure 4.4: Back-to-back BER performance of the CO-OOFDM modem for (DBPSK, DQPSK, 16-QAM, 32-QAM, 64-QAM, 128-QAM, and 256-QAM).

4.4.1.2 Quantization and Clipping Effect on CO-OOFDM

The impact of the quantization effect on the modem performance over AWGN channel is shown in Fig. 4.5, where the clipping ratio is chosen to be effectively large, so that the clipping noise can be neglected. It can be seen from Fig. 4.5 that the use of small quantization bits will result in a high quantization noise, leading to a high minimum OSNR required for achieving a BER of 10^{-3}. On the other hand, increasing the quantization bits will decrease the minimum OSNR reaching the saturation region. Over the optimum quantization bit region the quantization noise is negligible, as the corresponding minimum required OSNR is almost identical to that obtained for the back-to-back link, see Fig. 4.4. In addition, the optimum quantization bits are also modulation format dependent, resulting from the non-Gaussian nature of the quantization noise.

From Fig. 4.5, it can be seen that for a given modulation format such as DBPSK, using a low quantization bit such as 3 will require an OSNR of 9 dB to achieve a BER of 10^{-3}. However when larger valued quantization bits, such as 6 or more, are used the minimum OSNR value is 1 dB, which is identical to that obtained for achieving a BER of 10^{-3} for the back to back case

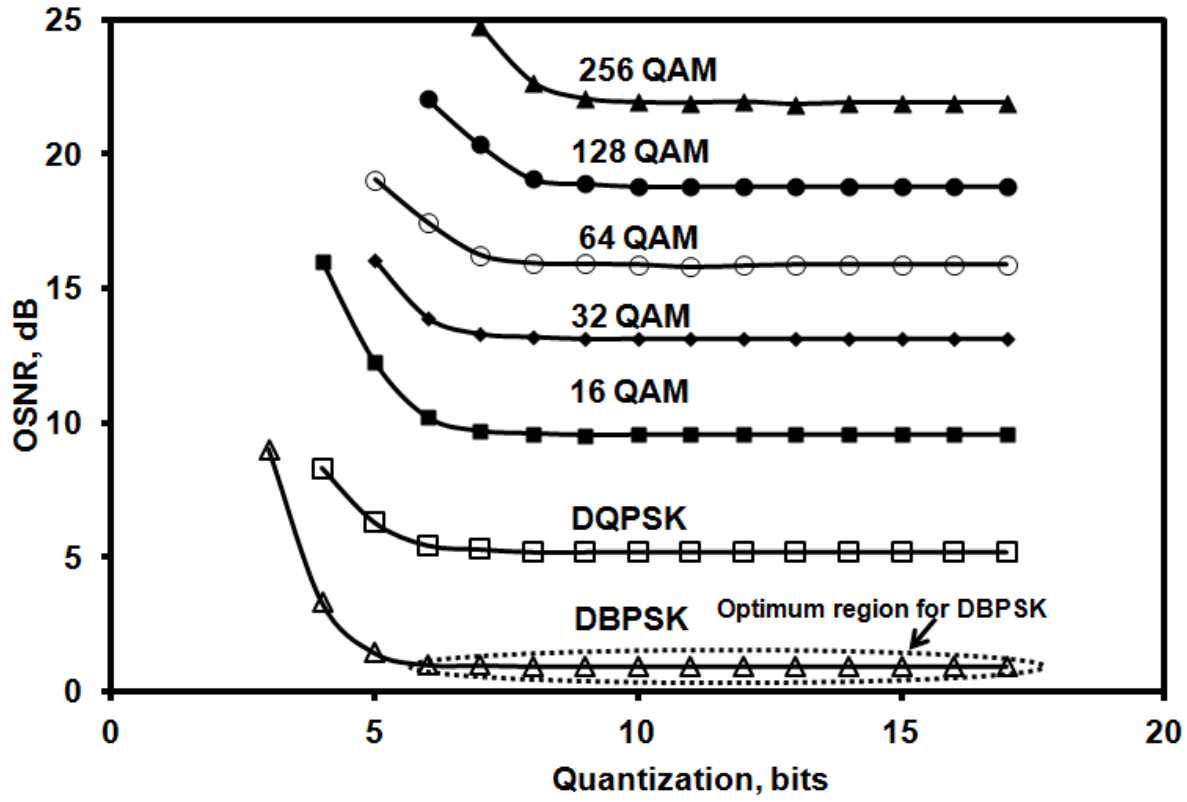

Figure 4.5: OSNR versus the quantization bits for a range of modulation schemes.

The clipping ratio effect on the modem performance over the AWGN channel can be seen in Fig. 4.6, where the quantization effect is eliminated by setting quantization bits to significantly higher values. It can be seen from Fig. 4.6 that, for a given signal modulation format such as DBPSK, using low clipping ratios (<10), will result in increased clipping noise level, thus leading to increase of OSNR. The minimum OSNR increases sharply for very larger values of clipping ratio (>30 dB). This is due to the increase in the quantization dynamic range and thus the quantization step size. Therefore, there exists an optimum clipping ratio which is signal modulation format dependent, it can be noticed that for the case of DBPSK the optimum clipping ratio exists in the region between (10 dB – 30 dB) at which the minimum OSNR is identical to that obtained for a BER of 10^{-3} for the back-to-back case. Similar to the behaviours observed in Fig. 4.5, the clipping noise is also negligible over the identified optimum clipping ratio region.

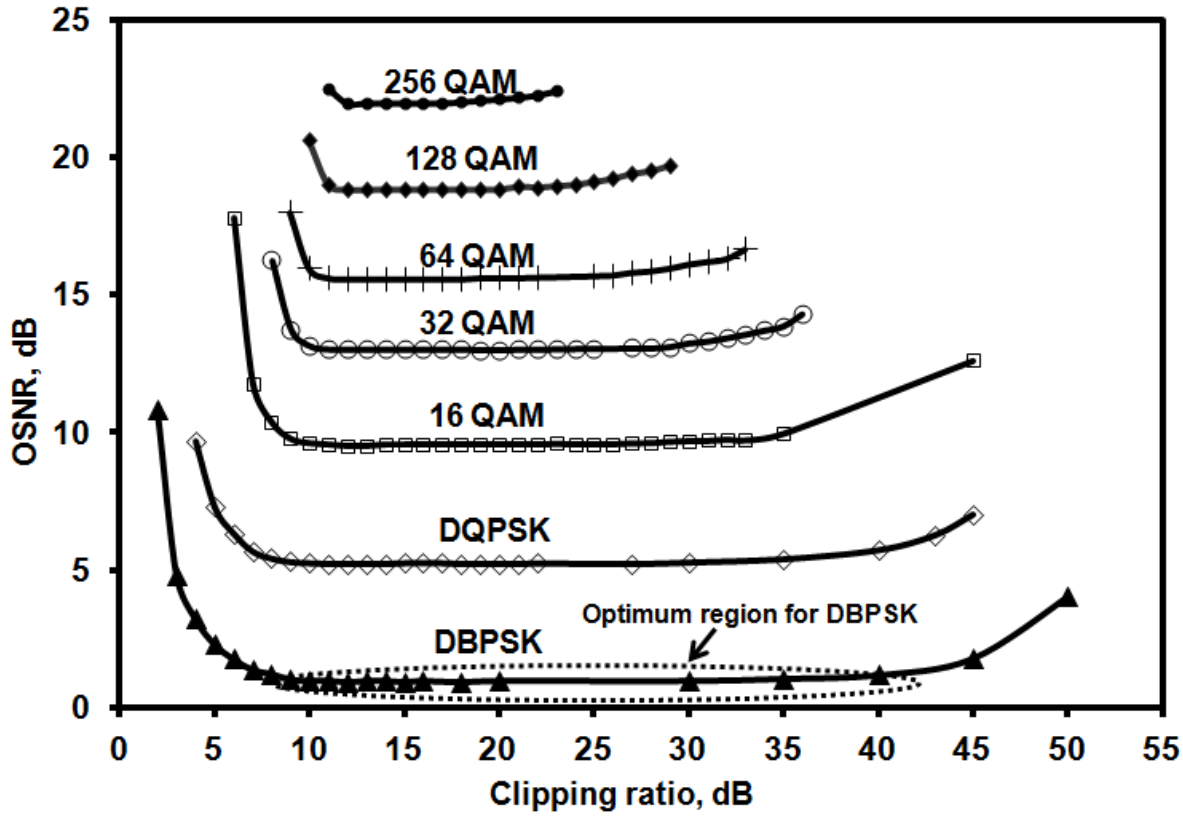

Figure 4.6: The minimum required OSNR against the clipping ratio for a range of modulation schemes.

4.4.2 Coherent Fast OFDM Performance in AWGN Links

4.4.2.1 Performance of Coherent Fast OFDM in AWGN Links

Under the same conditions of Fig.4.4, Fig. 4.7 shows the performance of Coherent Fast-OFDM and CO-OOFDM for a single dimensional array (M-ASK) under the AWGN channel. It can be seen that for a given modulation format, OFDM requires lower OSNR when compared with that required for achieving the same BER for Fast-OFDM. For OFDM system the OSNRs required for achieving a BER of 10^{-3} are 12.6 dB, 18.5 dB, and 24 dB for 4-ASK, 8-ASK, and 16-ASK, respectively and 13 dB, 19.5 dB and 25.3 dB for the same modulation formats when

Fast-OFDM modem is used. Consequently, 1 dB of penalty can be noticed when using Fast-OFDM. This is because Fast-OFDM subcarriers are closely backed together with less spacing if compared to the conventional OFDM subcarriers.

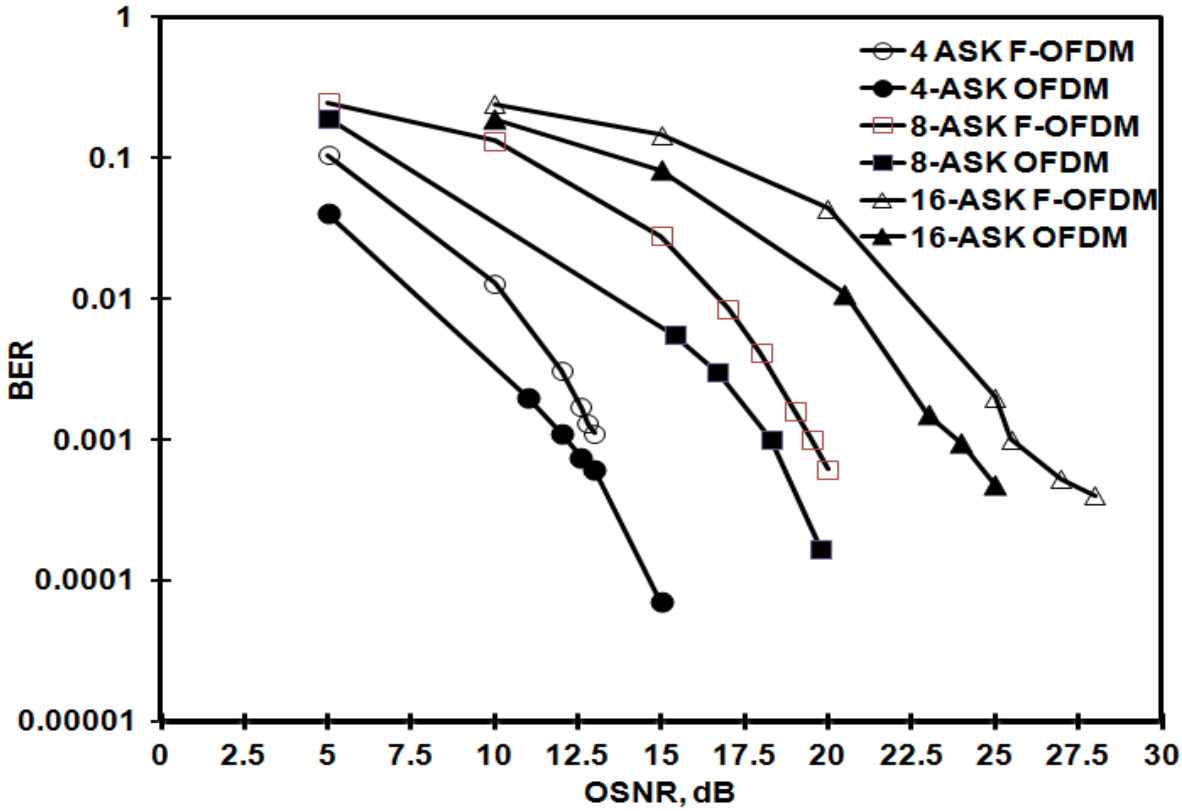

Figure 4.7: Back-to-back BER performance of the coherent Fast-OFDM modem for a range of modulation schemes.

4.4.2.2 Quantization and Clipping Effect on Fast-OFDM:

Fig. 4.8 represents the quantization effect on the performance of Fast-OFDM modem for arrange of modulation formats. The simulation results in this section obtained while fixing the OSNR to that required for achieving a BER value of 10^{-3} for the back-to-back case. it can be seen that, for a given modulation format, lower quantization bit values will give rise to a high quantization noise, thus higher BER value, moreover, using higher number of bits reduces the

quantization noise until a negligible quantization noise is reached over the flat region of the curve at which the optimum quantization bit is reached. From Fig. 4.8 it can be seen that for the 4-ASK modulation format using a quantization bit of < 7 will give rise to a BER of > 10^{-3}.

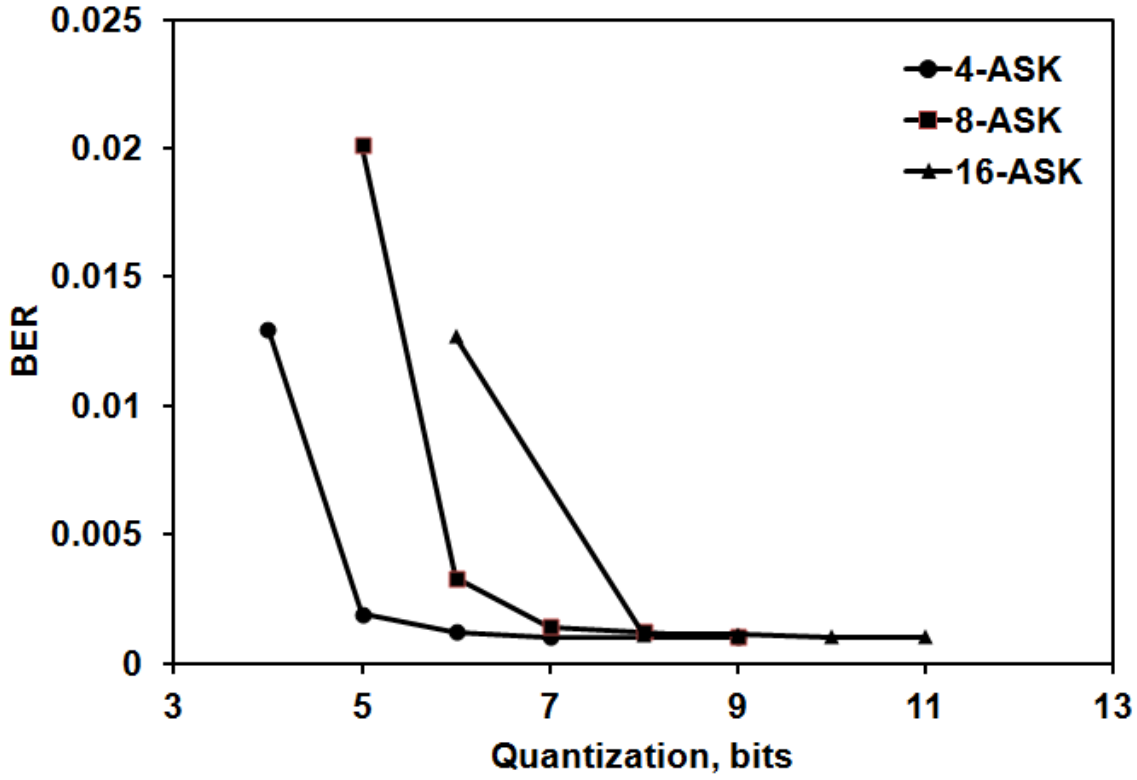

Figure 4.8: The BER performance against the quantization bits for a range of modulation schemes.

Similarly, Fig. 4.9 shows the effect of clipping for different modulation formats. The results were obtained while using a large quantization bit in order to effectively reduced or eliminate the quantization noise. This is fine for every signal modulation format when the minimum OSNR is used. When the ADC clipping ratio increases gradually it give rise to a negligible clipping noise over the flat region. It can be seen that (10 dB to 13 dB) can be considered as the optimum clipping ratio for the Fast-OFDM modem.

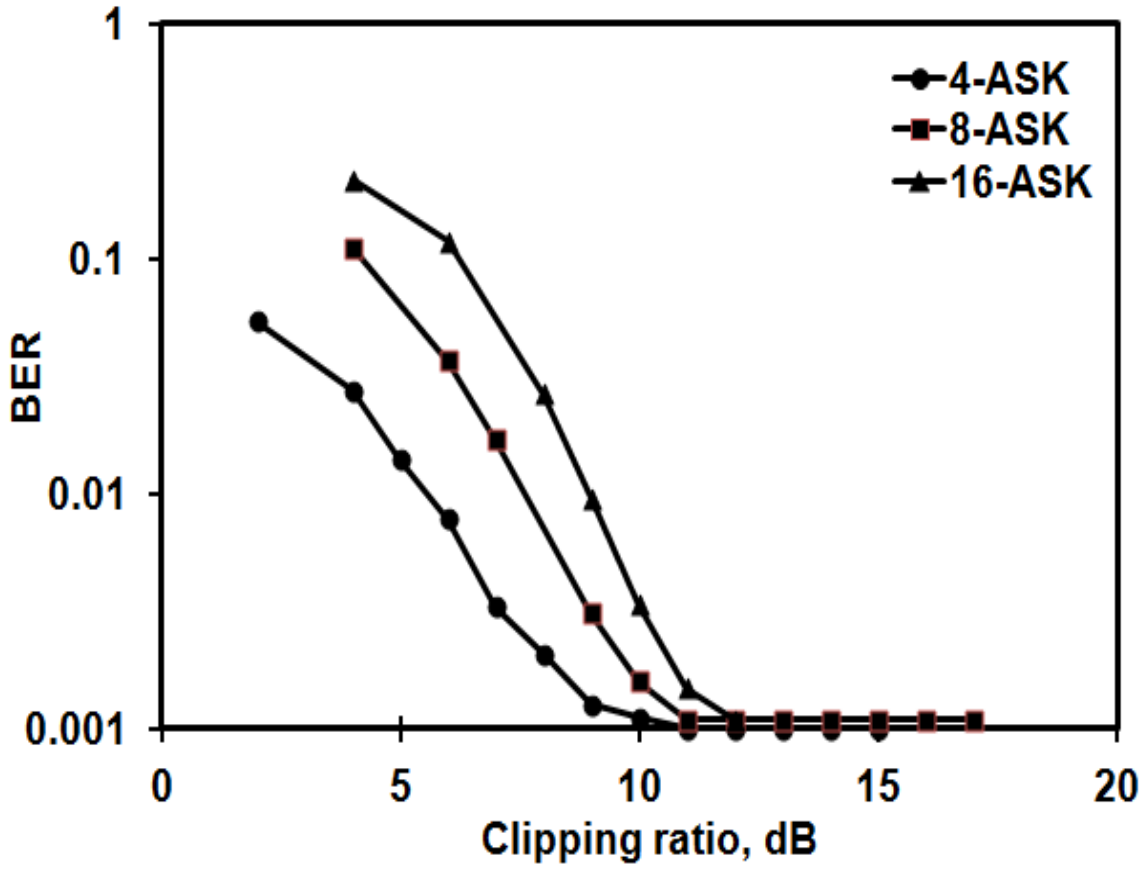

Figure 4.9: The BER performance against the clipping ratio for a range of modulation schemes.

4.5 CO-OOFDM versus Fast OFDM in The Presence of Fibre Dispersion Only

Having discussed and compared the performance of Fast-OFDM with OFDM in the AWGN channel, in this section the performance of the two modems in the presence of the SMF dispersion only is discussed. As can be seen from Fig. 4.10, that for a given BER value the conventional OFDM is more effective in combating the CD than Fast-OFDM.

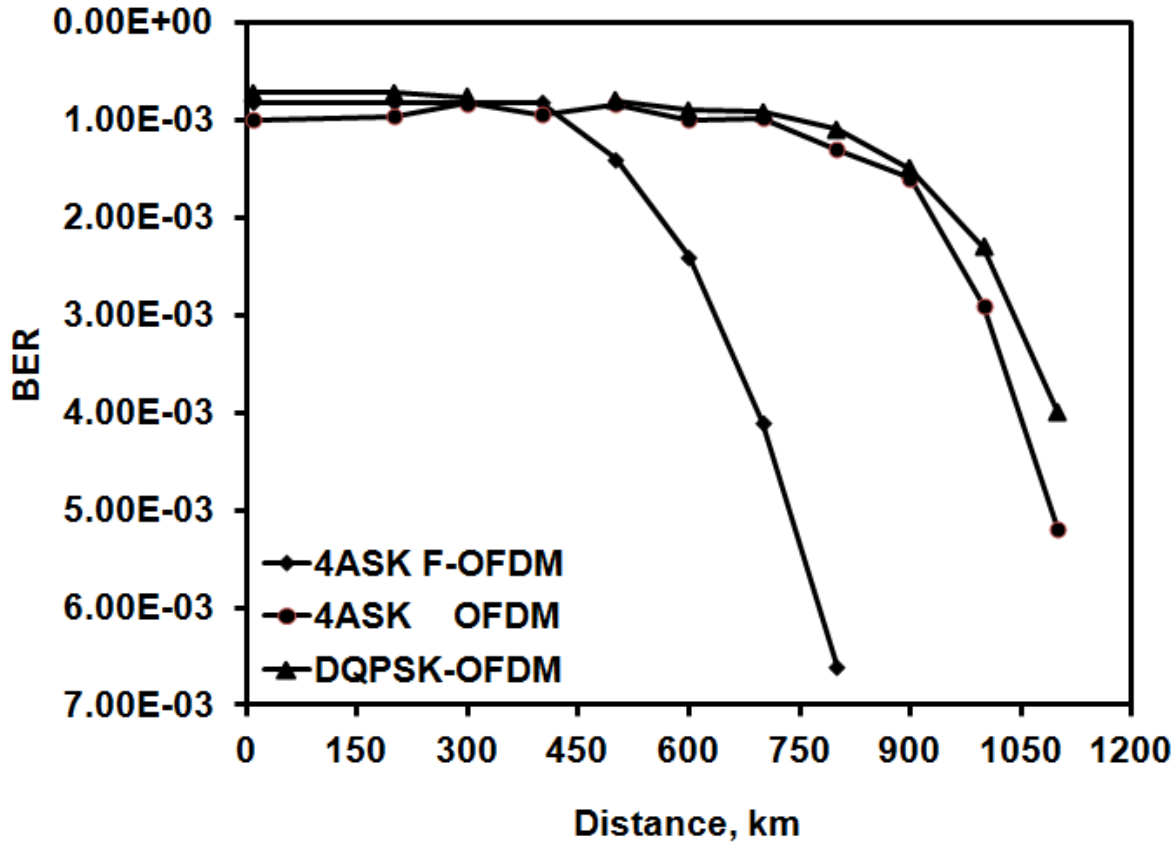

Figure 4.10: The BER performance against transmission distance for an OFDM and Fast-OFDM.

This is because Fast-OFDM backs the subcarriers closely together which makes them more susceptible to ISI effects. Moreover, the CP based guard interval (GI) cannot enable the ideal CD compensation using the one-tap equalizer. One solution is to use frequency or time domain equalization schemes before channel de-multiplexing. This however, increases the implementation complexity [127].

Moreover, it can be noticed from Fig. 4.10 that 4-ASK has the same performance as the DQPSK when using the OFDM modem. This is because both modulation techniques have the same number of constellation points, thus equal power distribution within the constellation domain. The 4-ASK Fast-OFDM constellation diagram at the transmitter is shown in Fig.

4.11, and thereafter at the receiver after propagating through 700 km of SMF when considering CD only is shown at Fig. 4.12. It can be seen from Fig. 4.11 and Fig. 4.12, that the transmitted data points are rotated to the right side of the constellation diagram due to the dispersion effect, this effect can be reversed using pilot tone or other type of equalizer.

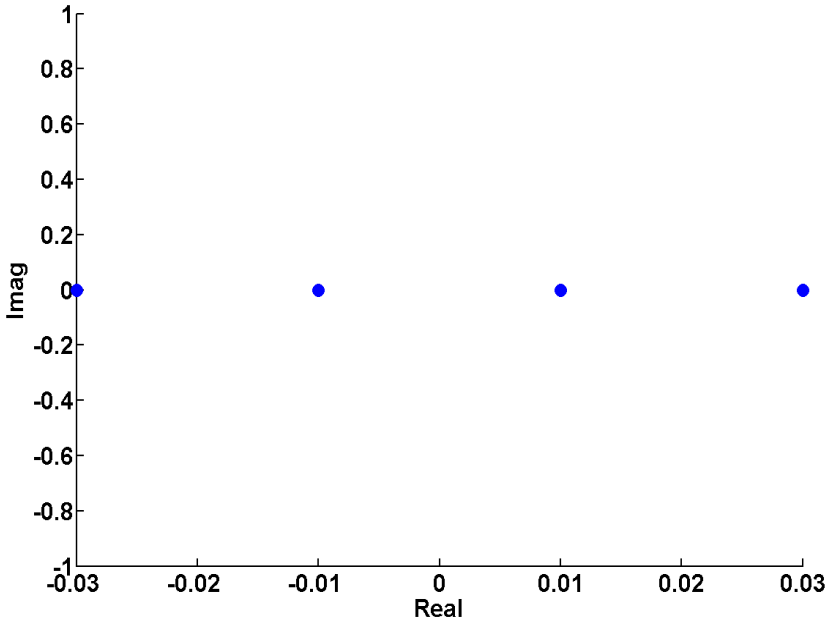

Figure 4.11: Fast-OFDM 4-ASK transmitted data constellation diagram.

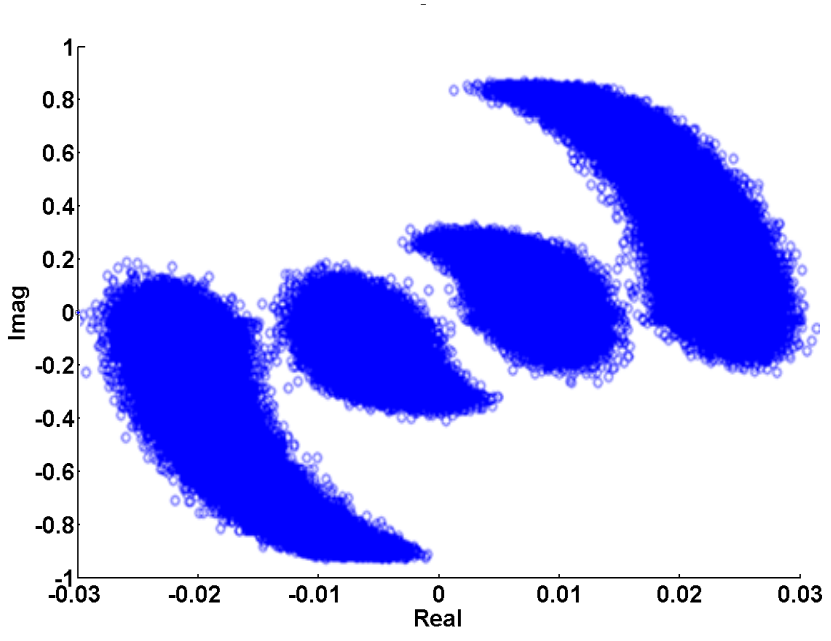

Figure 4.12: Fast-OFDM 4-ASK received constellation diagram for a link with dispersion.

4.6 Conclusions

For CO-OOFDM and Fast-OFDM modems, optimum clipping ratios and quantization bits have been identified for various modulations formats 256-QAM and M-ASK formats up to 16-ASK for the Fast-OFDM modem. These optimum ADC parameters are modulation format dependant, under which the clipping and quantization noises are negligible. This work is useful for the practical design of the optimum CO-OOFDM modems. Fast-OFDM offers reduced complexity in the DSP domain with the use of DCT and simple single-quadrature modulation formats when compared with the conventional OFDM. OOFDM is more resilient to fibre dispersion if compared to the Fast-OFDM modem; however, Fast-OFDM can be used in different applications where bandwidth can be traded with the distance.

Chapter5. Performance Analysis for CO-OOFDM Modems for SMF-Based Links

5.1 Introduction

In recent years, we have seen a growing interest in application of OFDM in mobile communication systems and networks. OFDM is a robust, cost effective, and a flexible scheme with high resilience to multipath induced inter-symbol interference (ISI), thus offering an improved transmission performance [3]. In [7, 130, 131] its optical version i.e. Optical OFDM (OOFDM) has been adopted for high-speed long haul optical fibre communication links to combat fibre-induced CD, PMD, and a high spectral efficiency. According to its applications, OOFDM can be subcategorized in to two main groups; (i) the IM-DD used in local and access networks [132], and (ii) CO-OOFDM which is utilized in long and ultra-long haul optical networks offering superior performance in spectral efficiency, receiver sensitivity and PMD [11].

The main challenges for high-speed long distance optical communication systems are the CD and fibre non-linearities. To address these technical challenges, especially for the CO-OOFDM modem a number of CD compensation schemes has been proposed. In [21] and [22] transmission of OSSB signals, which ensure transfer of optical phase into the electrical domain, allow linear electronic filters to be used for CD compensation. Several digital signal processing based schemes including EPD at the transmitter [24], the maximum likelihood sequence estimation (MLSE) [133] as well as the coherent phase and polarisation diversity reception [134] have been adopted for CD compensation. In long-haul optical system fibre non-linearity is a major problem, unless the optical power is kept at a low level [135].

Electronic pre-compensation approach has been applied for the compensation of fibre nonlinearities [136] and for PMD [137]. In [8] a simple signal processing at the transmitter in CO-OOFDM system adopted for CD compensation has been used to mitigate fibre non-linearities. A careful management of these effects leads to a successfully experimental demonstration of 20Gb/s CO-OOFDM signal transmission over 4160km SMFs using sub carriers multiplexing technique[134].

In WDM systems, the spectral efficiency is an important factor. In optical OFDM schemes, which are essentially an optical equivalent of the RF OFDM, the spectral efficiency of ~1 bit/s/Hz, in principle, could be achieved by utilizing the orthogonality between the spectral profiles of each channel. In [121], [138] it has been shown that a CO-OFDM modulation format employing a CP can tolerate fibre CD equivalent to 3,000 km standard SMF, and is also robust against the 2^{nd} order PMD.

In all the CO-OOFDM work published previously, the impact of key CO-OOFDM modem design parameters has, however, not been reported on the transmission length versus capacity performance of CO-OOFDM signals over SMF links. These parameters include, for example, the CP length, number of sub-carriers, sampling speed, quantization bits and clipping ratio associated with ADCs, and the modulation format type used for each individual subcarrier. All these parameters play significant roles in determining the maximum achievable transmission performance of CO-OOFDM modems.

Firstly, considering the physical nature of CP, it is clear that, if a CP time duration is smaller than the CD associated with a SMF link, the imperfectly compensated dispersion effect limits considerably the maximum achievable transmission performance of the CO-OOFDM signals.

In addition, a shorter length CP may also affect the sub-carrier orthogonality, resulting in a significant increase in the minimum required OSNR for a specific signal modulation format being taken on a sub-carrier [3]. On the other hand, if the CP is longer than the CD of the SMF link, for a fixed signal sampling speed, the CP wastes a large percentage of the transmitted signal power, giving rise to a degraded effective signal OSNR.

Secondly, for a given ADC, a large number of sub-carriers within one CO-OOFDM symbol increase the time duration of the CO-OOFDM symbol and thus the time duration of the CP. This gives rise to the enhanced dispersion tolerance, thus leading to the improved transmission performance. However, this also decreases the frequency spacing between adjacent sub-carriers, fibre nonlinear effects may; therefore affect the orthogonality between sub-carriers, thus leading to transmission performance degradation. Therefore, it is expected that there exists an optimum number of sub-carriers for a specific application scenario.

Thirdly, it is widely known that ADC have a wide range of sampling speeds, where low sampling rates can will increase the CD tolerance. However, considering fibre nonlinear effects, the sampling speed can affect the spacing between adjacent CO-OOFDM sub-carriers, which may affect sub-carriers orthogonality.

Fourthly, given the fact that CO-OOFDM signals suffers from the large PAPRs, which make the CO-OOFDM modems more sensitive to fibre nonlinearity. Similar to IM-DD OOFDM cases [9, 57], it is therefore expected that signal clipping and quantization associated with an ADC (DAC) are also crucial for determining the maximum achievable transmission performance of the modems.

The ADC is one of the crucial devices for the OFDM real-time implementation. ADCs and digital-to-analogue converters (DACs) sampling speeds, signal clipping and quantization levels affect the system tolerance to the CD and the overall system performance. In [10] it is shown that a combination of an adaptive modulated OOFDM and an adaptive CP can improve the transmission performance over multimode fibre links for the IM-DD OFDM schemes. However, adopting identical modulation formats for all CO-OOFDM sub-carriers may result in some sub-carriers suffering from higher distortion level than the others, because of the frequency response of the SMF link. Therefore, it is advantageous to employ dissimilar modulation formats on each subcarrier depending upon the link frequency response. However, the effects of CO-OOFDM modem parameters (i.e. number of sub-carriers, CP length, sampling speed and adaptive modulation) on the CD compensation tolerance for SMF links and transmission performance over SMF links has not been reported by the researchers. Finally, this chapter investigates the capability of the adaptive modulated CO-OOFDM schemes for compensation of the CD and fibre non-linearities. Moreover, CO-OOFDM mentioned above parameters impact on the CD tolerance for CO-OOFDM signal transmitted over a SMF link for different modulation schemes is also investigated.

In this chapter, numerical simulations are undertaken to investigate thoroughly the impact of the number of sub-carriers, CP length, sampling speed and ADC parameters on the modem performance over SMF links. It is shown that, an increase in the number of sub-carriers is more effective in combating CD, when compared to CP with a longer length. Moreover, in the presence of SMF non-linearities an optical power independent optimum number of subcarriers of 64 within one CO-OOFDM symbol is identified with and without utilizing the non-linearity compensation algorithm, optimum ADC parameters are shown to be dependent upon transmission distance for different data rates. In addition, for a fixed symbol length

reducing the sampling speed increases the system CD tolerance, however, in the presence of non-linearities this will result in a negative effect due to the reduction in the subcarriers spacing.

The present chapter is organized as follows: in Section 2 the CO-OOFDM modem model used in numerical simulations is outlined, along with the adopted system parameters. In Section 3, investigations are undertaken of the optimization of ADC parameters over SMF links. In Section 4, the effects of the number of sub-carriers and length of CP on the transmission performance of CO-OOFDM modems are explored based on which optimum modem parameters are obtained for different optical launch power also with and without non-linearity compensation. Moreover, in Section 5 the effect of sampling speed on the transmission performance is investigated based on transmission over SMF links. Section 6 investigates the effect of adopting adaptive modulation, which is proven to be effective in compacting fibre dispersion and non-linearity in IM-DD systems [35], on the performance of CO-OOFDM systems transmission over SMF links. Finally, the chapter is summarized in Section 7.

5.2 System Model

Figure 5.1 shows a top-level block diagram of a CO-OOFDM modem adopted in the numerical simulation. At the transmitter side, complex valued data streams are passed through a serial-to-parallel (S/P) converter producing a $N \times 1$ vector X_n prior to being mapped into N_d constellation symbols $\{X[k]\}_{k=0}^{N_{d-1}}$ using a number of modulation schemes including, differential binary phase shift keying (DBPSK), differential quadrature phase shift keying (DQPSK), 16-QAM, 32-QAM, 64-QAM, 128-QAM, and 256-QAM. The data symbol is

converted into a time domain CO-OOFDM symbols by N orthogonal sub-carriers by means of an inverse fast Fourier transform (IFFT) is given as:

$$x[n] = \frac{1}{\sqrt{N}} \sum_{k=0}^{N-1} X[k] e^{\frac{j2\pi nk}{N}}, \quad n = 0, \ldots, N-1 \tag{5.1}$$

The n^{th} OFDM symbol is constructed by adding a cyclic prefix of length G–sample to x_n the parallel symbols of the IFFT before being serialized to form a long digital complex data sequence. The in-phase (I) and quadrature (Q) components of the data sequence are separated and subsequently are applied to DACs. The outputs of DACs are applied to two identical MZMs with an integrated laser source at a wavelength of 1554.94 nm biased at the null biasing point and a 90-degree phase shifter. Finally, the optical signal propagating through a SMF is amplified using a number of EDFA at a regular interval to cover the total link span.

For simulating a SMF link, the widely adopted split-step Fourier method is employed to model the propagation of the optical signal down a SMF [60]. It is well known that for a sufficiently small fibre split-step length, this theoretical treatment yields an accurate approximation to the real effects. In the SMF model, the effects of loss, CD and optical power dependence of the refractive index are included. The effect of fibre nonlinearity-induced phase noise to intensity noise conversion is also considered upon the photon detection in the receiver.

To set the OSNR to a specified value, an optical noise-loading module is employed in the receiver. This module performs the function of a simple saturating optical amplifier with a variable noise figure, and can be characterised as an optical attenuator followed by a gain block.

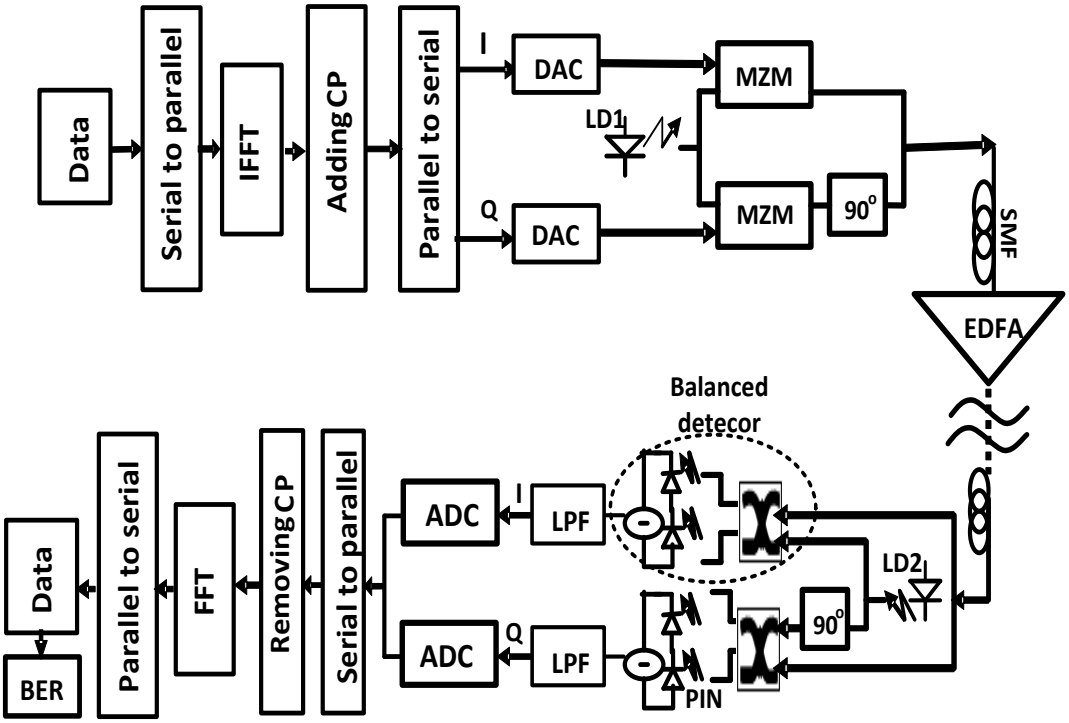

Figure 5.1: A base-band model of CO-OOFDM adopted for numerical simulations.

At the receiver side, the CO-OOFDM signal is detected using two identical optical coherent balanced detectors acting as an optical-to-electrical OFDM I/Q converter, where I/Q components of a locally generated carrier are mixed with the optical signal to obtain the electrical I/Q components. Each coherent detector consists of a pair of couplers and PIN detectors [139]. The low pass filters transfer functions attenuate the sub-carriers close to the Nyquist frequency, thus reducing the usable bandwidth as the attenuated sub-carriers cannot be used for data transmission. The outputs of DACs are passed through a serial-parallel module prior to remove the CP.

Having described CO-OOFDM modem and SMF-based coherent transmission link, this section details the most important parameters adopted in the numerical simulations. The simulation was performed using the Matlab software, and all the key parameters adopted throughout the simulation are given in next section below

5.2.2 Simulation Parameters

Having described the theoretical CO-OOFDM modem and SMF-based coherent transmission link, this section details the parameters adopted in the numerical simulations. In all simulations, 64 sub-carriers are used, onto which identical signal modulation formats are applied. The modulation formats employed range from DBPSK, DQPSK, and 16-QAM to 256-QAM. For the cases of DBPSK and DQPSK the receiver does not apply any channel estimation method, however, for the rest of the modulation formats as it is complex to perform a differential decoding, channel estimation technique such as the pilot tone is necessary for the decoding process [11] [140].

It is assumed that ADCs have fixed a sampling rate of 12.5 GS/s and variable clipping ratios and quantization bits. All the parameters for DACs and ADCs used in the transmitter and the receiver are set to be identical. Under the above-mentioned conditions, signal bit rates of 10 Gb/s, 20 Gb/s, 40 Gb/s, 50 Gb/s, 60 Gb/s, 70 Gb/s, and 80 Gb/s corresponds to DBPSK, DQPSK, 16-QAM, 32-QAM, 64-QAM, 128-QAM, and 256-QAM, respectively.

The operating parameters used for the optical link simulations are: a wavelength of 1550 nm, a laser source with a line width of 100 kHz, -6 dBm optical power coupled into the input facet of the link, PIN responsibility of 0.9, SMF span of 80 km length, fibre chromatic dispersion of 17 ps/nm/km, 0.2 dB/km loss and a nonlinear Kerr-coefficient of 2.6×10^{-20} m^2/W.

The adopted MZM modulation amplitude has a sinusoidal transfer function with a modulation index is of 0.3. The modulation index can be as high as 0.5 without introducing

any significant penalty when the modulator is based at the null biasing point [121], however, investigating the modulation index effect on the transmission performance is beyond the scope of this chapter.

In each fibre span, the fibre loss is compensated by an EDFA with an optical gain and a noise figure of 16 dB and 6 dB, respectively. Note that in this work the following assumptions have been made: state that no laser phase noise is considered, and transmitter and receiver laser local oscillators (LO) are assumed to be matched, sampling clock at the receiver side is ideal. It should be pointed out, in particular, that other parameters that are not mentioned above will be addressed explicitly in the corresponding text parts where necessary.

5.3 ADC/DAC Parameter Optimisation in SMF Links

The magnitude of each complex signal sample is calculated and compared with the threshold magnitude. Samples that exceed the threshold are then clipped (limited) to a value that is equal to the clipping ratio multiplied by the signal average power. In chapter 3 the ADC/DAC quantization and clipping effect on the minimum OSNR required for achieving a BER of 1.0×10^{-3} over optical additive white Gaussian noise AWGN channels for different modulation formats. Consequently, a set of an optimum quantization and clipping ratios were identified.

Having described the impact of ADC/DAC parameters on the CO-OOFDM modem performance in optical AWGN channels, this section further explores the quantization, clipping and sampling speed effects on the transmission performance of the CO-OOFDM modems in SMF links. Based on a fixed modulation format of DQPSK (corresponding to a

signal bit rate of 20 Gb/s), Fig. 5.2 and Fig. 5.3 present the minimum required OSNR as a function of the quantization bit and clipping ratio, respectively, for different transmission distances. In calculating these two figures, both CD and fibre nonlinearity are considered and EDFAs are also utilised to amplify the attenuated optical signals.

In obtaining Fig. 5.2 (Fig. 5.3), the clipping (quantization) effect is effectively switched off by adopting a sufficiently large clipping ratio of 13 dB (a sufficiently large quantization bit value of 10) in both the transmitter and the receiver. It can be seen in Fig. 5.2 that, for a given transmission distance, the use of a small quantization bit value leads to a high minimum required OSNR due to the strong quantization noise effect. On the other hand, for a very large quantization bit value, a flat minimum required OSNR region occurs, corresponding to which optimum quantization bits can be found.

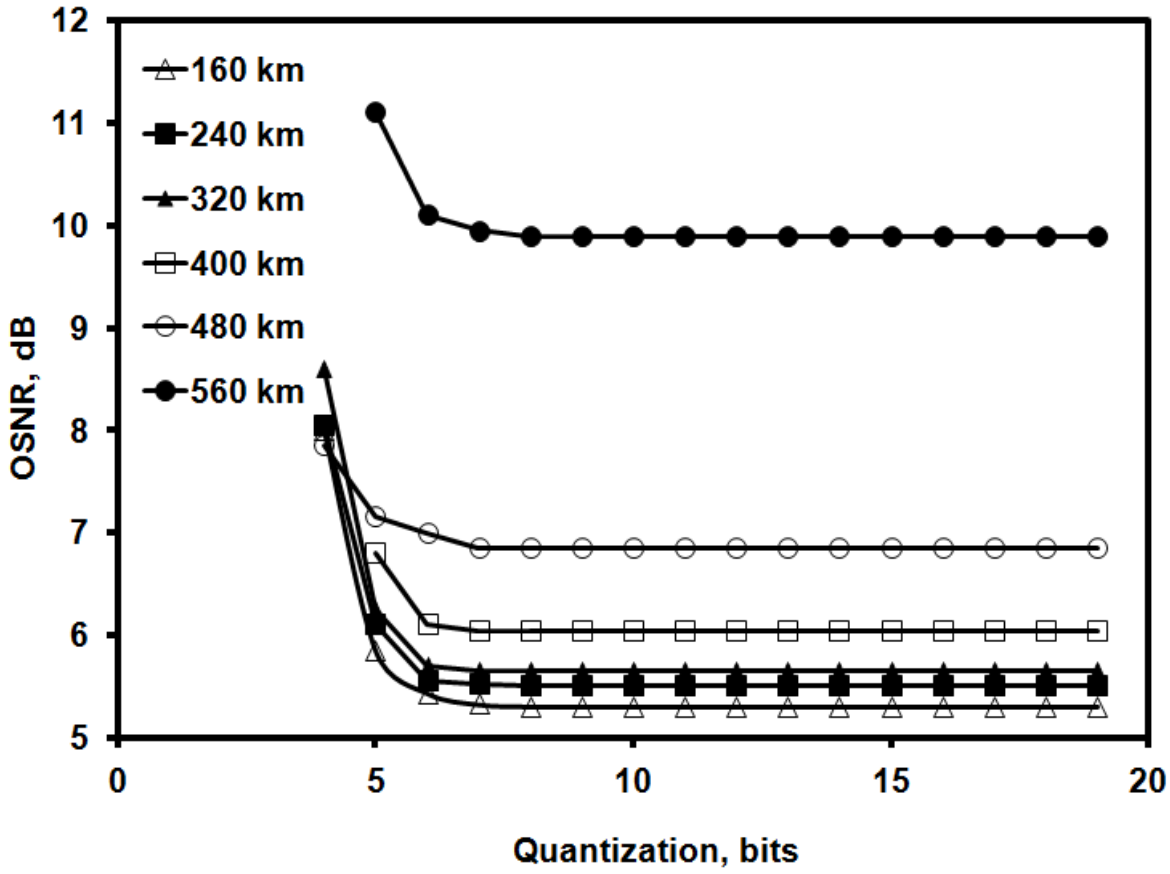

Figure 5.2: Minimum required OSNR versus quantization bit, using 20 Gb/s for different transmission distances.

Over that flat region, the quantization noise effect is negligible, as the corresponding minimum required OSNR is identical to that required for that given transmission distance. In addition, the identified optimum quantization bit value is dependent upon the transmission distance, because of the non-Gaussian nature of the quantization noise.

The signal clipping effect on the minimum required OSNR is illustrated in Fig. 5.3, which shows that, for a fixed signal transmission distance, a low clipping ratio leads to a high minimum required OSNR due to an increase in the clipping noise effect. For a very large clipping ratio, the minimum required OSNR grows sharply because of an increase in the quantization dynamic range and thus quantization step size. As a direct result of the above-

mentioned effects, an optimum clipping ratio region is observed in Fig. 5.3, over which the lowest required OSNR can be found. Similar to those observed in Fig. 5.3, the optimum-clipping ratio gives rise to the negligible clipping noise effect and is also transmission distance dependent.

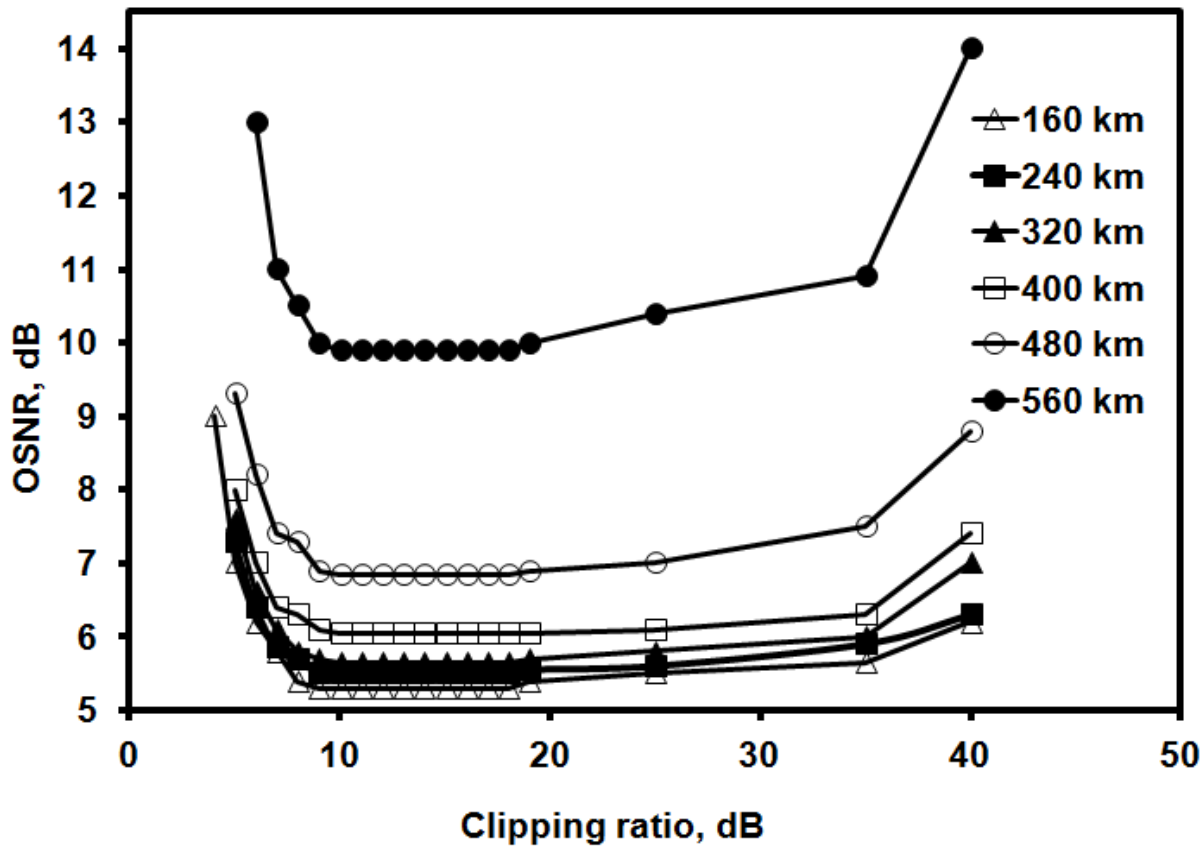

Figure 5.3: Minimum required OSNR versus clipping ratio using 20Gb/s for different transmission distances.

To illustrate explicitly the transmission distance dependent optimum ADC parameters, the minimum optimum quantization bit and clipping ratio are plotted in Fig. 5.4 and Fig. 5.5, respectively, as a function of transmission distance for different modulation schemes and signal bit rates. Here the minimum optimum quantization bits (clipping ratio) refer to as a

minimum value corresponding to which a minimum OSNR is observed for a specific transmission distance.

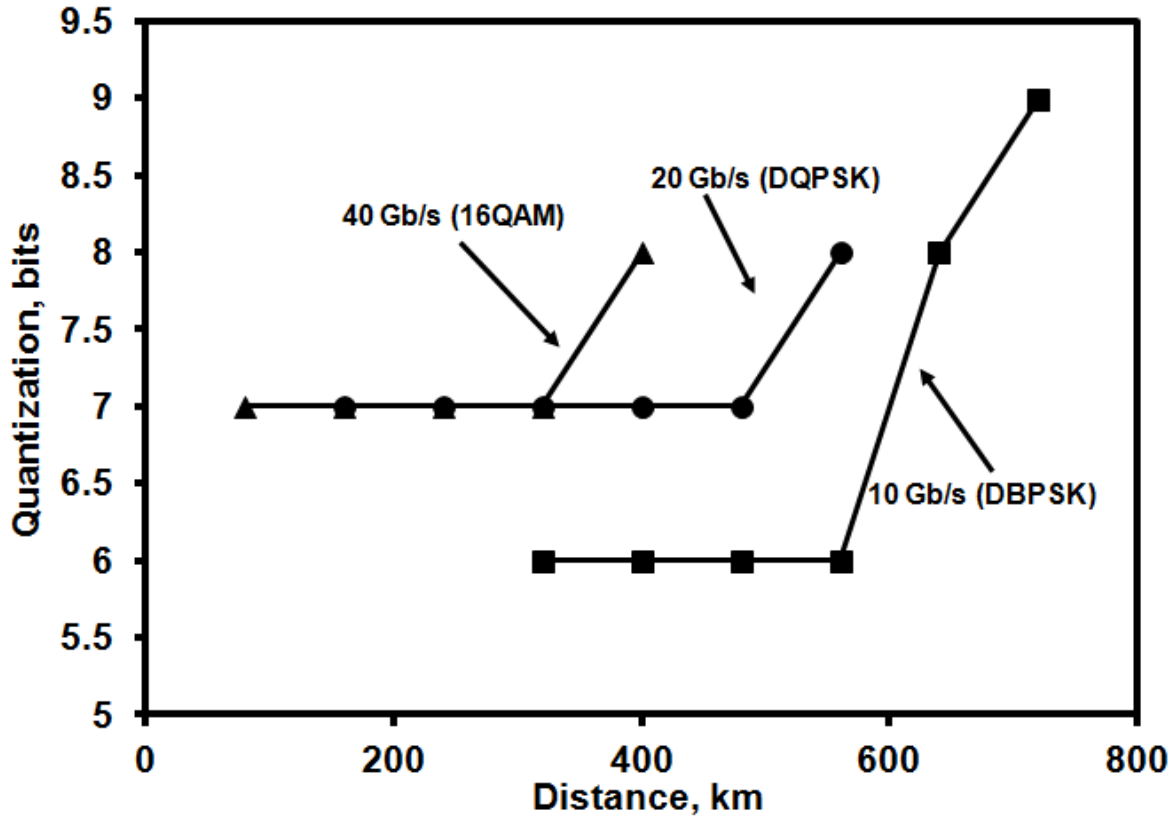

Figure 5.4: Quantization bit effect versus transmission distance for 16-QAM, DQPSK and DBPSK at different data rates.

Fig. 5.4 (Fig. 5.5) shows that, for a given modulation scheme and the signal bit rate, there exists a fibre length threshold, within which the optimum quantization bits shown in chapter 4 at Fig. 5.3 (clipping ratio shown in Fig. 5.4) are capable of supporting quantization (clipping) noise free transmission performance. 16-QAM and DQPSK show a higher quantisation bits compared to DBPSK, except when the link span is greater than 560 km, where the latter increases sharply. Beyond the fibre length threshold (~300 km. ~480 km and ~570 km for 16-QAM, DQPSK and DBPSK, respectively), the required minimum

quantization bits (clipping ratio) increases at a slope of 1 bit (2 dB) per 100 km, which is, however, independent of the signal bit rates. This indicates that, for such a transmission distance scenario, the quantization (clipping) noise effect is the dominant factor. For clipping ratio (Fig. 5.4) 16-QAM display higher profile than DQPSK and DBPSK for all the fibre span.

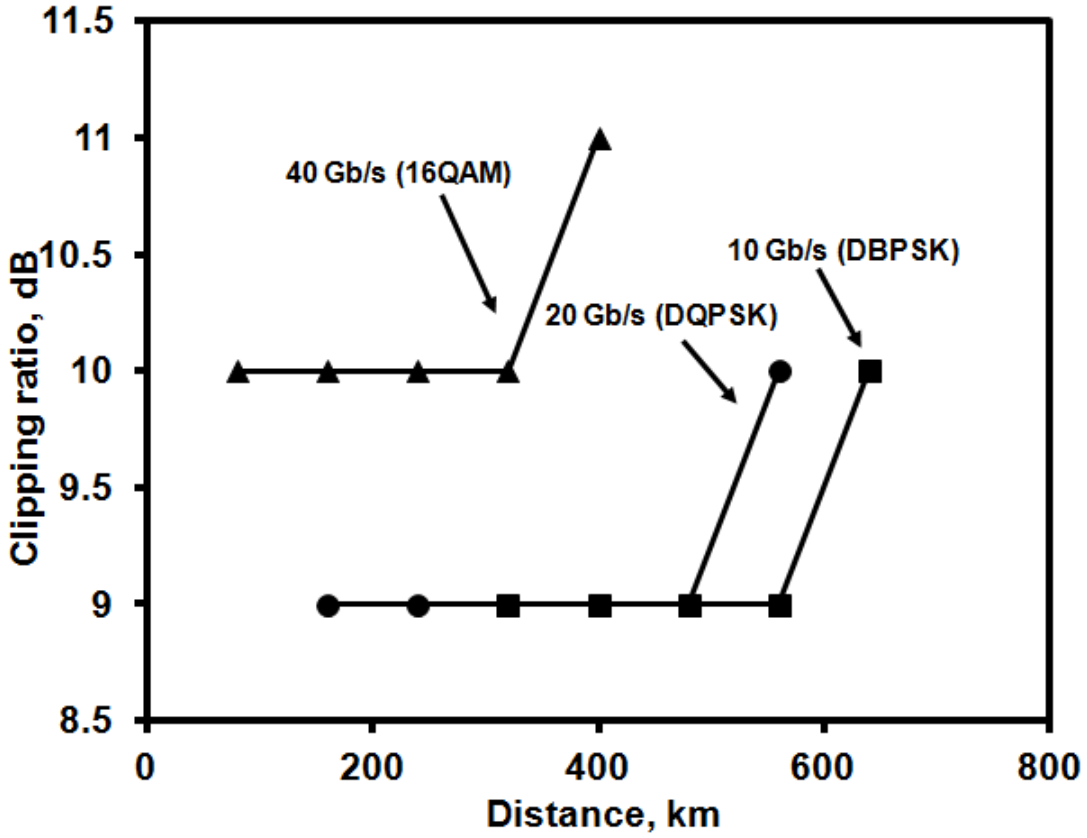

Figure 5.5: Clipping ratio effect versus transmission distance for 16-QAM, DQPSK and DBPSK at different data rates.

Fig. 5.4 and Fig. 5.5 also show that, the fibre length threshold decreases with increasing signal bit rates. This is due to the accumulated effects of various noises mainly contributed by EDFAs and FWM.

5.4 Optimisation of Number of Sub-carriers and Cyclic Prefix

This section discusses the impact of the number of sub-carriers on the CO-OOFDM signal transmission performance in SMF links. To highlight such effects, in this section, numerical simulations are performed by setting the quantization bits and clipping ratio to be 10 and 13dB, respectively. Here dispersion tolerance and transmission reach are defined as the maximum fibre length at which a 1 dB increase in the minimum required OSNR is required with respect to the minimum required OSNR for back-to-back cases as explained previously in chapter 3 section 3.4.1.

5.4.1 Effect of Number of Sub-carriers and Cyclic Prefix on Dispersion Tolerance

Figure 5.6 demonstrates the effect of the number of sub-carriers and CP on the channel capacity over a link span of 2500 km and considering only fibre CD. Simulations reveal that, for a fixed signal data rate 80 Gbps and a CP of 25%, increasing the number of sub-carriers from 32 to 128 increases the link span is from 104 km to 600 km (a factor of up to 5.7). However, for a fixed number of subcarriers, dispersion tolerance can also be increased by increasing the CP length.

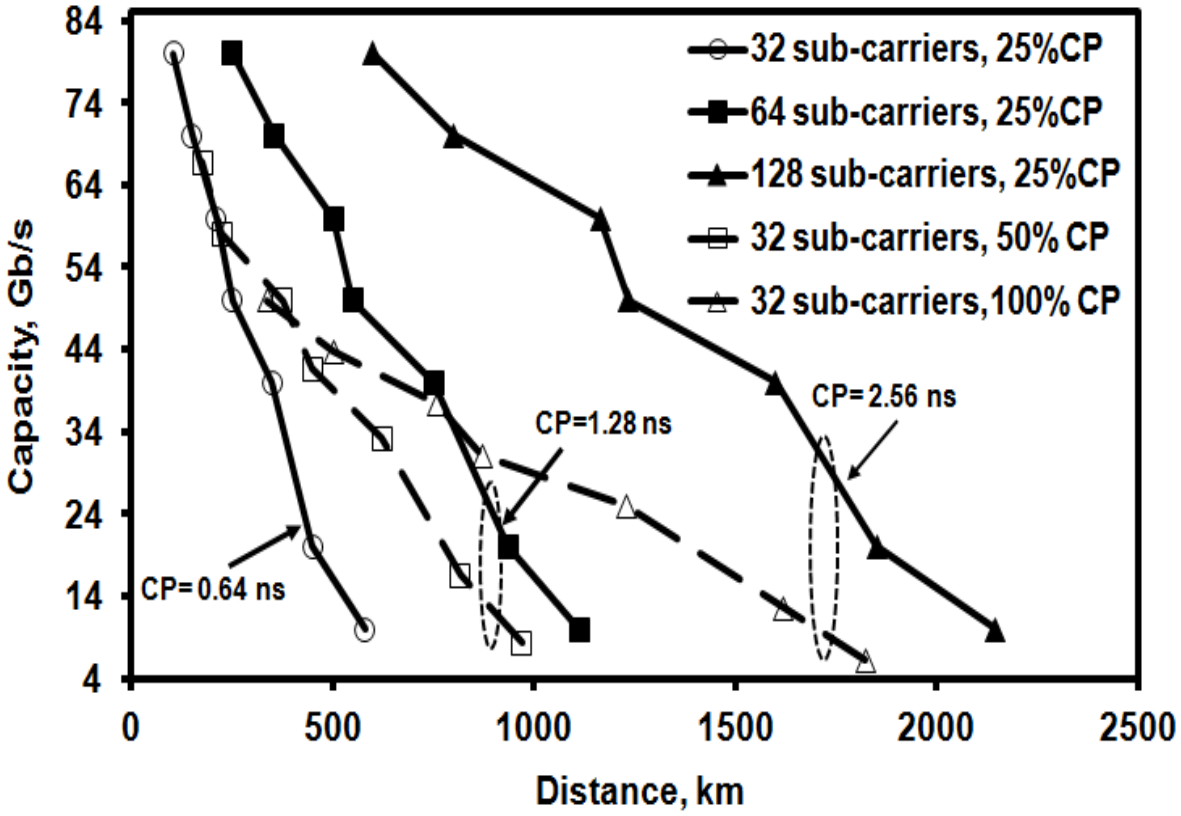

Figure 5.6: Channel capacity against the link span for a range of sub-carrier and cyclic prefix and with fibre chromatic dispersion only.

As shown in Fig. 5.6 that for 32 sub-carriers increasing the CP length from 25% to 100% can improve the dispersion tolerance by a factor of 2.7 for low data rates of up to 25 Gb/s. Note that this effect is more significant for low signal data rates. However, for higher data rates, increasing the CP length means that higher modulation formats are required to achieve the same data rate as that can be obtained with employing lower CP lengths. This is the reason behind the low impact of increasing the CP length for the above-mentioned condition.

The physical reason behind the ability of CP length to combat the dispersion in SMF links can be understood as follow. When CO-OOFDM symbols are transmitted over a dispersive link, they will suffer a frequency dependent delay and consequently the slow sub-carriers will

cross the symbol boundary, thus leading to ISI. Moreover, this can destroy the orthogonality between adjacent sub-carriers causing ICI impact [7]. Therefore, a larger CP length helps in maintaining the orthogonality between the subcarriers and combating both ISI and ICI.

In comparison with employing a long CP, the use of a large number of sub-carriers is more effective in combating the fibre dispersion. This is can be explained as increasing the number of sub-carriers will increase the CP length. Moreover, for a fixed sampling frequency, an increase in the number of sub-carriers reduces the frequency spacing between sub-carriers and the dispersion induced walk off [8]. This results in the better use of the link bandwidth under investigation. Therefore, considerable distortions occur within a lower percentage of sub-carriers.

5.4.2 The Effect of Number of Sub-carriers in SMF Links with Both Dispersion and Non-linearity

Having investigated the effect of the number of sub-carriers on the dispersion tolerance, this sub-section takes the investigation further to study the impact of the number of sub-carriers on modem performance in the presence of fibre non-linearities.

For 64 subcarriers, the OSNR required for achieving a BER value of 10^{-3} is plotted against the transmission distance for a range of data rates, and modulation schemes ranging from DBPSK (10Gb/s), DQPSK(20Gb/s) and 16-QAM(40Gb/s) to 128-QAM (70Gb/s) is shown in Fig. 5 7.

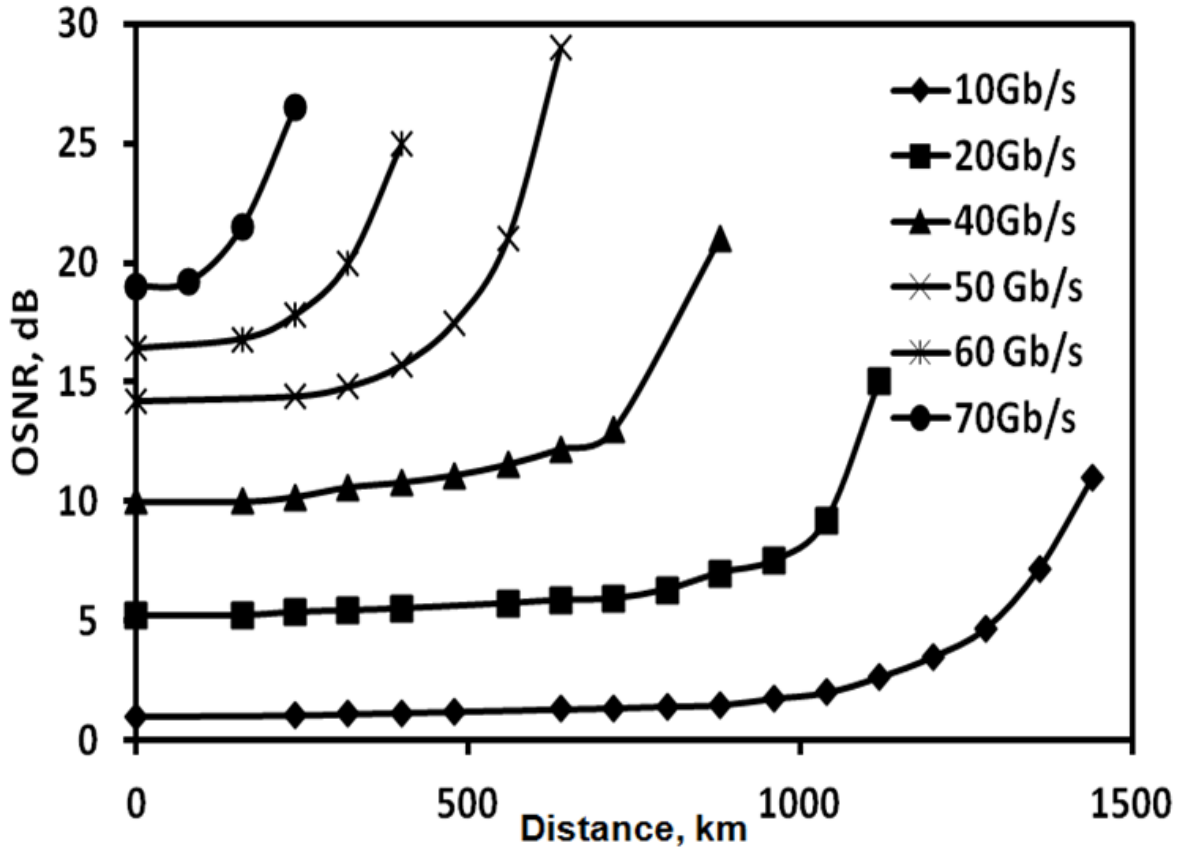

Figure 5.7: Transmission distance against OSNR for 64 sub-carriers and BER of 10^{-3}, for a range of channel data rates.

From the above figure it can be seen that for a given data rate the transmission reach is considered after an increase of 1 dB in the OSNR, which is called OSNR-min as mintioned previously. More over its clear that for the same transmission distance, increasing the data rate requires higher OSNR this is due to the need of higher modulation formats as the data rate increases.

The impact of the number of sub-carriers on the CO-OOFDM signals transmitted over SMF links is shown in Fig. 5.8, where the signal data rate is plotted as a function of transmission distance for various numbers of sub-carriers.

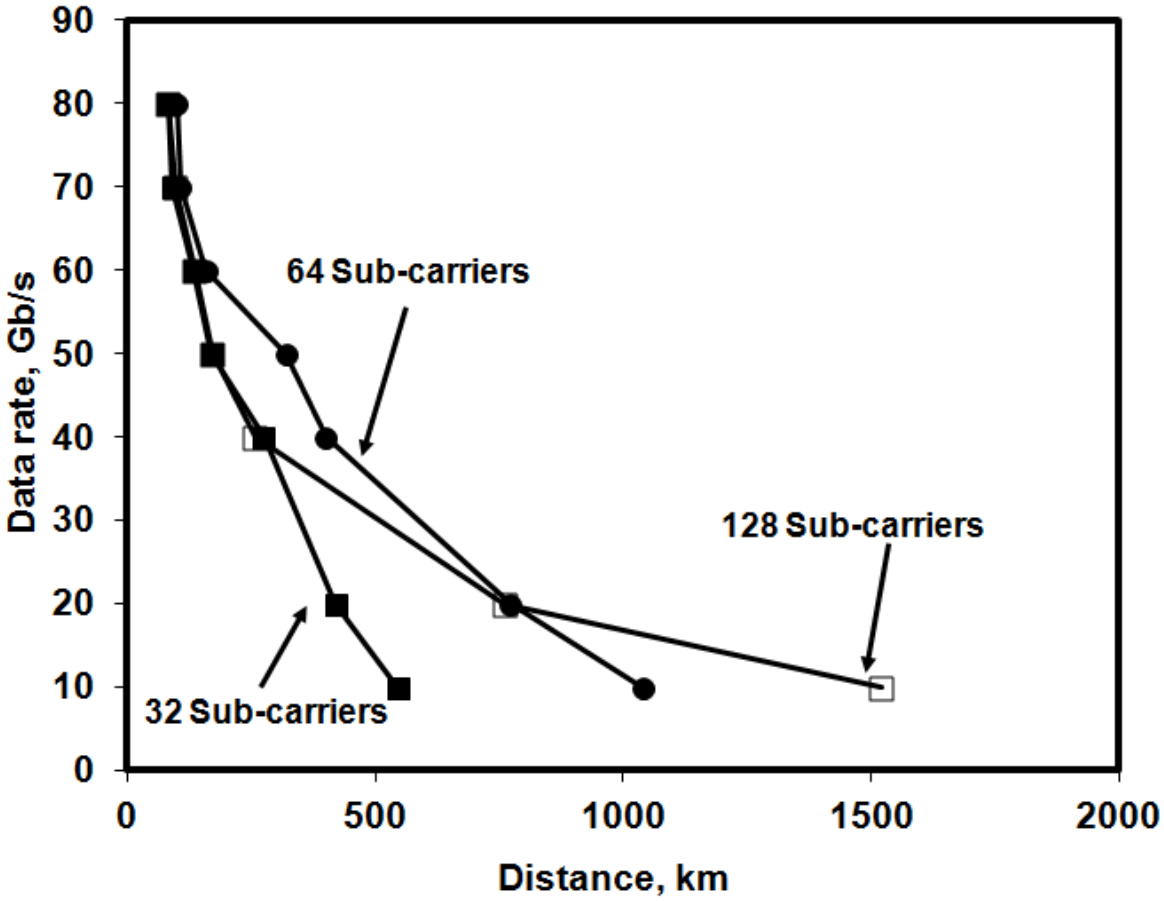

Figure 5.8: Channel capacity against the link span for a different number of subcarriers.

It is shown that increasing the number of sub-carriers improves the data rate for the link length > ~300 km. This can be explained by considering the fact that for a fixed ADC sampling rate, the duration of the CP length increases with the increase of the number of sub-carriers, thus leading to an enhanced dispersion tolerance. In addition, it is also important to address the fact that for a fixed bandwidth, increasing the number of sub-carriers reduces the frequency spacing between adjacent sub-carriers. This may cause sub-carrier intermixing effect if the perfect orthogonality between sub-carriers cannot be maintained [8] [141]. However, it can be seen that for 10 Gb/s data rate increasing the number of sub-carriers from 64 to 128 results in an increase transmission distance performance. This is may be due to the

ability of low modulation formats such as DBPSK to preserve the orthogonality and combat the fibre non-linearity.

Figure 5.8 shows that, for data rates > 10 Gb/s, using 128 sub-carriers will degrade the modem performance when compared with that achieved using 64 sub-carriers. This is because of the increase of intermixing effect as the frequency spacing between adjacent numbers of sub-carriers decreases. Consequently, 64 sub-carriers can be considered as an optimum number of sub-carriers for the CO-OOFDM modems.

5.4.3 The Effect of Launch Power on the CO-OOFDM Modem Performance In SMF Links

For CO-OOFDM modem the optical launch power affects the signal transmission performance over SMF links [8], therefore, this section investigates the launch power effect on the CO-OOFDM modem performance for data rates up to 80 Gb/s, for different number of sub-carriers. For 20 Gb/s, Fig. 5.9 shows the effect of launch power on CO-OOFDM signals reach. It is clear that -6 dBm induces the highest transmission distance if compared with 0 dBm, -3 dBm and -9 dBm. This is because a large launch power such as 0 dBm can excite fibre non-linearities, on the other hand attenuating the launch powers values to < -6 dBm will give rise to extra signal distortion due to the EDFA noise, which in both cases results in degradation of the system performance.

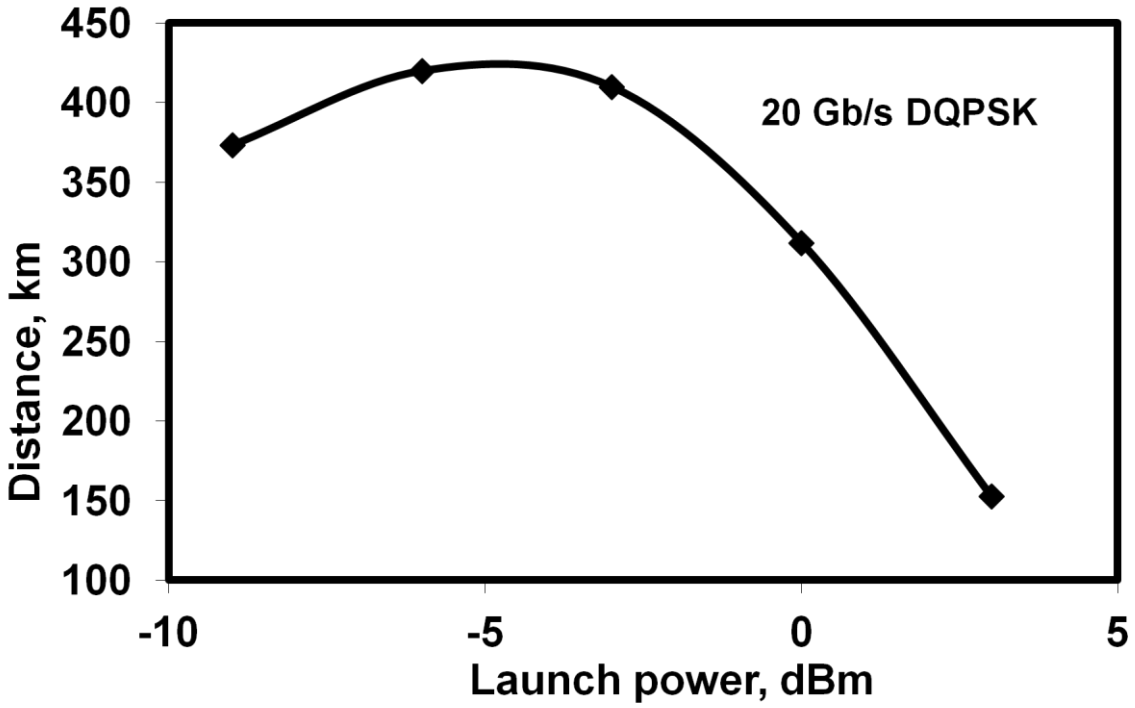

Figure 5.9: Launch power against the transmission distance for a data rate of 20 Gb/s.

The power must be large enough to provide an acceptable OSNR at the output of the transmission link but below the limit where excited fibre nonlinearities distort the signal. Consequently, -6 dBm is considered as the optimum launch power for the CO-OOFDM modem.

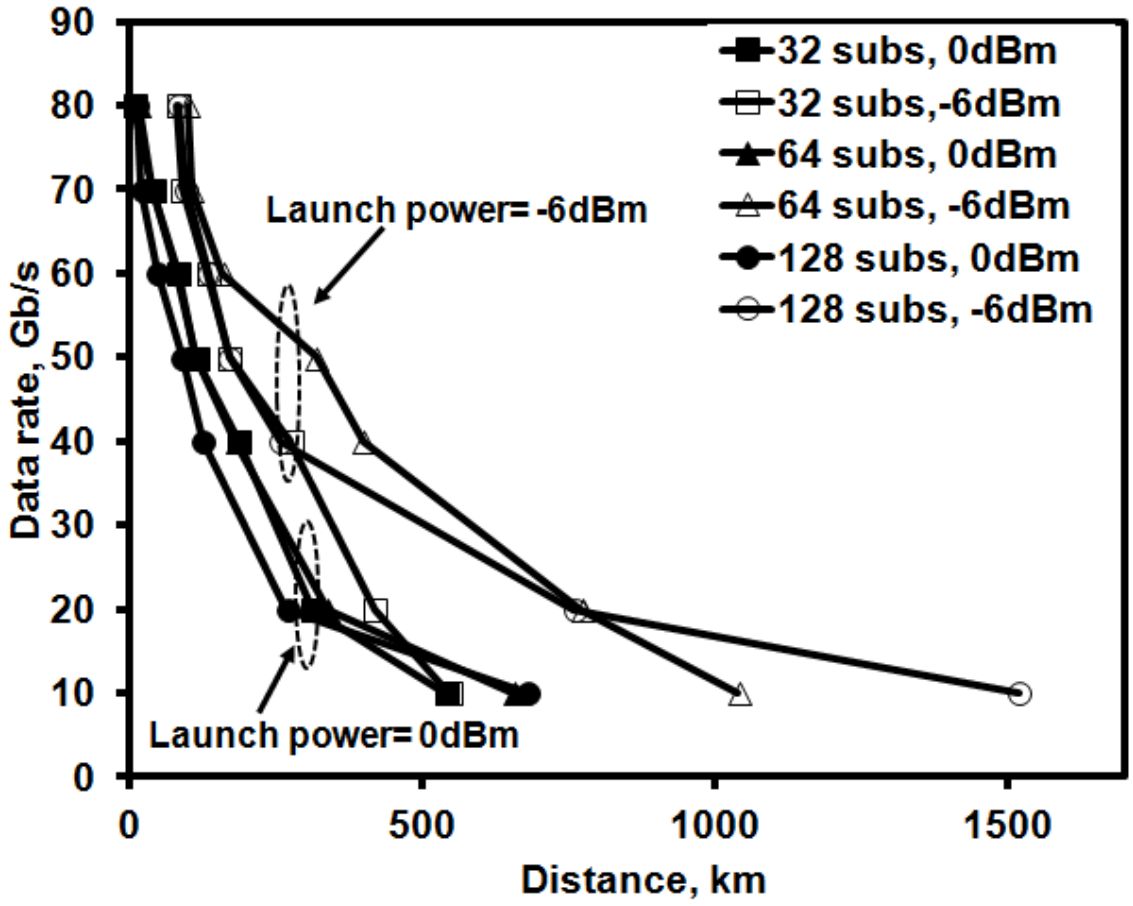

Figure 5.10: Channel data rate against the link span for different number of subcarriers using different launch power.

It is shown in Fig. 5.10 that for different number of subcarriers attenuating the launch power to -6 dBm can improve the modem performance by an average factor of 2.9 times when compared with that obtained by utilizing 0 dBm launch power. Moreover, it can be seen that 64 sub-carriers can be considered as the optimum number of subcarriers for 0 and -6 dBm launch power conditions.

5.4.4 Effect of Number of Sub-Carriers on Transmission Performance in Fibre Links with Non-linearity Compensation

In order to improve the CO-OOFDM modem performance, a recently proposed algorithm in [10], has been used to compensate for Kerr non-linearity impairments in SMF links. Figure 5.11 illustrates the effect of the non-linearity mitigation algorithm on different numbers of sub-carriers. It is shown that, the non-linearity compensation algorithm does not increase the transmission distance significantly. This effect is a direct result of utilizing an optimum launch power of -6 dBm. However, other nonlinearities such as FWM are dominant and not compensated for, which results in a low improvement in the performance when using the compensation process.

It can be seen that for 32 and 64 sub-carriers the results obtained in Fig. 5.11 are very close to that obtained from Fig. 5.6. However, this is not valid for 128 sub-carriers even when the non-linearity compensation algorithm is used. This is because the non-linearity compensation algorithm effectively compensates for fibre Kerr non-linearities only; therefore, as explained previously, using 128 sub-carriers will increase the FWM effect as a direct result of reducing the frequency spacing between sub-carriers.

For 0 dBm launch power, Fig. 5.12 illustrates the effect of utilizing the non-linearity compensation algorithm on CO-OOFDM based transmission link performance.

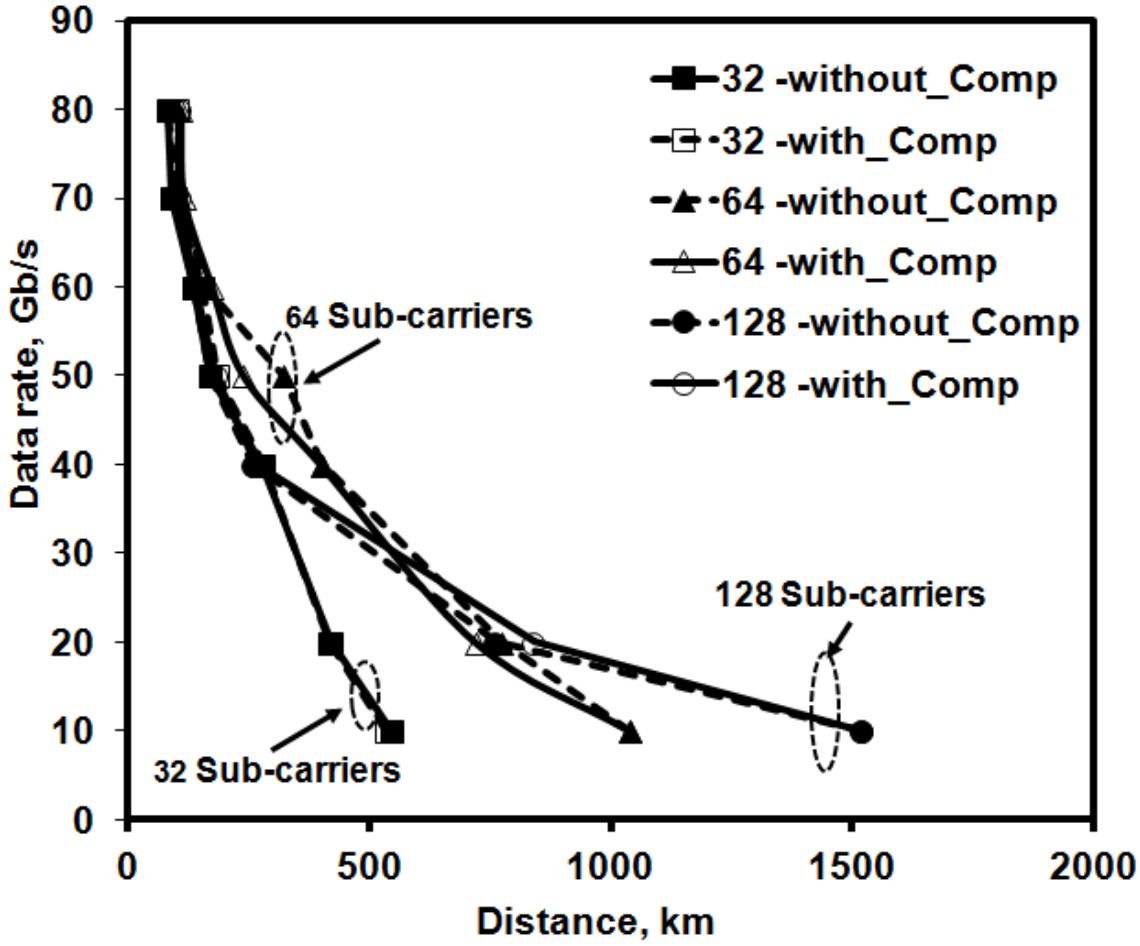

Figure 5.11: Channel data rate against the link span for different number of subcarriers with and without using the compensation algorithm at -6 dBm launch power.

By comparing Fig. 5.11 and Fig. 5.12, it can be seen that for 0 dBm launch power the compensation algorithm effect is more significant than it is for -6 dBm launch power. Moreover, such an effect is higher for high data rates (i.e. 80 Gb/s), where utilizing the compensation algorithm increases signals transmission distance from 16 km to 89 km (a factor of 5.6 times) when 64 subcarriers are used. This can be explained as Kerr non-linearities are launch power dependent, for higher data rates the signals transmission distance is short; consequently Kerr non-linearities are the dominant factor, which limits the performance. However, the compensation algorithm has less impact for low data rates (i.e. 10Gb/s) where non-linearities such as FWM effect increases with the transmission distance.

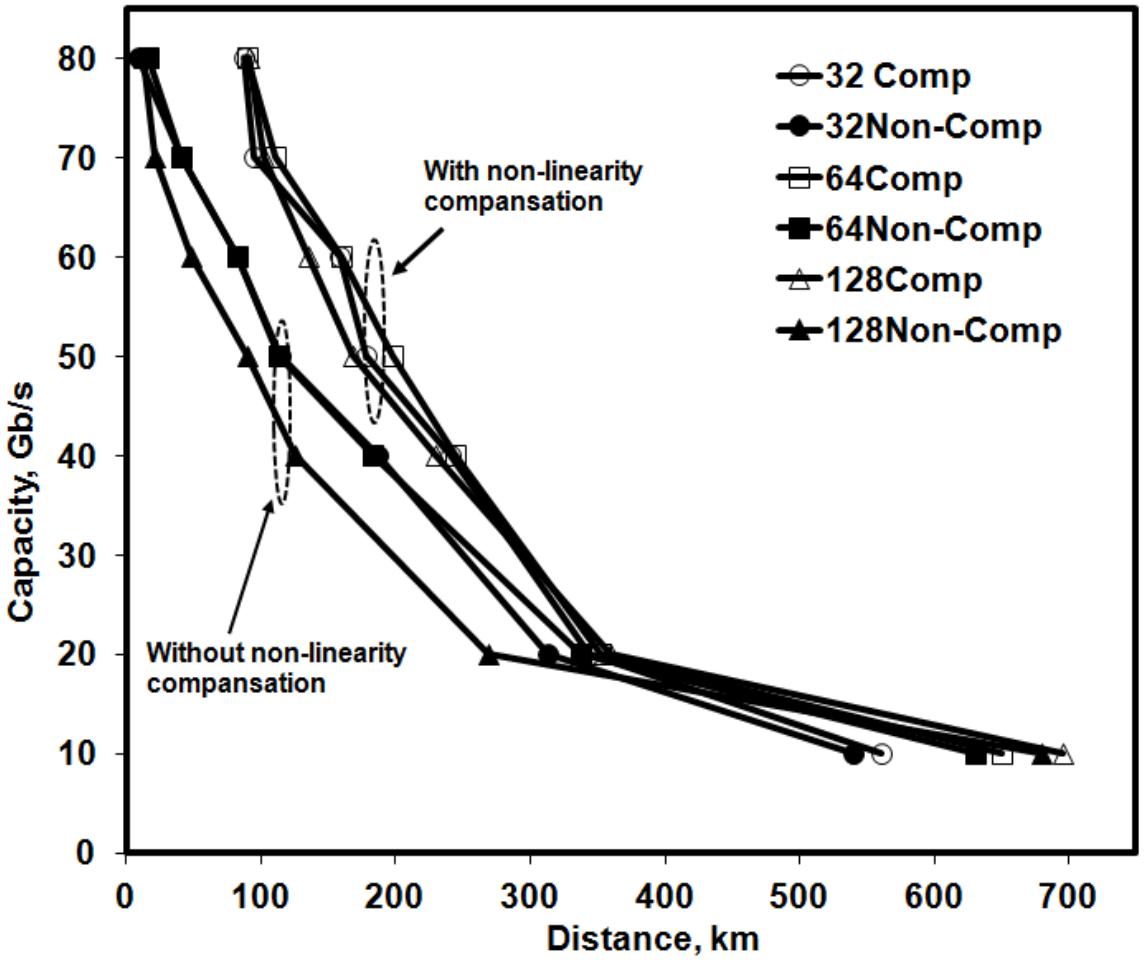

Figure 5.12: Channel capacity against the link span for different number of subcarriers with and without using the compensation algorithm at 0 dBm launch power.

For different data rates and number of subcarriers an average improvement of 2.9 times can be realized when the non-linearity compensation algorithm is employed while utilizing 0 dBm optical launch power. Moreover, it can be seen from Fig. 5.12 that using 64 sub-carriers results in a longer transmission distance if compared with the 32 and 128 subcarriers, therefore it is considered as the optimum number of subcarriers with and without the non-linearity compensation scheme.

It should be noted that the optimum number of sub-carriers is closely related to signal sampling speeds, as a high sampling speed gives a short symbol period and thus decreases the fibre dispersion tolerance. All the above-mentioned facts indicate that the optimum number of sub-carriers may vary with sampling speed.

5.5 Effect of Sampling Speed on Transmission Performance in Fibre Links

It is well known that ADC's sampling speed play a significant role in determining the symbol period; therefore, this section discusses the impact of the sampling speed on the CO-OOFDM transmission link performance. Numerical simulations are carried out by adopting 64 sub-carriers and setting the ADC's quantization bit resolution and the clipping ratio to 10 and 13dB, respectively. Figure 5 13 illustrates the data rate against the link span for 64 and 128 sub-carriers, symbol length of 6.4 ns and 12.8 ns, and for two sampling speeds of 6.25 and 12.5 giga sample/second (GS/s). Doubling the symbol length increases the link span in particular at lower data rates.

For a symbol period of 12.8 ns and at low data rates adopting a sampling speed of 6.25 GS/s can increase the dispersion tolerance by an average factor of 1.5 compared to the case with a sampling speed of 12.5 GS/s. However, at lower sampling speed higher order modulation formats could be used to achieve the same data rate as that of higher sampling speed. This can be explained as follow. For a fixed symbol length, at lower sampling speed, the number of high frequency sub-carriers that could be used is reduced and consequently this result in a lower OSNR-min requirement for a specific modulation format adopted for a sub-carrier.

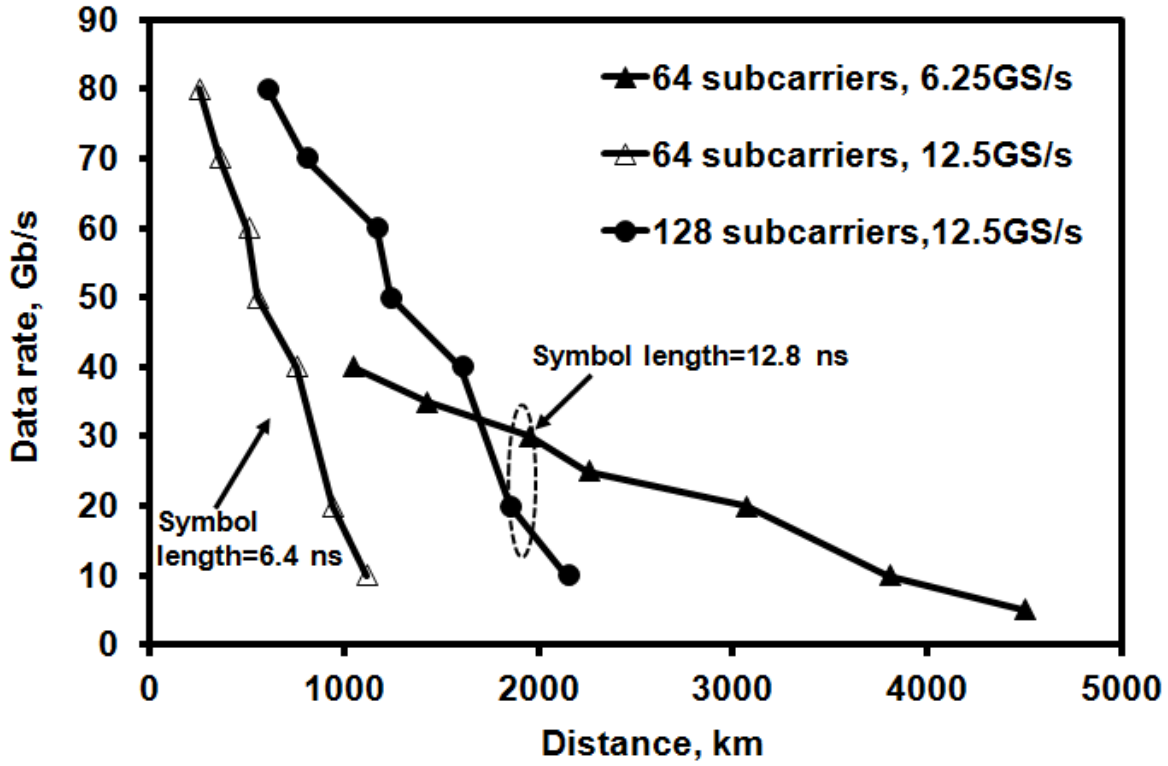

Figure 5.13: Channel data rate against the link span for a range of sampling speed effect fibre chromatic dispersion only.

At a data rate of 40 Gbps adopting a sampling speed of 12.5 GS/s is more effective in combating fibre dispersion than at 6.25 GS/s. This is due to the requirement of utilizing high order modulation formats such as 256-QAM with a 6.25 GS/s sampling rate compared to 16-QAM with a sampling rate of 12.5 GS/s. For 64 sub-carriers, utilizing a sampling speed of 6.25 GS/s can increase the dispersion tolerance by a factor of 2.5 when compared to a sampling rate of 12.5 GS/s. This is due to the increased CP length as a result of increased symbol period as well as decreased signal bandwidth.

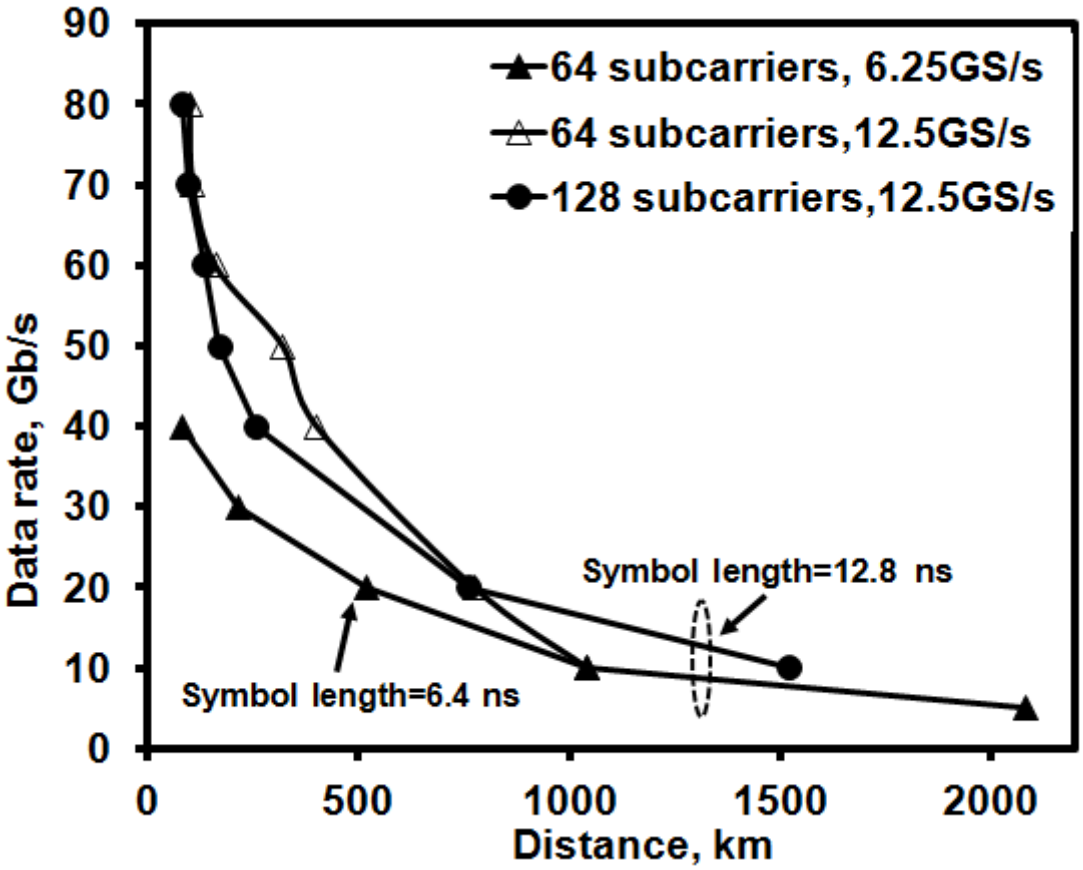

Figure 5.14: Channel data rate against the link span for a range of sampling speeds while transmitting over SMF links.

Considering the SMF non-linearities, Fig. 5.14 illustrates the data rate against the link span for the symbol length of 6.4 and 12.8 ns for 64 and 128 sub-carriers. For the data rates > 10 Gbps reducing the sampling speed does not improve the transmission capacity versus the reach performance. However, at lower sampling speed, where the spacing between the sub-carriers is reduced, FWM effects become prominent.

5.6 Adaptive CO-OOFDM

CO-OOFDM sub-carrier signals will experience amplitude distortion that depends upon the frequency response of the transmission link, consequently certain sub-carrier components will endure higher distortion than the others. To address this problem CO-OOFDM with the adaptive modulation (CO-AMOOFDM) applied to all sub-carriers is proposed where low and high order modulation formats are used for the sub-carriers with higher and low distortions, respectively. As a direct consequence of this, CO-AMOOFDM technique has a unique feature of effectively utilizing the entire transmitted signal spectrum.

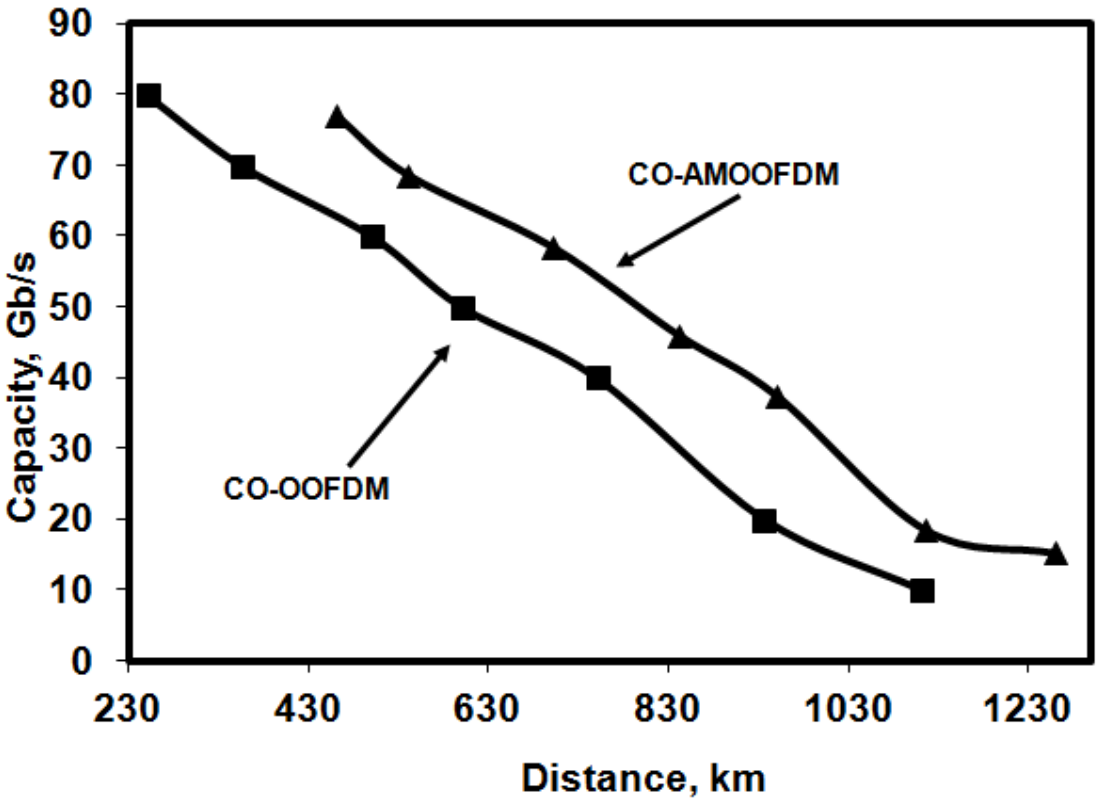

Figure 5.15: Channel data rate against the link span for CO-OOFDM identical and dapative modulation formats.

Figure 5 15 depicts the data rate against the link span for CO-OOFDM with identical and adaptive modulation formats adopted for all sub-carriers while considering only the CD effect. The latter scheme displays an increase in the link span by a factor of 1.4. On the other hand, when considering both the fibre non-linearities and dispersion, figure 5.16 illustrates the advantage of utilizing CO-AMOOFDM over the traditional CO-OOFDM scheme.

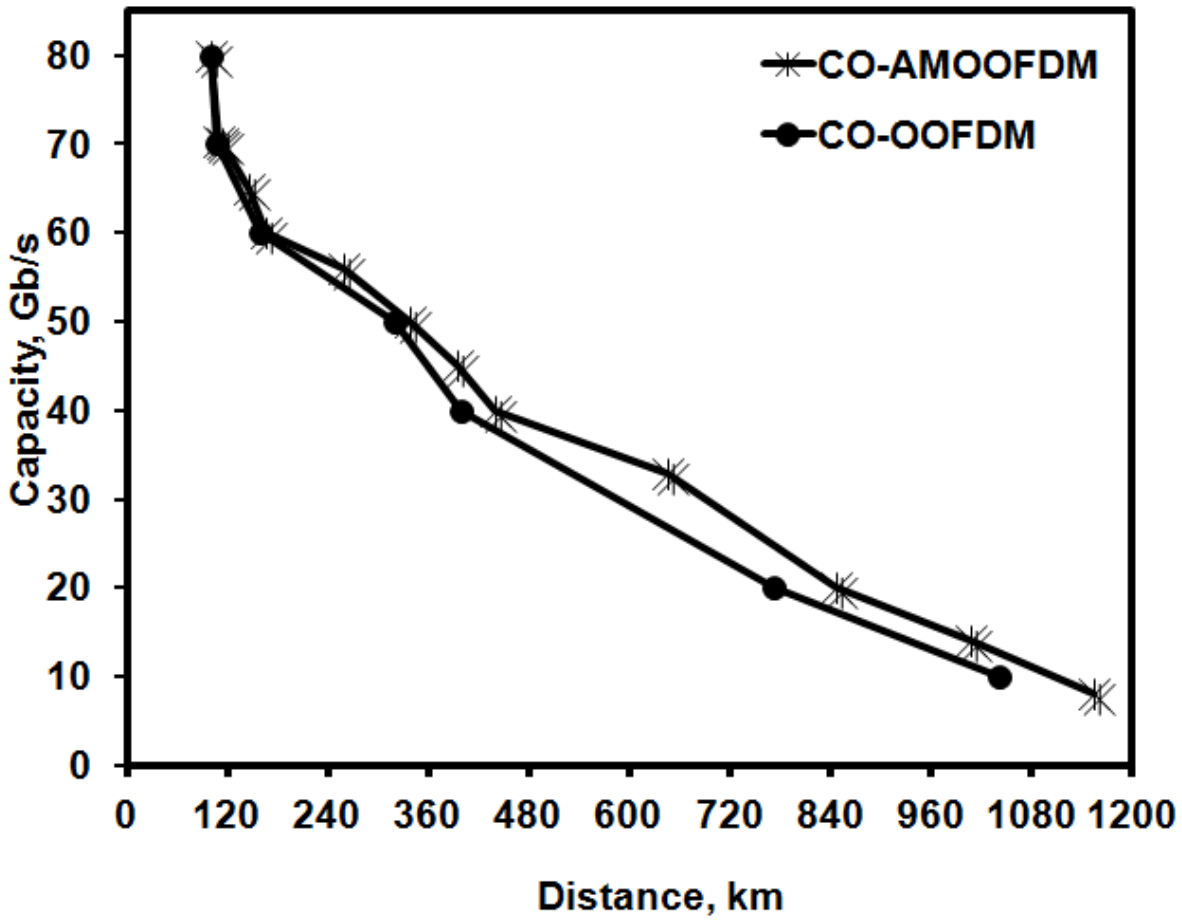

Figure 5.16: Channel capacity against the link span for CO-OOFDM identical and CO-AMOOFDM formats in the presence of fibre non-linearity.

At lower link span (< 280 km) both schemes offer similar data rates. However, at higher link spans CO-AMOOFDM offers an average improvement of 1.15 times that of CO-OOFDM. In this research we have focused on the adaptive modulation schemes which improves spectrum usage efficiency, thus resulting in higher tolerance to the CD when compared to the case where an identical modulation formats are adopted across all the sub-carriers.

5.7 Conclusions

For CO-OOFDM modems, in comparison with the OFDM employing a long CP, the use of a large number of sub-carriers is more effective in combating the fibre CD. For a fixed number of sub-carriers, dispersion tolerance can also be increased by increasing the CP length from 25% to 100% can improve the dispersion tolerance by a factor of 2.7 for lower data rates of up to 25 Gbps. We have shown that with the SMF fibre non-linearities adopting 64 sub-carriers can increase the transmission distance when compared to 32 and 128 sub-carriers. The aid of the non-linearity compensation algorithm is more effective for high launch powers, such as 0dBm, and high data rates, than it is for lower launch power such as -6dBm. Moreover, with the use of the non-linearity compensation algorithm the optimum number of subcarriers can be found, as 64 sub-carriers. ADC sampling speed play a significant role in determining the symbol period. Reducing the sampling speed can increase the symbol length and limit the number of high frequency components from propagating along fibre, which increases the CD tolerance. However, for a fixed symbol length a lower sampling speed does not necessarily lead to CD improvement, since higher order modulation formats are needed to achieve the same data rate as the higher sampling rates. Moreover, reducing the sampling speed further reduces the spacing between sub-carriers, thus resulting in increased FWM effect.

We have shown that employing adaptive modulation schemes have a unique feature of effectively utilizing the entire transmitted signal spectrum, thus addressing the amplitude distortion experience by all the CO-OOFDM sub-carrier signals. It has been shown that the link span increases by factors of 1.4 and 1.2 for dispersion only and both dispersion and fibre non-linearities, respectively.

Chapter 6. Artificial Neural Network Equalizer for CO-OOFDM Modems

6.1 Introduction

The coherent transmission system, in particular CO-OOFDM, has recently seen a growing interest within the optical research community. This is mainly due to the inherited OFDM properties such as higher data rates, resilience to the noise and the ICI.

High performance optical networks, such as CO-OOFDM, are very sensitive to the degradation introduced by the linear and non liner impairments introduced by the fibre channels; therefore, many techniques have been introduced in order to reduce the channel effect on the transmission system performance [49]. Consequently, to increase the CO-OOFDM system tolerance to the CD and fibre non-linearities, a number of methods has been proposed including: (i) including low-cost DSP techniques such as EDC that provides a simpler solution to compensated for the fibre CD [21], and OSSB for CD compensation at the receiver [23], (ii) EPD at the transmitter [24] as well as non-linear electrical post-compensation at the receiver [25], and (iii) the optimization of modem parameters such as the CP, multiple number of subcarriers and ADC [37, 49].

A careful management of CO-OOFDM modems key parameters such as CP, number of subcarriers, and phase noise of the laser source has lead to a successful experimental demonstration of 20 Gb/s CO-OOFDM signal transmission over 4160 km of SMF using the sub-carriers multiplexing technique [11]. Moreover, it has been shown in simulation and practical experiments that CO-OOFDM is a candidate for the 100 Gbit/s Ethernet and beyond [142, 143]. In [144]a backward propagation equalization method has been introduced, where by the Fourier split step length method has been modified to reduce the complexity of the computationally expensive original split step method [8]. However, it only compensates for

Kerr non linearity which have a greater effect for higher optical launching power and cannot compensate for low optical power and other types of non linearities such as self phase modulation and four wave mixing (FWM), therefore, this algorithm proven to be in efficient and may be incapable of performing the equalization task [49].

For a time and frequency-varying channel such as SMF links, equalization based on filters is the non-optimum classification strategy as filters have a linear decision boundary [77, 145]. Therefore, the optimum technique would be to have a nonlinear decision boundary based equalizer such as ANN and MLPs. ANN is an attractive alternative for compensating the linear and non-linear distortions of optical fibre communications [146, 147], and its applications has been explored for the communication systems for a variety of channels, including optical fibre, optical wireless and wireless) [113, 146-148], where it can offer similar or better performance compared to the traditional finite impulse response filter equalizers [149]. ANNs have the capability of achieving a complex mapping between its input and output spaces, moreover are capable of forming complex decision regions with nonlinear decision boundaries, consequently ANN of different architecture have been used in the channel equalization [91]. It has been shown that the ANN techniques have also been adopted for compensating for the impartment introduced by communication link in OFDM modems in the wireless domain [150, 151]. However, no research in all the CO-OOFDM published literature, the use of artificial intelligence in particular ANN to compensate for the distortion experienced by signals while propagating through SMF link has been reported.

This chapter investigated the performance of the ANN equalizer when used to compensate for CD and fibre nonlinear impairments induced by the SMF links for CO-OOFDM. Consequently, numerical simulations are undertaken to investigate the impact of the ANN

equalizer on the modem performance over SMF links. It is shown that for a given transmission distance utilizing the proposed equalization scheme results in reduced bit error ratio (BER) while considering CD only in the presence of other nonlinear impairments. Moreover, for a given OSNR the transmission distance is doubled when transmitting over SMF links.

The present chapter is organised as follows: The CO-OOFDM modem model used in numerical simulations along with the adopted system parameters are presented in Section 6.2. In Section 6.3, the equalizer design is illustrated, and in Section 6.4, represents results of the performance of the proposed equalizer using different ANN equalizer learning algorithms, while transmitting over SMF links that considers CD only. In Section 6.5, the performance of the ANN equalizer is reported in the presence of nonlinear fibre impairments for a different transmission distance. Finally, the paper is concluded in Section 6.6.

6.2 Transmission Link Models and Simulation Parameters

6.2.1 Transmission Link Simulations

Figure 6.1 describes a typical block diagram of the CO-OOFDM modem adopted in numerical simulations. After passing through a serial to parallel converter, the encoded complex data are first mapped onto various CO-OOFDM subcarriers. The inverse fast Fourier transform (IFFT) is then applied to convert the *N* number of sub-carriers into time-domain CO-OOFDM symbols. The IFFT is given as:

$$x[n] = \frac{1}{\sqrt{N}} \sum_{k=0}^{N-1} X(k) e^{2j\pi k/N}, \quad n=0,\ldots,N\text{-}1. \tag{6.1}$$

The *n*-th OFDM symbol is constructed by adding a CP of length G samples, which is added to *x*[*n*], the parallel symbols of the IFFT, before being serialized to form a long digital complex data sequence. The real (I) and imaginary (Q) parts of the data sequence are separated and subsequently inputted into two DACs. The OFDM electrical-to-optical conversion is accomplished by feeding the OFDM I and Q components to the corresponding I/Q ports of the two optical MZMs. The optical modulators that have a sinusoidal transfer function are biased at the null biasing point; moreover, a 90-degree phase shifter is applied to the output of the second MZM.

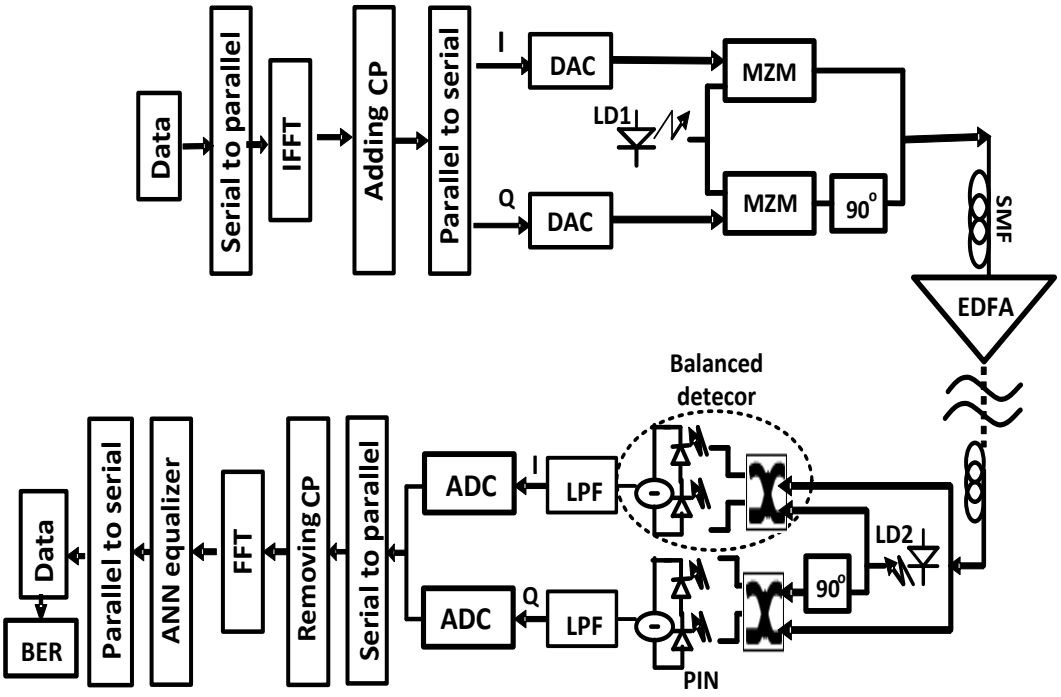

Figure 6.1: CO-OOFDM modem diagram used in numerical simulations.

Finally, the optical signal is coupled to the SMF link of several spans with erbium-doped fibre amplifiers (EDFAs) inserted between them. At the receiver side, the CO-OOFDM signal is detected using two identical optical coherent balanced detectors acting as an optical-to-electrical OFDM I/Q converter, in which I/Q components of a locally generated carrier are

mixed with the optical signal to obtain the electrical I/Q components. Each coherent detector consists of a pair of couplers and PIN detectors [139]. The low-pass filters attenuate the sub-carriers close to the Nyquist frequency, thus reducing the usable bandwidth as the attenuated sub-carriers cannot be used for the data transmission.

The outputs of DACs are passed through a serial–parallel module prior to removing the CP. Owing to the CP, the linear convolution between the transmitted signal and the channel becomes a circular convolution; hence, the output of the FFT can be written as a production the matrix form given by [152].

$$r_n = diag(X_n).H_n + W_n, \tag{6.2}$$

Where H_n = $F_n.h_n$ is the frequency response of the channel with the length L, $[F]_{n,k} = N^{-\left(\frac{1}{2}\right)}e^{-\left(\frac{2j\pi kn}{N}\right)}$ the FFT matrix, W_n the $N \times 1$ vector of the white Gaussian noise with $E[W_n W_n^H] = \sigma_n^2 I_N$ [22], H_n the $A = N \times 1$ vector, h_n the channel response, N the number of equally spaced subcarriers, H the Hermitian transpose and *diag* the diagonal matrix. The FFT unit is followed by the ANN equalizer which is in turn followed by a parallel to serial converter and a decoder in order to recover the data.

It should be pointed out that such a CO-OOFDM modem model has been widely adopted in both theoretical simulations and non-real-time experimental measurements [7, 11, 37, 49]. For simulating a SMF link, the widely adopted split-step Fourier method is employed to model the propagation of the optical signal down a SMF [8, 11, 144]. It is well known that for a sufficiently small fibre split-step length, this theoretical treatment yields an accurate approximation to the real effects. In the SMF model, the effects of loss, CD, and optical power dependence of the refractive index are included. The effect of fibre non-linearity-

induced phase noise to the intensity noise conversion is also considered upon the photon detection in the receiver. This model has been successfully used in [37].

To mitigate fibre non-linearity, here ANN nonlinear feed-forward equalizers based on multilayer perception (MLP) method is proposed, which by training the ANN applies the opposite effect of fibre impairments occurring in the transmission link under investigation to the CO-OOFDM signals at the transmitter. To validate the ANN compensation method adopted here, results obtained using the modem for a wireless channel shows an improvement of transmission SNR same as that obtained by [151]. In the simulation to set the OSNR to a specified value, an optical noise-loading module is employed at the receiver. This module performs the function of a simple saturating optical amplifier with variable noise figure, and can be characterized as an optical attenuator followed by a gain block.

6.2.2 Simulation Parameters

Having described the theoretical CO-OOFDM modem and the SMF-based coherent transmission link, this section details the most important parameters adopted in the numerical simulations, which was shown to be the optimum parameters for the modem by [37, 49]. In simulations, 64 sub-carriers are used, onto which identical 16-QAM signal modulation formats corresponding to 40 Giga bit/ second (Gb/s) are applied.

It is assumed that ADCs and DACs have fixed sampling rates, clipping ratio, and quantization bit of 12.5 GS/s, 13 dB, and 10 bits, respectively which give rise to a negligible clipping and quantization noses [37].

The operating parameters used for optical link simulations are a laser with a wavelength of 1550 nm and with a 100 kHz line width, -6 dBm optical power coupled into the input facet of the link, a PIN responsibility 0.9, SMF spans of 80 km, a fibre CD of 17 ps/nm/km and a loss of 0.2 dB/km, and a non-linear Kerr-coefficient of 2.6 $x10^{-20}$ m^2/W.

The adopted MZ modulator modulation amplitude is a sinusoidal transfer function with a modulation index of 0.3, as the modulation index can be as high as 0.5 without producing any significant penalty when the modulator is based at the null biasing point, this is in order to obtain signals amplitudes in the optical domain as close as possible to the amplitude of the real and imaginary components at the electrical domain [153]; however, investigating the modulation index effect on the transmission performance is beyond the scope of this paper. In each span, the fibre loss is compensated by an EDFA with 16 dB optical gain and a noise figure of 6 dB. It is important to state that no laser phase noise is considered, and the transmitter local oscillator (LO) and receiver LO are matched, moreover a perfect sampling clock synchronisation between the transmitter and receiver is assumed. It should be pointed out, in particular, that other parameters that are not mentioned above will be addressed explicitly in the corresponding parts where necessary.

6.3 ANN Equalizer Design

One of the major receiver components is the equalizer that has the task of recovering the transmitted symbols based on the channel observations. The output of the channel is represented by equation (6.2). As the CO-OOFDM signal consists of (k) number of subcarriers, it is shown in Fig.6.2 that ANN equalizer consists of k sub-neural networks, each sub-network is designated for a different subcarrier. From the Fig. 6.2 the error is given as:

$$e(k) = s(k) - \hat{s}(k). \tag{6.3}$$

The k-th estimated output of the neural network $\hat{s}(k)$ of the k-th subcarrier is given by the following equation:

$$\hat{s}(k) = \sum_{i=1}^{16} w_{k,i}\, \varphi_{k,i}\big(r(k)\big). \tag{6.4}$$

It is important to mention that number of neurons in every neural sub-net is as suggested to be equal to the number of different transmitted OFDM symbols which is in the case of 16-QAM modulation format equals to 16 neurons [151].

In Fig. 6.2, the symbols $r(k)$ corresponds to the received k-th subcarrier information, $w(k,n)$ is the weight value for a given subcarrier and neuron, $\hat{s}(k)$ is the output of the equalizer, $s_i(k)$ is the training vector i.e. the pre-known transmitted subcarrier set, and finally is the MMSE algorithm, which is standard in the new-feed forward network, which according to the weight values are updated.

From Fig. 6.2 firstly a sets of previously known 16-QAM symbols $s_i(k)$ are OFDM modulated and transmitted over the SMF channel.

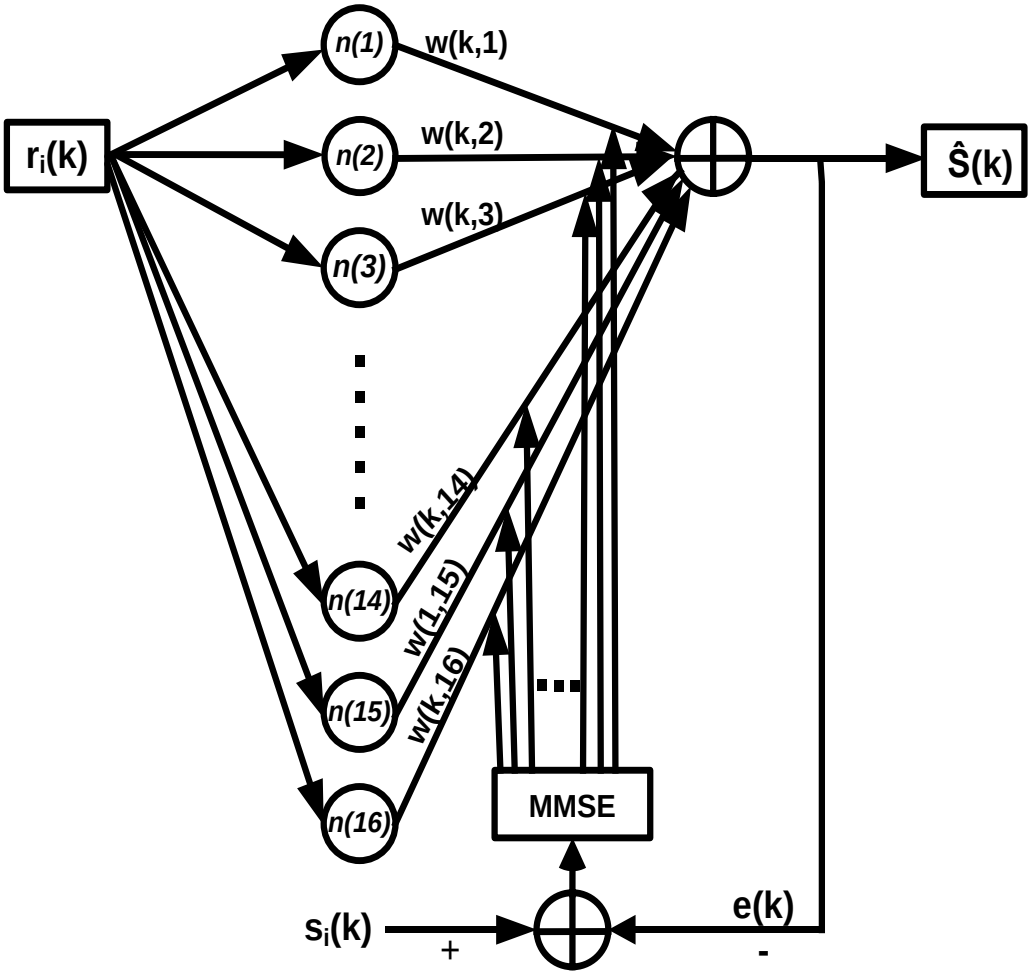

Figure 6.2: ANN sub neural network equalizer schematic.

The received symbols of every 16-QAM subcarrier $r_i(k)$ are feed into the equalizer neurons where received symbols are multiplied with weights of corresponding neurons, then the output of all the neurons are summed to give the sub-network output $\hat{s}(k)$. The pre-known transmitted subcarrier symbols $s_i(k)$ are then feed together with the instant sub-network output to the MMSE algorithm to calculate the error value and update the weights. This is a continues process until a required error value is reached, which means at that point the sub-network output match the transmitted (undistorted) subcarrier symbols.

In this chapter the ANN is based on the new feed-forward network, which uses the Riedmiller's Resilient back propagation algorithm (RP) [154], training function that updates the weight and bias values according to the resilient less computationally cost effective back propagation algorithm (BP), which is one of the most popular learning algorithms to train a neural network performing an approximation to the global minimization achieved by the steepest descent [155].

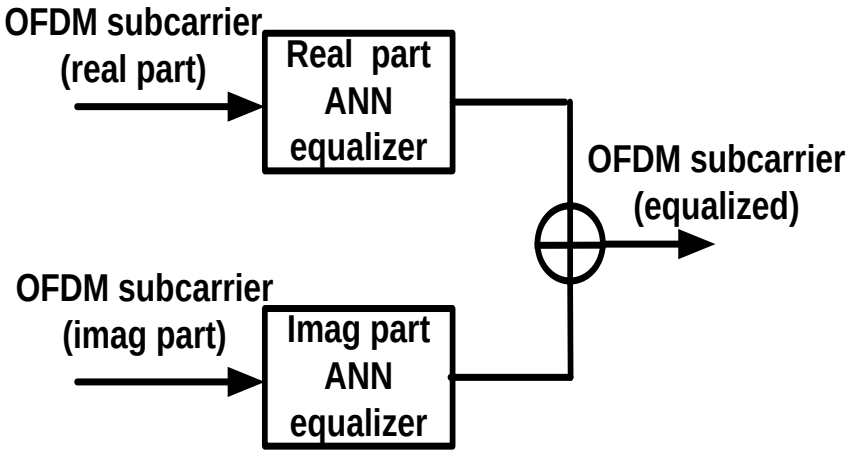

Figure 6.3: ANN equalizer for complex input signals.

Hence as mentioned BP minimizes the deference between the ANN output and the desired output i.e. the target, and this is applicable for the real data only. Therefore, it has been suggested by [156] that the OFDM complex data should be divided into two parts the real and image and fed separately to two ANN networks and the output is recombined at the exit of the ANN equalizer according to (6.5), the process also illustrated in Fig. 6.3.

$$\hat{s}_{Final}(k) = \hat{s}_{Real}(k) + \hat{s}_{Imag}(k). \tag{6.5}$$

For simulation the employed transfer functions are differentiable transfer function such as the hyperbolic tangent function suggested by Beneinto and Pizzo [97] for the hidden layer, and the linear function purelin for the output layer which was explained previously in Chapter 3.

6.4 Effect of ANN Equalizer on CD

The first set of simulation results illustrates the effect of the proposed ANN equalizer on the bit error rate performance when considering only the CD.

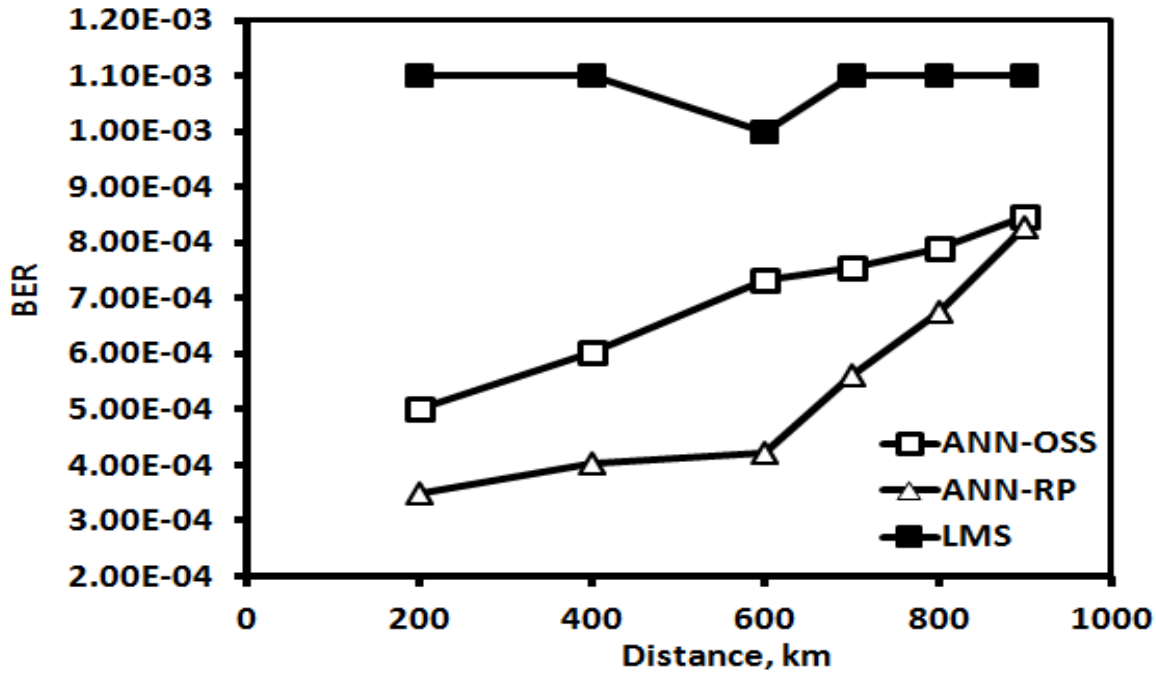

Figure 6.4: Transmission distance against BER when utilizing LMS, and ANN equalizers that uses OSS or RP training algorithm while transmitting over SMF link that considers only dispersion.

Figure 6.4 shows the BER performance comparison between the traditional equalization technique of the least mean square (LMS) and the two proposed ANN equalizers based on the

RP and the one step secant (OSS) training algorithms. In this figure for every particular transmission distance the minimum required OSNR (OSNR-Min) was utilized [37].

As recommended in [97], the length of the training sequence for every subcarrier is 60% of the target sequence length, and the utilization of ANN equalizer with either RP or OSS algorithm offers an average 50% improvement in terms of the BER performance when compared to the traditional LMS equalization method (see Fig. 6.4).

Moreover, Fig. 6.4 illustrate a comparison curve in terms of BER for different transmission distances between LMS method and two variants of ANN equalizers, where the first network uses the RP training algorithm and the second is using OSS algorithm [157]. It can be seen that the RP network is in terms of the BER performance is outperforming the network that uses the OSS algorithm. This can be explained as RP is a back propagations algorithm, which results in an enhancement of the learning process while training the neural network, consequently the ANN equalizer with the RP learning algorithm will be adopted for the rest of the chapter. From the same figure, it can also be observed that both back propagation algorithms can outperform the LMS equalizer.

The effect of equalization can be illustrated further from looking at the constellation diagram for 700 Km transmission as shown in Fig. 6.5. It can be seen that ANN has the ability of condensing the constellation points at the centre of each constellation point compared to LMS, therefore it is considered that the ANN equalizer has improved performance.

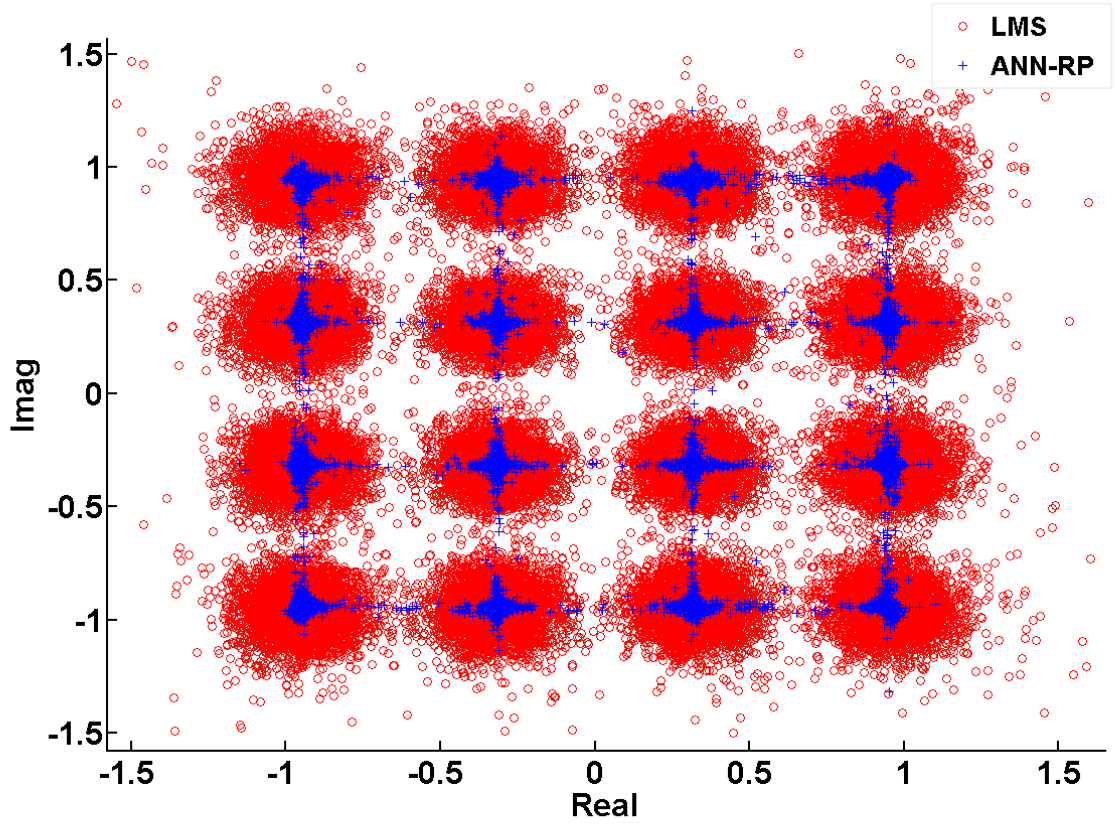

Figure 6.5: Constellation diagram of the equalized performance.

The effect of ANN equalizer on the BER performance per subcarrier is shown at Fig. 6.6, it can be seen that the ANN equalizer performs better for those subcarriers with higher values of BER.

Figure 6.7 illustrate the effect of the proposed ANN equalization scheme on the OSNR penalty while transmitting CO-OOFDM signals over SMF that only considers the CD effect. The figure shows results of the BER against the transmission distance while fixing the OSNR value during all transmission distances to that required for achieving a BER of 10^{-3} at 400 km, before and after the utilization of the proposed ANN equalization scheme.

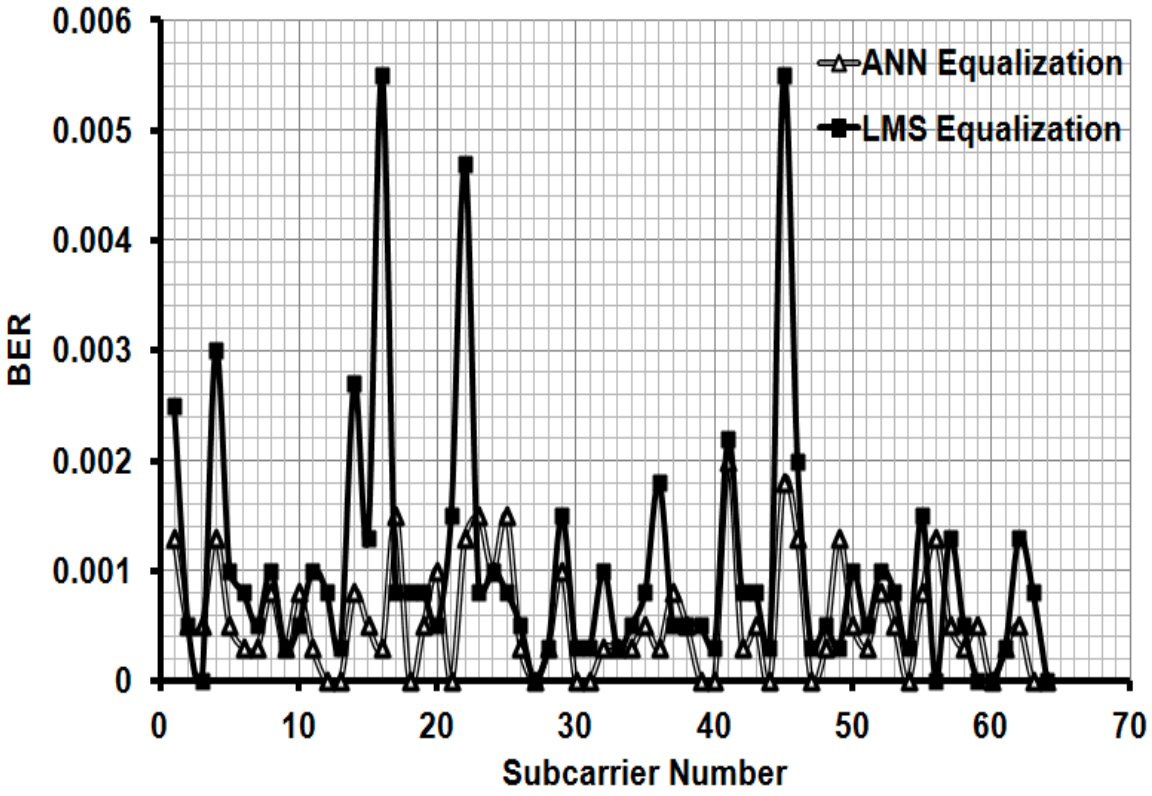

Figure 6.6: Number of subcarriers versus BER, with and without utilizing the ANN equalizer for the SMF link.

It can be realized that the transmission distance increases from 400 km (LMS) to 750 km (ANN) while maintaining a BER of 10^{-3}, moreover from the OSNR vs. distance curve the corresponding OSNR-Min for 400 km is 10.5 dB and for 750 km is 12 dB, thus offering 1.5 dB improvement when using the proposed ANN method with the RP learning algorithm.

SMF dose not only include linear time invariant (LTI) impartment's such as CD; but it also suffers from non LTI impairments such as Kerr, FWM, and self phase modulation (SPM). Consequently, it is important to study the effect of the ANN equalizer on the transmission performance in the presence CD as well as fibre nonlinearities.

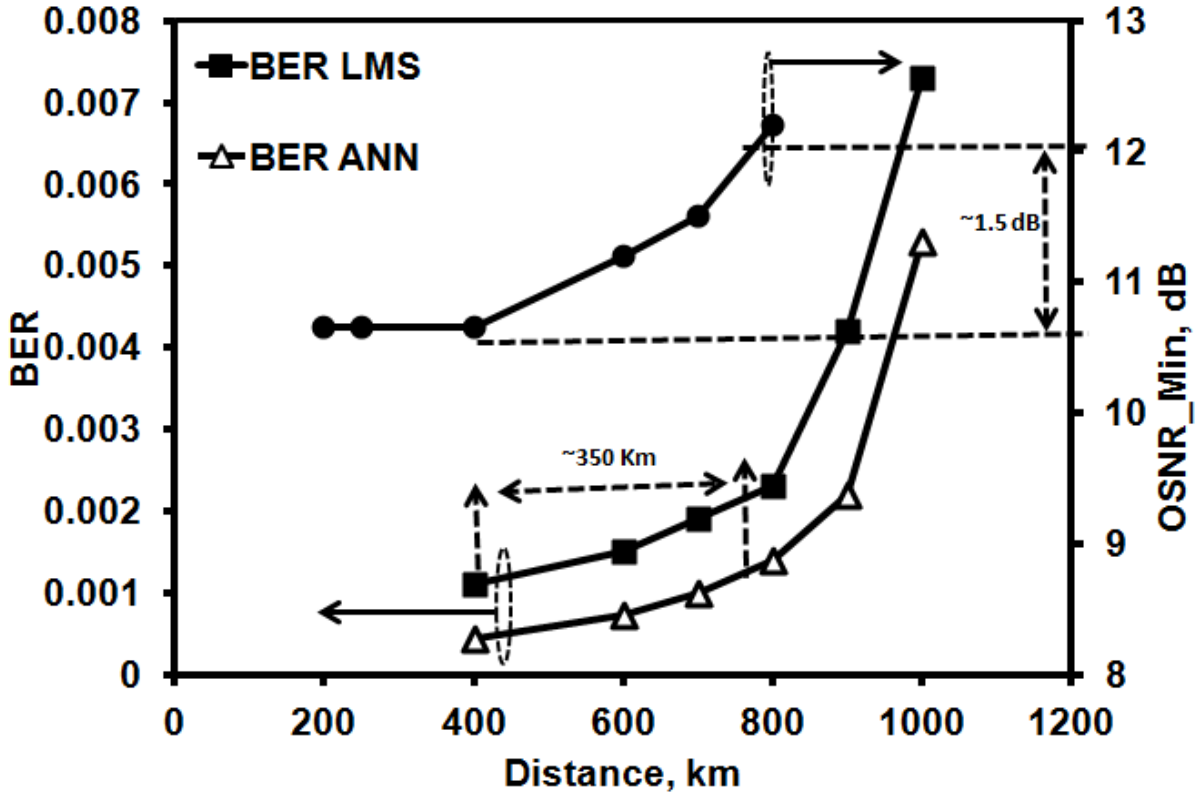

Figure 6.7: Transmission distance against BER, when ANN equalizer is used while considering only CD and fixing OSNR to 10.5 dB.

6.5 Effect of ANN Equalizer on Transmission Performance over SMF Links

In this section, the first set of the simulation results illustrate the effect of the ANN equalizer on the BER performance against the transmission distance while considering fibre non-linearity and CD.

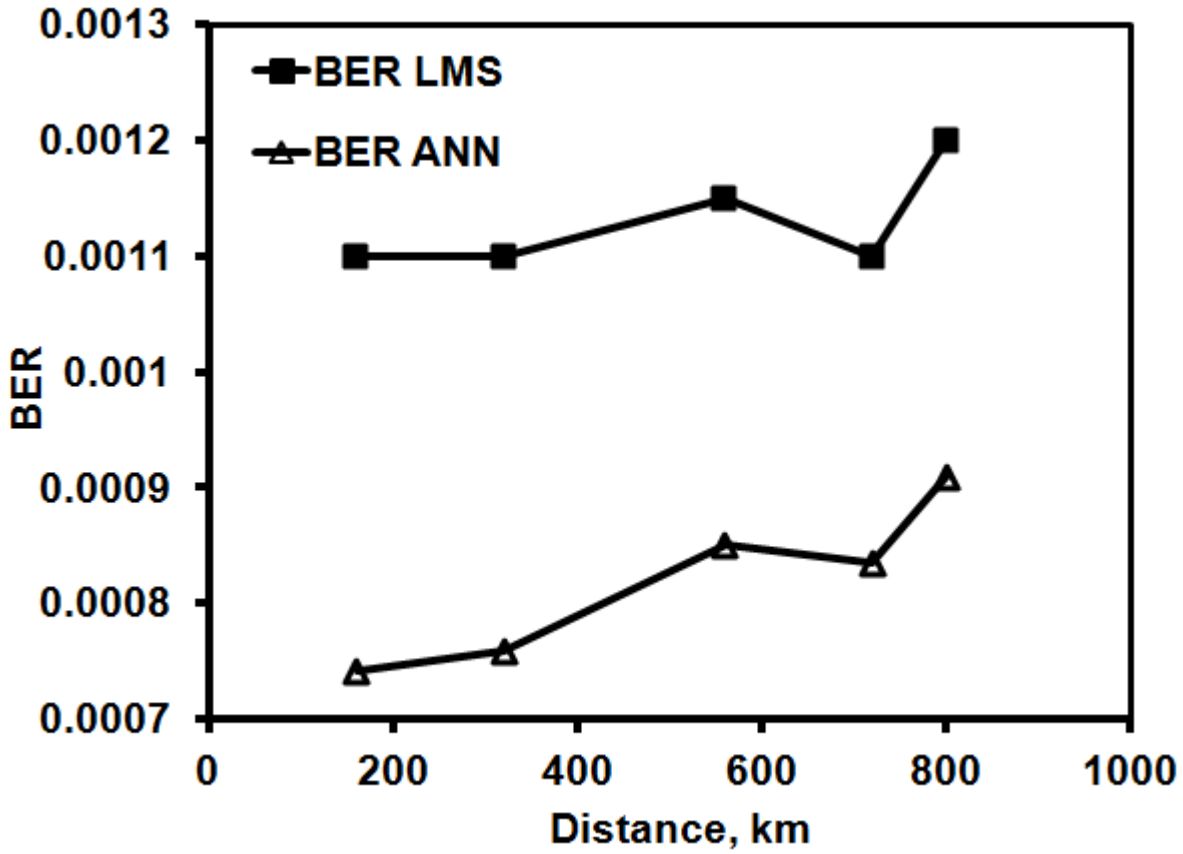

Figure 6.8: Transmission distance against BER with and without utilizing the ANN equalizer for the SMF link.

For obtaining the results shown in Fig. 6.8, for each transmission distance the corresponding OSNR-Min which gives rise to 10^{-3} BER was adopted, therefore, it can be seen that ANN equalizer with RP learning algorithm is superior to the traditional LMS equalizer, moreover it can be seen from the Fig. 6.8 that ANN equalizer can proved an enhancement of the system's BER figure by an average of 70%, when compared with the LMS equalizer.

Figure 6.9 illustrates the effect of the proposed ANN equalization scheme on the OSNR penalty while transmitting CO-OOFDM signals over SMF. During simulations, the OSNR is set to OSNR-Min that is required for achieving a BER of 10^{-3} at 160 km transmission distance. It is clear that with the aid of the ANN equalizer this distance is doubled to 320 km

while keeping the same BER penalty of 10^{-3}, which means an improvement in OSNR of about 0.65 dB, see Fig. 6.9.

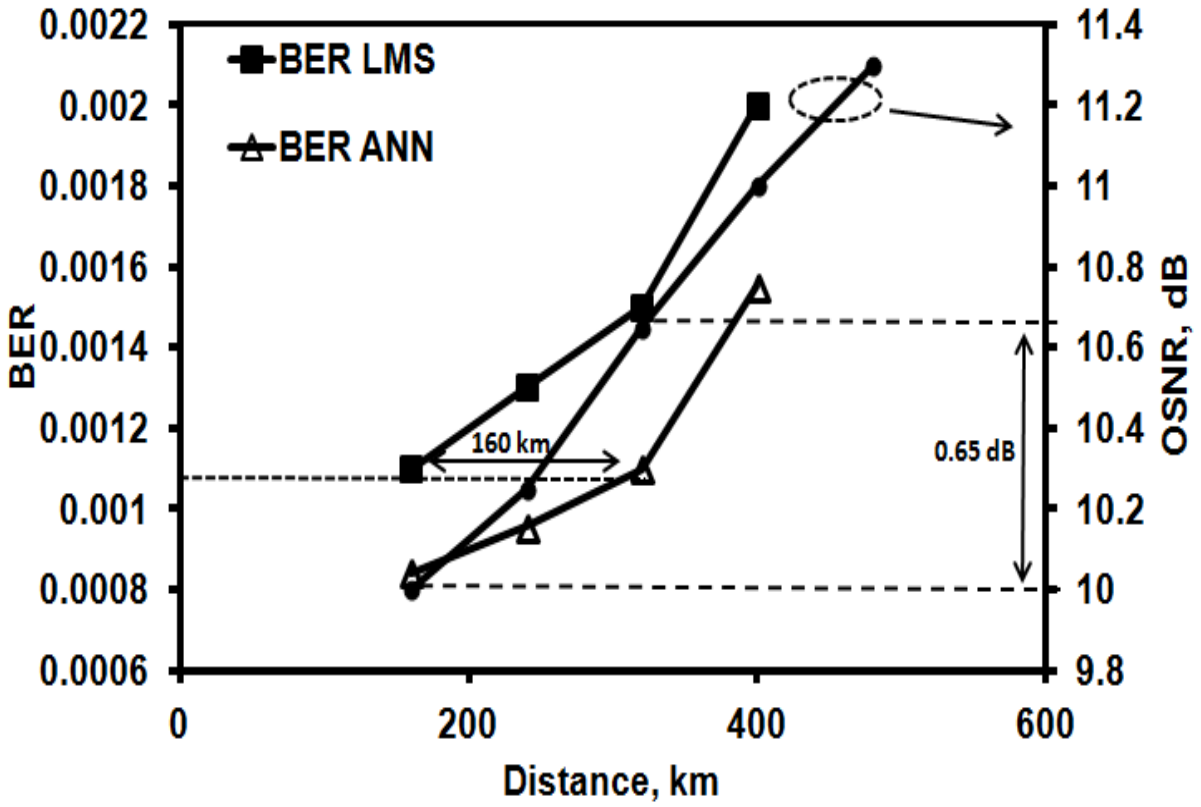

Figure 6.9: Transmission distance against BER, when ANN equalizer is used while fixing OSNR to 10 dB.

In the literature there are a number of techniques for dispersion and Kerr non-linearity compensation [8]. The split step Fourier algorithm is one of them where signals are assumed to be propagating through a virtual fibre in the electrical domain. The accuracy of this technique is highly dependent of the split step length and it can be a very computational expensive and inefficient, moreover it does not function under a low optimum launch power of -6 dBm such as that used in this chapter.

CD, and other non-linear impartments are together the limiting factor for SMF transmission systems, consequently the ANN equalizer has the ability to compensate effectively for both impairments regardless of the launch power condition, which is beyond the scope of this chapter. For the adopted optimum modem parameter, which are illustrated in section (6.2.2), when comparing the proposed equalizer performance with that obtained in [37], it can be noticed that for a given transmission distance the split step length equalizer provides an average improvement in OSNR of about 0.1 dB , which is 6.5 times greater than the ANN equalizer.

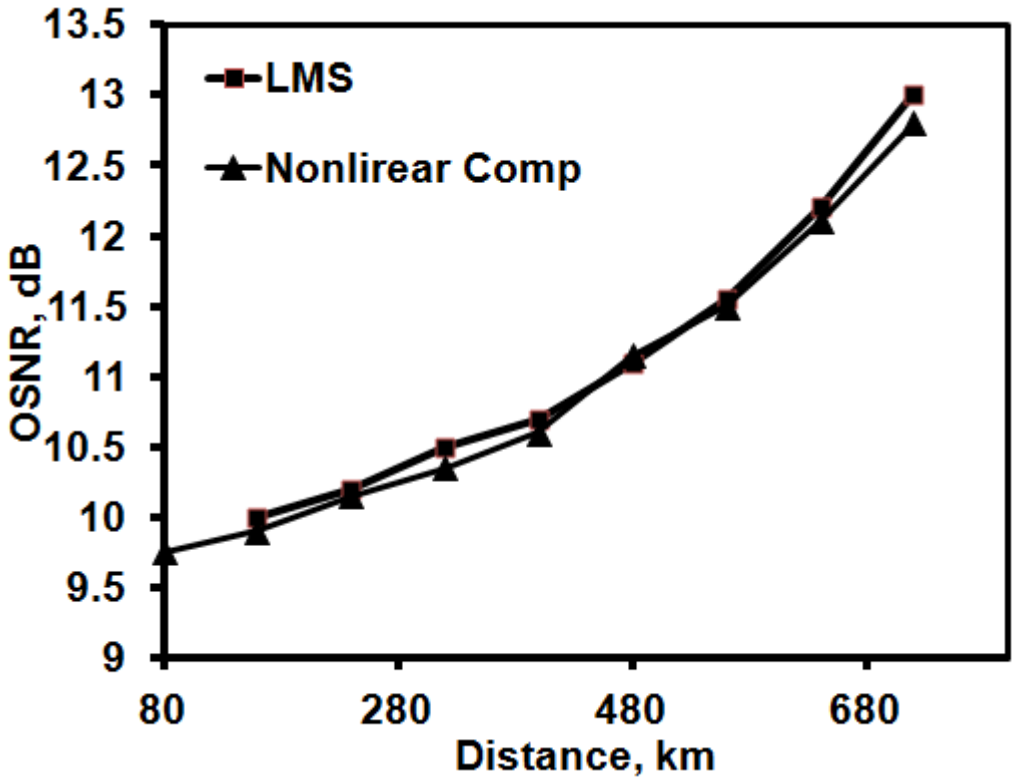

Figure 6.10: Transmission distance versus OSNR, for the proposed ANN equalizer and the equalizer proposed by [3] while transmitting through SMF links.

This is because the non-linearity compensation algorithm [8] effectively compensates for the fibre Kerr non-linearities only; therefore, as explained previously utilizing the optimum

launch power reduces the Kerr non-linear effect to its minimum value, thus making the compensation algorithm effect almost negligible see Fig. 6.10.

6.6 Conclusions

For CO-OOFDM modem, an ANN based equalization method with the RP learning algorithm was proposed and simulated and proved to be more effective in combating CD when compared with the ANN equalizer with OSS learning algorithm and the traditional LMS equalization technique. Considering SMF non-linearities, the aid of ANN equalizer reduces the BER value by an average of 70%, moreover doubles the transmission distance while not changing the OSNR value when compared with the LMS equalizer. It was noticed that the proposed ANN equalization scheme can outperform the Fourier split step length by 7.

Chapter 7. Conclusions and Future Work

7.1 Conclusions

CO-OOFDM has been considered as a promising technique for future high-capacity optical networks, its practical application has been mainly determined by its tolerance to the optical fibre CD and susceptibility to the fibre nonlinearity particularly at high data rates and high optical power levels. Therefore, addressing these technical challenges and increasing CO-OOFDM system tolerance to CD and fibre non-linearities was the main focus of this thesis, for which, a comprehensive investigation (both theoretically and by means of simulation) have been undertaken in order to investigate the feasibility of the OOFDM technique in coherent optical transmission systems with and without the aid of artificial neural network equalizer.

The thesis has discussed the concept of CO-OOFDM and Fast-OFDM, which are widely considered as long-term solutions for long haul networks. CO-OOFDM systems are susceptible to SMF CD and nonlinearities, therefore in this thesis, extensive numerical investigations have been undertaken to optimize the proposed CO-OOFDM modem parameters such as the cyclic prefix, number of subcarriers, ADC associated clipping, quantization, and sampling speed, and the adaptive modulation, moreover the investigation were carried a step further to propose an ANN equalizer for CD and nonlinearities compensation.

The second Chapter of the thesis provided a review of the OOFDM modem components including optical components associated with the IM-DD and coherent transmission, together with a description of the SMF link impairments and characteristics. Whereas the need for equalization, in particular ANN based equalizers, as well as the concept of ANN including

neurons, artificial neural network different architectures, and training algorithms were covered in Chapter three.

In Chapter 4, the optimum ADC key parameters were found for the AWGN channel, for CO-OOFDM and Fast-OFDM modems, consequently the optimum clipping ratios and quantization bits were identified for various modulation formats up to 256-QAM and M-ASK format up to16-ASK when employing the Fast-OFDM modem. It was shown that these optimum ADC parameters are modulation format dependant; therefore, clipping and quantization noises were considered to be negligible. This finding is valuable for the practical design of optimum CO-OOFDM modems. With the aid of the DCT, Fast-OFDM offers reduced complexity when compared with the conventional OFDM; moreover, Fast-OFDM can be used in different application where bandwidth can be traded with the distance. The thesis next investigated the affects of modem key parameters on the transmission performance over SMF links. As for CO-OOFDM modems, in comparison with employing a long cyclic prefix, the use of a large number of sub-carriers is more effective in combating the fibre CD.

For a fixed number of sub-carriers, increasing the cyclic prefix length from 25% to 100% did improve the dispersion tolerance by a factor of 2.7 for lower data rates up to 25 Gbps. It was shown that with SMF fibre non-linearities adopting 64 sub-carriers can increase the transmission distance when compared to 32 and 128 sub-carriers. Employing a non-linearity compensation algorithm is more effective for higher launch power (i.e. 0 dBm), and higher data rates, than for lower launch power (i.e. -6 dBm). Moreover, with the use of the non-linearity compensation algorithm the optimum number of subcarriers was found to be 64 sub-carriers.

ADC sampling speed plays a significant role in determining the symbol period. Reducing the sampling speed can increase the symbol length and limit the number of high frequency components from propagating along fibre, which increases the CD tolerance. However, for a fixed symbol length a lower sampling speed does not necessarily lead to CD improvement, since higher order modulation formats are needed to achieve the same data rate as the higher sampling rates. Moreover, reducing the sampling speed further reduces the spacing between sub-carriers, thus resulting in increased FWM effect. It was shown that employing adaptive modulation schemes have a unique feature of effectively utilizing the entire transmitted signal spectrum, thus addressing the amplitude distortion experience by all the CO-OOFDM sub-carrier signals. By doing so the link span was increased by factors of 1.4 and 1.2 and for dispersion only and both dispersion and fibre non-linearities cases.

Chapter 6 has outlined the ANN equalizer design for the CO-OOFDM transmission system. The proposed artificial neural network based equalization method based upon the RP learning algorithm proved to be more effective in combating the CD when compared to the artificial neural network equalizer employing the OSS learning algorithm and the traditional LMS equalization technique. Considering SMF fibre non-linearities, adopting the artificial neural network equalizer reduced the BER value by 70% and doubled the transmission distance while the OSNR value was left unchanged when compared to the traditional LMS. It was observed that the proposed artificial neural network equalization scheme can outperform the split step length back ward propagation by a magnitude of seven.

7.2 Future Work

Although extensive research has been undertaken in this thesis, a number of issues related to CO-OOFDM-based long haul transmission may still be worth investigating in the future. This research work is summarised as follow:

- **Experimental demonstration of CO-AMOOFDM transmission using real-time OOFDM transceivers:** Real-time experimental demonstrations of AMOOFDM transmission is critical for evaluating the true potential of the AMOOFDM transmission,

- **Exploring the use of CO-AMOOFDM transmission in WDM- passive optical networks PONs using CO-OOFDM transceivers:** Due to a number of issues related to passive optical networks (PONs) such as the utilization of cheap optical/electrical O/E and E/O converters, PON has been considered as a solution for LAN and MAN networks. As PONs are dominant technologies for today's access networks due to their mature standards and massive global deployment, the evolution of PON technologies and standards is also overviewed, their potential in coherent networks has not yet been explored for CO-OOFDM modems.

- **Investigating the effect of modem key parameters such as the CP, the number of subcarriers and the ADC parameters such as the sampling speed, clipping and quantization on the capacity versus reach performance of the Fast-OFDM modem when transmitting over SMF links:** Fast-OFDM inherited an excellent energy concentration property of DCT, which results in an enhanced robustness to frequency offset when compared to conventional OFDM. Furthermore because Fast-OFDM uses

only the real arithmetic, it has a reduced complexity thus implementation cost and increased resilience to in-phase/quadrature imbalance.

- **Utilization of Fast-OFDM for next generation (NG)-coherent PONs:** Fast-OFDM has the ability to reduce frequency spacing between subcarriers by half in contrast to conventional OFDM. Investigations on Fast-OFDM can trigger a new generation of bandwidth-efficient optical networks including a new breed of next generation (NG)-Coherent passive optical networks (PONs).

- **Evaluate the performance of the wavelet transform CO-OOFDM in comparison with the conventional CO-OOFDM**: In OFDM the modulation/ demodulation can be efficiently implemented using IFFT/FFT electronically. On the other hand in the wavelet transforms (WTs) by which a signal is expanded in an orthogonal set called wavelets, where by the subcarriers orthogonality still can be reserved similar to the case of FFT OFDM, however, the basic functions are wavelets instead of sinusoids [158]. Since wavelets have finite length unlike sinusoids, which are infinitely long in the time domain. Therefore, WTs have both frequency and time localization, moreover, can provide better spectral roll-off and to remove the need for CP. In addition, wavelets can provide more freedom in system design [158]; therefore, it is important to evaluate the performance of the wavelet transform OOFDM, and compare the performance with the conventional OOFDM for long haul networks.

References

[1] P. M. Watts, R. Waegemans, M. Glick, P. Bayvel, and R. I. Killey, "An FPGA-based optical transmitter using real-time DSP for implementation of advanced signal formats and signal predisortion," in *The European Conference on Optical Communications, ECOC*, pp. 1-2, 2006.

[2] M. Franceschini, G. Bongiorni, G. Ferrari, R. Raheli, F. Meli, and A. Castoldi, "Fundamental limits of electronic signal processing in direct-detection optical communications," *Journal of Lightwave Technology*, vol. 25, pp. 1742-1753, 2007.

[3] L. Hanzo, S. X. Ng, T. Keller, and W. Webb, "*Quadrature amplitude modulation:From basics to adaptive trellis-coded, turbo-equalised and space-time coded OFDM, CDMA and MGCDMA systems*": Wiley, 2004.

[4] J. Heiskala and J. Terry, "*OFDM wireless LANs: a theoretical and practical guide*". Indianapolis: IN: Sams, 2002.

[5] N. E. Jolley, H. Kee, R. Rickard., J. M. Tang, and K. Cordina, "High-speed transmission of adaptively modulated optical OFDM signals over multimode fibers using directly modulated DFBs," Presented at the Optical Fiber Communication Conference, and the National Fiber Optic Engineers Conference. OFC, Anahiem, CA, 2005.

[6] X. Q. Jin, J. M. Tang, P. S. Spencer, and K. A. Shore, "Optimization of adaptively modulated optical OFDM modems for multimode fiber-based local area networks," *Journal of Optical Networking*, vol. 7, pp. 198-214, Feb 2008.

[7] W. Shieh, H. Bao, and Y. Tang, "Coherent optical OFDM: theory and design," *Optics Express*, vol. 16, pp. 841–859, 2008.

[8] A. J. Lowery, "Fibre nonlinearity pre- and post compensation for long-haul optical links using OFDM," *Optics Express,* vol. 15, pp. 12965–12970, 2007.

[9] J. A. L. Silva, A. V. T. Cartaxo, and M. E. V. Segatto, "A PAPR reduction technique based on a constant envelope OFDM approach for fiber nonlinearity mitigation in optical direct-detection systems," *Journal of Optical Communications and Networking, IEEE/OSA*, vol. 4, pp. 296-303, 2012.

[10] E. Giacoumidis and J. Tang, "Improved transmission performance of adaptively modulated optical OFDM signals over MMFs using adaptive cyclic prefix," Presented at the OECC/ACOFT, pp. 1-2, 2008.

[11] S. L. Jansen, I. Morita, N. Takeda, and H. Tanaka, "20-Gb/s OFDM transmission over 4160-km SSMF enabled by RF-pilot tone phase noise compensation," Presented at the Optical Fiber Communication Conference and Exposition, and the National Fiber Optic Engineers Conference. OFC, Anaheim, CA, pp.1-3, 2007.

[12] W. Shieh, X. Yi, and Y. Tang, "Transmission experiment of multi-gigabit coherent optical OFDM systems over 1000km SSMF fibre," *Electronics Letters,* vol. 43, pp. 183-184, 2007.

[13] W. Shieh, X. Yi, Y. Ma, and Y. Tang, "Theoretical and experimental study on PMD-supported transmission using polarization diversity in coherent optical OFDM systems," *Optics Express,* vol. 15, pp. 9936-9947, 2007.

[14] H. Sun, K.-T. Wu, and K. Roberts, "Real-time measurements of a 40 Gb/s coherent System," *Optics Express*, vol. 16, pp. 873-879, 2008.

[15] Y. Xingwen, W. Shieh, and T. Yan, "Phase estimation for coherent optical OFDM," *Photonics Technology Letters, IEEE*, vol. 19, pp. 919-921, 2007.

[16] http://www.alcatcl-lucent.com, accessed at 12-Dec-2009.

[17] Y. Xingwen, N. K. Fontaine, R. P. Scott, and S. Yoo, "Tb/s coherent optical OFDM systems enabled by optical frequency combs," *Journal of Lightwave Technology*, vol. 28, pp. 2054-2061, 2010.

[18] M. Yiran, Y. Qi, T. Yan, C. Simin, and W. Shieh, "1-Tb/s per channel coherent optical OFDM transmission with subwavelength bandwidth access," Presented at the *Optical Fiber Communication. OFC*, pp. 1-3, 2009.

[19] W. Shieh, Q. Yang, and Y. Ma, "107 Gb/s coherent optical OFDM transmission over 1000-km SSMF fiber using orthogonal band multiplexing," *Optics Express*, vol. 16, pp. 6378–6386, 2008.

[20] D. Hillerkuss, T. Schellinger, R. Schmogrow, M. Winter, T. Vallaitis, R. Bonk, A. Marculescu, J. Li, M. Dreschmann, J. Meyer, S. Ben Ezra, N. Narkiss, B. Nebendahl, F. Parmigiani, P. Petropoulos, B. Resan, K. Weingarten, T. Ellermeyer, J. Lutz, M. Moller, M. Huebner, J. Becker, C. Koos, W. Freude, and J. Leuthold, "Single source optical OFDM transmitter and optical FFT receiver demonstrated at line rates of 5.4 and 10.8 Tbit/s," presented at the *Optical Fiber Communication, collocated National Fiber Optic Engineers Conference.OFC*, pp. 1-3, 2010.

[21] A. J. Lowery, D. Liang Bangyuan, and J. Armstrong, "Performance of optical OFDM in ultralong-haul WDM lightwave systems," *Journal of Lightwave Technology*, vol. 25, pp. 131-138, 2007.

[22] M. Cavallari, C. R. S. Fludger, and P. J. Anslow, "Electronic signal processing for differential phase modulation formats," Presented at the *Optical Fiber Communication Conference. OFC*, pp. 422-425 , 2004.

[23] A. J. Lowery, D. Liang, and J. Armstrong, "Orthogonal frequency division multiplexing for adaptive dispersion compensation in long haul WDM systems," presented at the *Optical Fiber Communication Conference, and the National Fiber Optic Engineers Conference. OFC*, pp. 1-3, 2006.

[24] B. J. C. Schmidt, A. J. Lowery, and J. Armstrong, "Experimental demonstrations of electronic dispersion compensation for long-haul transmission using direct-detection optical OFDM," *Journal of Lightwave Technology*, vol. 26, pp. 196-203, 2008.

[25] A. J. Lowery, "Fiber nonlinearity mitigation in optical links that use OFDM for dispersion compensation," *Photonics Technology Letters, IEEE*, vol. 19, pp. 1556-1558, 2007.

[26] Q. Dayou, H. Ming-Fang, E. Ip, H. Yue-Kai, S. Yin, H. Junqiang, and W. Ting, "High capacity/spectral efficiency 101.7-Tb/s WDM transmission using PDM-128QAM-OFDM over 165-km SSMF within C- and L-bands," *Journal of Lightwave Technology*, vol. 30, pp. 1540-1548, 2012.

[27] D. Ayyagari and C. Wai-chung, "Comparison of TDM and OFDMA access methods for powerline OFDM systems," Presented at the *Second IEEE Consumer Communications and Networking Conference. CCNC*, pp. 364-368, 2005,.

[28] E. Giacoumidis, I. Tomkos, and J. M. Tang, "Performance of optical Fast-OFDM in MMF-based links," Presented at the *Optical Fiber Communication Conference and Exposition, and the National Fiber Optic Engineers Conference. OFC*, pp. 1-3,.2011

[29] Z. Jian and A. D. Ellis, "Discrete-Fourier transform based implementation for optical fast OFDM," Presented at the *European Conference on Optical Communications. ECOC*, pp1-3, 2010.

[30] Z. Jian and A. Ellis, "Transmission of 4-ASK optical Fast OFDM with chromatic dispersion compensation," *Photonics Technology Letters, IEEE,* vol. 24, pp. 34-36, 2012.

[31] B. Haji, B. Naeeni, and H. Amindavar, "Performance of per tone hammerstein and bilinear recurrent neural network equalizer for wireless OFDM systems," Presented at the *9th International Symposium on Signal Processing and Its Applications. ISSPA*, pp. 1-4, 2007.

[32] X. Chen, Y. Li, G. Hu, and W. Shen, "Blind adaptive time domain equalizer for OFDM system," Presented at the *International Conference on Communications and Mobile Computing. CMC*, pp. 274-277, 2009.

[33] S. Rajbhandari, Z. Ghassemlooy, and M. Angelova, "Bit error performance of diffuse indoor optical wireless channel pulse position modulation system employing artificial neural networks for channel equalisation," *Optoelectronics, IET*, vol. 3, pp. 169-179, 2009.

[34] S. Rajbhandari, "Application of wavelets and artificial neural network for indoor optical wireless communication systems," PhD Thesis, Northumbria University, Newcastle, 2009.

[35] E. Giacoumidis, J. L. Wei, A. Tsokanos, A. Kavatzikidis, E. Hugues-Salas, J. M. Tang, and I. Tomkos, "Performance optimization of adaptive loading algorithms for SMF-based optical OFDM transceivers," Presented at the *16th European Conference on Networks and Optical Communications. NOC*, pp. 56-59, 2011.

[36] E. Giacoumidis, J. L. Wei, and J. M. Tang, "Adaptive modulation induced WDM impairment reduction in optical OFDM PONs," Presented at the *Future Network and Mobile Summit*, pp. 1-12, 2010.

[37] M. A. Jarajreh, Z. Ghassemlooy, and W. P. Ng, "Improving the chromatic dispersion tolerance in long-haul fibre links using the coherent optical orthogonal frequency division multiplexing," *Microwaves, Antennas & Propagation, IET*, vol. 4, pp. 651-658, 2010.

[38] R. Ramaswami and K. N. Sivarajan, "*Optical networks: A practical perspective*, ". NewYork: Academic Press Inc, 2002.

[39] T. D. Nga, "Etude de techniques de modulation multi-porteuse OFDM' pour la montee en debit dans le reseau d'acces optique," PhD Thesis, University of Rennes, Rennes, 2010.

[40] C. F. Lam, "*Passive optical networks: principles and practice*:" Academic Press, 2007.

[41] D. Burstein, "*DSL,"*. New York: John Wiley and Sons, 2007.

[42] L. Bin, J. M. Cioffi, S. Jagannathan, and M. Mohseni, "Gigabit DSL," *IEEE Transactions on Communications*, vol. 55, pp. 1689-1692, 2007.

[43] I. E. Telatar, "Capacity of multi-antenna gaussian channels tech. MIMO," *Bell Laboratories, Lucent Technologies, Published in Euopean Transaction on Tclecommunications,*. vol. 10, pp. 585-595, 1995.

[44] R. Lassalle and M. Alard, "Principles of modulation and channel coding for digital Broadcasting for mobile receivers," *EBU Tech.Rev,* pp. 168-190, 1987.

[45] B. J. Dixon., R. D. Pollard., and S. lezekiel., "Orthogonal frequency-division multiplexing in wireless communication systems with multimode fiber feeds," *IEEE Transactions on Microwave Theory and Techniques,* vol. 49, pp. 1404-1409, 2001.

[46] Z. Jia, J. Yu, D. Qian, and G. K. C. Ellinas, "Experimental demonstration for delivering 1-Gb/s OFDM signals over 80-km SSMF in 40-GHz radio-over-fiber access systems," Presented at the Optical Fiber Communication Conference, and the National Fiber Optic Engineers Conference. OFC, paper JWA108, 2008.

[47] E. Giacoumidis, J. L. Wei, X. L. Yang, A. Tsokanos, and J. M. Tang, "Adaptive-modulation-enabled WDM impairment reduction in multichannel optical OFDM transmission systems for next-generation PONs," *Photonics Journal, IEEE,* vol. 2, pp. 130-140, 2010.

[48] X. Q. Jin., R. P. Giddings., E. Hugues-Salas., and J. M. Tang., "Real-time experimental demonstration of optical OFDM symbol synchronization in directly modulated DFB laser-based 25km SMF IMDD systems," *Optics Express,* vol. 18, pp. 21100-21110, 2010.

[49] M. A. Jarajreh, J. L. Wei, J. Tang, Z. Ghassemlooy, and W. P. Ng, "Effect of number of sub-carriers, cyclic prefix and analogue to digital converter parameters on coherent

optical orthogonal frequency division multiplexing modem's transmission performance," *Journal of IET Communications*, vol. 4, pp. 213- 233, 2010.

[50] L. W. Couch, "*Digital and analog communication systems*, " Prentice Hall, 2006.

[51] J. L. WeI, "Intensity modulation of optical OFDM signals using low-cost semiconductor laser devices for next-generation PONs," PhD Thesis, Bangor University, Bangor, 2010.

[52] A. Peled and A. Ruiz, "Frequency domain data transmission using reduced computational complexity algorithms," Presented at the *IEEE International Conference on Acoustics, Speech, and Signal Processing. ICASSP*, pp. 964-967, 1980.

[53] X. Zheng, "Advanced Optical OFDM Transceivers for Optical Access Networks," PhD Thesis, Bangor Univesity, 2011.

[54] J. M. Tang, P. M. Lane, and K. A. Shore, "30 Gb/s transmission over 40 km directly modulated DFB laser-based SMF links without optical amplification and dispersion compensation for VSR and metro applications," Presented at the *Optical Fiber Communication Conference, and the National Fiber Optic Engineers Conference. OFC*, pp. 3, 2006.

[55] J. M. Tang, P. M. Lane, and K. A. Shore, "High-speed transmission of adaptively modulated optical OFDM signals over multimode fibers using directly Modulated DFBs," *Journal of Lightwave Technology*, vol. 24, pp. 429-441, 2006.

[56] J. M. Tang, P. M. Lane, and K. A. Shore, "Transmission performance of adaptively modulated optical OFDM signals in multimode fiber links," *Photonics Technology Letters, IEEE*, vol. 18, pp. 205-207, 2006.

[57] J. M. Tang and K. A. Shore, "Maximizing the transmission performance of adaptively modulated optical OFDM signals in multimode-fiber links by optimizing analog-to-digital converters," *Journal of Lightwave Technology,* vol. 25, pp. 787-798, 2007.

[58] W. Shieh and I. Djordjevic, "*Orthogonal frequency division multiplexing for optical communications,* " Academic Press, 2010.

[59] E. Giacoumidis., "Adaptive optical OFDM for local and access networks," PhD Thesis, Bangor University, Bangor, 2011.

[60] G. P. Agrawal, "*Nonlinear fibre optics,* ": Academic Press.Inc, 1995.

[61] P. Gysel and R. K. Staubli., "Statistical properties of Rayleigh back scatterinb in single-mode fibers," *Journal of Lightwave Technology,* vol. 8, pp. 561-567, 1990.

[62] Y. Lianshan. "Tunability helps mitigate polarization mode dispersion effects, ". *SPIE Newsroom magazine,Optoelectronics & Communications,General Photonics Corp., 2007.*

[63] J. M. Tang, P. M. Lane, and K. A. Shore, "High-speed transmission of adaptively modulated optical OFDM signals over multimode fibers using directly Modulated DFBs," *Journal of Lightwave Technology,* vol. 24, pp. 429-441, 2006.

[64] W. K. Pratt, "*Laser Communication Systems:"*, 1st ed. New York: John Wiley & Sons, 1969.

[65] P. Wasiu., "Subcarrier intensity modulated free-space optical communication systems," PhD Thesis, Northumbria University Newcastle, 2009.

[66] S. H. Qureshi, "Adaptive equalization," *Proceedings of the IEEE,* vol. 73, pp. 1349-1387, 1985.

[67] S. Haykin, *Neural Networks* - "*A comprehensive foundation*, " New York: Macmillan, 2006.

[68] S. Haykin, "*Adaptive filter theory*, ". NJ, USA: Englewood Cliff,Prentice Hall, 1991.

[69] D. R. Guha, "Artificial neural network based channel equalization," Master Thesis, Department of Electronics and Communication Engineering, National Institute of Technology, Rourkela, 2011.

[70] K. Burse, R. N. Yadav, and S. C. Shrivastava, "Complex channel equalization using polynomial neuron model," in *International Symposium on Information Technology. ITSim*, pp. 1-5, 2008.

[71] B. Widrow and M. E. Hoff, "Adaptive switching circuits," *IRE WESCON Confrence*, vol. 4, pp. 94–104, August 1960.

[72] R. W. Lucky, "Techniques for adaptive equalization of digital communication systems," *J.Bell System Tech*, pp. 255-286, Feb 1966.

[73] F. Magee and J. Proakis, "Adaptive maximum-likelihood sequence estimation for digital signaling in the presence of intersymbol interference (Corresp.)," *IEEE Transactions on Information Theory*, vol. 19, pp. 120-124, 1973.

[74] G. D. Forney, "The viterbi algorithm," *IEEE*, vol. 61, pp. 268-278, 1973.

[75] S. H. Bang and B. J. Sheu, "A neural network for detection of signals in communication," *IEEE Transactions on Circuits and Systems I: Fundamental Theory and Applications,* vol. 43, pp. 644-655, 1996.

[76] L. Chee-Peng and R. F. Harrison, "Online pattern classification with multiple neural network systems: an experimental study," *IEEE Transactions on Systems, Man, and Cybernetics, Part C: Applications and Reviews,* vol. 33, pp. 235-247, 2003.

[77] P. Savazzi, L. Favalli, E. Costamagna, and A. Mecocci, "A suboptimal approach to channel equalization based on the nearest neighbor rule," *Journal on Selected Areas in Communications, IEEE,* vol. 16, pp. 1640-1648, 1998.

[78] G. Forney, Jr., "Maximum-likelihood sequence estimation of digital sequences in the presence of intersymbol interference," *IEEE Transactions on Information Theory,* vol. 18, pp. 363-378, 1972.

[79] S. K. Nair and J. Moon, "A theoretical study of linear and nonlinear equalization in nonlinear magnetic storage channels," *IEEE Transactions on Neural Networks,* vol. 8, pp. 1106-1118, 1997.

[80] B. Widrow and M. A. Lehr, "30 years of adaptive neural networks: perceptron, Madaline, and backpropagation," *Proceedings of the IEEE,* vol. 78, pp. 1415-1442, 1990.

[81] A. K. Jain, M. Jianchang, and K. M. Mohiuddin, "Artificial neural networks: a tutorial," *Computer,* vol. 29, pp. 31-44, 1996.

[82] G. Nagy, "Neural networks-then and now," *IEEE Transactions on Neural Networks,* vol. 2, pp. 316-318, 1991.

[83] F. Rosenblatt, "The perceptron, A perceiving and recognizing automation," Cornell Aeronautical Laboratory,1957.

[84] B. Krose and P. S. Smagt., "*Introduction to neural networks,* " 8th ed, The University of Amsterdam, 1996.

[85] T. Kondo and A. S. Pandya, "Medical image recognition by using logistic GMDH-type neural networks," Presented in the *Proceedings of the 40th SICE Annual Conference.*, pp. 259-264, 2001.

[86] F. Pourboghrat, "Aplications of neural networks in the controller design," in *Electro International*, pp. 498-501, 1991.

[87] R. Kota, K. A. Abdelhamied, and E. L. Goshorn, "Isolated word recognition of deaf speech using artificial neural networks," Presented in the *Proceedings of the Twelfth Southern on Biomedical Engineering Conference,* pp. 108-110, 1993.

[88] A. Kantsila, M. Lehtokangas, and J. Saarinen, "Complex RPROP algorithm for neural network equalization of GSM data bursts," *Neurocomputing,* vol. 61, pp. 339–360, 2004.

[89] T. Kondo, "Feedback GMDH-type neural network algorithm using prediction error criterion for self-organization," Presented in the *SICE Annual Conference*, pp. 1044-1049, 2008.

[90] T. Balandier, A. Caminada, V. Lemoine, and F. Alexandre, "170 MHz field strength prediction in urban environment using neural nets," Presented at the *Sixth IEEE International Symposium on Personal, Indoor and Mobile Radio Communications,*

1995. PIMRC'95. 'Wireless: Merging onto the Information Superhighway', vol. 1, pp. 120-124, 27-29 Sep 1995.

[91] J. C. Patra, R. N. Pal, R. Baliarsingh, and G. Panda, "Nonlinear channel equalization for QAM signal constellation using artificial neural networks," *IEEE Transactions on Systems, Man, and Cybernetics, Part B: Cybernetics,* vol. 29, pp. 262-271, 1999.

[92] S. K. Patra and B. Mulgrew, "Fuzzy implementation of a Bayesian equaliser in the presence of intersymbol and co-channel interference," *IEE Proceedings-Communications, ,* vol. 145, pp. 323-330, 1998.

[93] L. Tsu-Tian and J. Jin-Tsong, "The Chebyshev-polynomials-based unified model neural networks for function approximation," *IEEE Transactions on Systems, Man, and Cybernetics, Part B: Cybernetics,* vol. 28, pp. 925-935, 1998.

[94] Y. H. Pao, *Adaptive pattern recognition and neural network*. Reading: Addison Wesley, 1989.

[95] J. C. Patra and R. N. Pal, "A functional link artificial neural network for adaptive channel equalization," The Elsevier Signal Processing, vol.43,pp. 181-195, 1995.

[96] R. Pandey, "Fast blind equalization using complex valued MLP," *Neural Process. Letters,* vol. 21, pp. 215–225, Jun. 2005.

[97] N. Benvenuto and F. Piazza, "On the complex backpropagation algorithm," *IEEE Transactions on Signal Processing,* vol. 40, pp. 967-969, 1992.

[98] G. M. Georgiou and C. Koutsougeras, "Complex domain backpropagation," *IEEE transactions on Circuits and systems II: analog and digital signal processing,* vol. 39, pp. 330-334, 1992.

[99] T. Kim and T. Adali, "Fully complex multi-layer perceptron network for nonlinear signal processing," *Journal of VLSI Signal Process*, vol. 32, pp. 29–43, 2002.

[100] M. Ibnkahla and J. Yuan, "A neural network MLSE receiver based on natural gradient descent: application to satellite communications," in *The Seventh International Symposium on Signal Processing and Its Applications*, pp. 33-36, 2003.

[101] L. Chun, S. Bingxue, and C. Lu, "BG: a hybrid algorithm for MLP," in *The IEEE Asia-Pacific Conference on Circuits and Systems. IEEE APCCAS*, pp. 360-363, 2000.

[102] T. Ying, W. Jun, and J. M. Zurada, "Nonlinear blind source separation using a radial basis function network," *IEEE Transactions on Neural Networks*, vol. 12, pp. 124-134, 2001.

[103] X. Nan and L. Henry, "Blind equalization using a predictive radial basis function neural network," *IEEE Transactions on Neural Networks*, vol. 16, pp. 709-720, 2005.

[104] L. Ming-Bin and E. Meng-Joo, "Channel equalization using self-constructing fuzzy neural networks with extended Kalman Filter (EKF)," in *IEEE International Conference on Fuzzy Systems, IEEE World Congress on Computational Intelligence, FUZZ-IEEE*, pp. 960-964, 2008.

[105] S. Han, I. Lee, and W. Pedrycz, "Modified fuzzy c-means and Bayesian equalizer for non-linear blind channel," *Appl. Soft Comput*, vol. 9, pp. 1090–1096, 2009.

[106] A. N. Ramesh, C. Kambhampati, J. R. T. Monson, and P. J. Drew, "Artificial intelligence in medicine," *Annals of The Royal College of Surgeons of England*, vol. 86, pp. 334-338, 2004.

[107] H. B. Burke, "Evaluating artificial neural networks for medical applications," Presented at the international Conference on Neural Networks, Houston, TX, USA, vol. 4, pp. 2494-2495, 1997.

[108] S. C. B. Lo, J. S. J. Lin, M. T. Freedman, and S. K. Mun, "Application of artificial neural networks to medical image pattern recognition: detection of clustered microcalcifications on mammograms and lung cancer on chest radiographs " *Journal of VLSI Signal Processing*, vol. 18, pp. 263-274, 1998.

[109] A. M. Nogueira, D. O. Rosario, P. Salvador, R. Valadas, and A. Pacheco, "Using neural networks to classify Internet users," Presented at the Advanced Industrial Conference on Telecommunications/Service Assurance with Partial and Intermittent Resources, pp. 183-188, 2005.

[110] S. Walczak, "An empirical analysis of data requirements for financial forecasting with neural networks," *Journal of Management Information Systems*, vol. 17, pp. 203-222, 2001.

[111] F. Yue and T. Chai, "Neural-network-based nonlinear adaptive dynamical decoupling control," *IEEE Transactions on Neural Networks* vol. 18, pp. 921-925, 2007.

[112] G. Dorffner, "Neural networks for time series processing," *IEEE Transactions on Neural Network World*, vol. 6, pp. 447-468, 1996.

[113] A. Patnaik, D. E. Anagnostou, R. K. Mishra, C. Christodoulou, and J. C. Lyke, "Applications of neural networks in wireless communications," *Antennas and Propagation Magazine, IEEE*, vol. 46, pp. 130-137, 2004.

[114] D. MacKay, "*Information theory, inference, and learning algorithms,"*. Cambridge, Cambridge University press, 2003.

[115] K. Hornik, M. Stinchcombe, and H. White, "Multilayer feedforward networks are universal approximators," *IEEE Transactions on Neural Networks* vol. 2, pp. 359 - 366, 1989.

[116] S. Haykin, "*Neural networks: A comprehensive foundation*, " 2nd ed. New Jersey, USA: Prentice Hall, 1998.

[117] D. P. Mandic and J. A. Chambers, "*Recurrent neural networks for prediction*, " John Wiley and Sons Ltd, 2001.

[118] L. Behera, S. Kumar, and A. Patnaik, "On adaptive learning rate that guarantees convergence in feedforward networks," *IEEE Transactions on Neural Networks,* vol. 17, pp. 1116-1125, 2006.

[119] A. Toledo, M. Pinzolas, J. J. Ibarrola, and G. Lera, "Improvement of the neighborhood based Levenberg-Marquardt algorithm by local adaptation of the learning coefficient," *IEEE Transactions on Neural Networks,* vol. 16, pp. 988-992, 2005.

[120] U. Windhorst and H. Johansson, "*Modern techniques in neuroscience research* ,": Springer-Verlag Berlin and Heidelberg GmbH & Co, 1999.

[121] W. Shieh and C. Athaudage, "Coherent optical orthogonal frequency division multiplexing," *Electronics Letters,* vol. 42, pp. 587-589, 2006.

[122] W. Shieh, "PMD-supported coherent optical OFDM systems," *Photonics Technology Letters, IEEE*, vol. 19, pp. 134-136, 2007.

[123] K. Li and I. Darwazeh, "System performance comparison of fast-OFDM with overlapping MC-DS-CDMA and MT-CDMA systems," Presented at the *The 6th International Conference on Information, Communications & Signal Processing*, pp. 1-4, 2007.

[124] S. K. Ibrahim, Z. Jian, D. Rafique, J. A. O'Dowd, and A. D. Ellis, "Demonstration of world-first experimental optical Fast OFDM system at 7.174Gbit/s and 14.348Gbit/s," Presented at the *36th European Conference and Exhibition on Optical Communication. ECOC*, pp. 1-3, 2010.

[125] Z. Jian and A. D. Ellis, "Discrete-Fourier transform based implementation for optical fast OFDM," in *European Conference on Optical Communications. ECOC*, pp. 1-3, 2010.

[126] E. Giacoumidis, I. Tomkos, and J. M. Tang, "Performance of optical Fast-OFDM in MMF-based links," Presented at the *Optical Fiber Communication Conference and Exposition, and the National Fiber Optic Engineers Conference.OFC*, pp. 1-3, 2011.

[127] Z. Jian, S. K. Ibrahim, D. Rafique, P. Gunning, and A. D. Ellis, "Symbol synchronization exploiting the symmetric property in optical Fast OFDM," *Photonics Technology Letters, IEEE*, vol. 23, pp. 594-596, 2011.

[128] K. Li, "Fast orthogonal frequency division multiplexing (Fast-OFDM) for wireless communications," PhD Thesis, Electrical and Electronic Engineering, University of College London, London, 2008.

[129] X. Fuqin, "M-ary amplitude shift keying OFDM system," *IEEE Transactions on Communications*, vol. 51, pp. 1638-1642, 2003.

[130] P. L. Nippon Telegraph and Telephone Corporation, "Optical orthogonal frequency division multiplexing (Optical OFDM)," p. 1, Nov 2003.

[131] Y. Tanaka, T. Komine, and S. Haruyama, "A basic study of optical OFDM system for indoor visible communication utilizing plural white LEDs as lighting," Presented at the Proc. 8th National Conf. Symp. on Microwave and Optical Technology. ISMOT Montreal, Canada, 2001.

[132] A. J. Lowery and J. Armstrong, "10 Gb/s multimode fiber link using power-efficient orthogonal-frequency-division multiplexing," *Optics Express*, vol. 13, pp. 10003–10009, 2005.

[133] A. Färbert, S. Langenbach, N. Stojanovic, C. Dorschk, T. Kupfer, C. Schulien, J. P. Elbers, H. Wernz, H. Griesser, and C. Glingener, "Performance of a 10.7Gb/s receiver with digital equaliser using maximum likelihood sequence estimation," Presented at the Proc. of the 30th European Conference on OpticalCommunications. ECOC Stockholm, Sweden, 2004.

[134] K. Roberts, "Electronic dispersion compensation beyond 10 Gb/s " Presented at the Digest of the IEEE LEOS Summer Topical Meetings, Portland Oregon, USA, 2007.

[135] T. Li and I. Kaminow, "*Optical fiber telecommunications IVB,"*. San Diego, CA: Academic, 2002.

[136] C. Weber, J. K. Fischer, C. A. Bunge, and K. Petermann, "Electronic precompensation of intrachannel nonlinearities at 40 gb/s," *Photonics Technology Letters, IEEE*, vol. 18, pp. 1759-1761, 2006.

[137] S. Hellerbrand, N. Hanik, and W. Weiershausen, "Optical metro networks and short-haul systems," Presented at the Proc. of the SPIE, 2009.

[138] W. Shieh, W. Chen, and R. S. Tucker, "Polarisation mode dispersion mitigation in coherent optical orthogonal frequency division multiplexed systems," *Electronics Letters*, vol. 42, pp. 996-997, 2006.

[139] L.-D. Gagnon, K. Katoh, and K.Kikuchi, "Unrepeated 210-km transmission with coherent detection and digital signal processing of 20-Gbs QPSK signal," Presented at the Tech. Dig. OFC Anaheim, CA, USA, 2005.

[140] L. Hanzo, M. Münster, B. Choi, and T. Keller, "*OFDM and MC-CDMA for broadband multi-user communications, WLANs and broadcasting,"*. New York: Wiley, 2003.

[141] A. J. Lowery, A. Wang, and M. Premarant, "Calculation of power limit due to fibre nonlinearity in optical OFDM systems," *Optics Express*, vol. 15, pp. 13282-13287, 2007.

[142] S. L. Jansen, I. Morita, T. C. W. Schenk, and H. Tanaka, "121.9-Gb/s PDM-OFDM transmission With 2-b/s/Hz spectral efficiency over 1000 km of SSMF," *Journal of Lightwave Technology*, vol. 27, pp. 177-188, 2009.

[143] Q. Yang, Y. Tang, Y. Ma, and W. Shieh, "Experimental demonstration and numerical simulation of 107-Gb/s high spectral efficiency coherent optical OFDM," *Journal of Lightwave Technology*, vol. 27, pp. 168–176., 2009.

[144] B. D. Liang and A. J. Lowery, "Improved single channel backpropagation for intra-channel fiber nonlinearity compensation in long-haul optical communication systems," *Optics Express,* vol. 18, pp. 17075-17088, 2010.

[145] L. Hanzo, C. H. Wong, and M. S. Yee, "Neural networked based equalization, adaptive wireless transceivers," *Wiley, IEEE Press,* pp. 299-383, 2002.

[146] S. Rajbhandari, Z. Ghassemlooy, and M. Angelova, "Effective denoising and adaptive equalization of indoor optical wireless channel with artificial light using the discrete wavelet transform and artificial neural network," *Journal of Lightwave Technology,* vol. 27, pp. 4493-4500, 2009.

[147] C. L. N. Veiga, L. S. Encinas, and A. C. Zimmermann, "Neural networks improving robustness on fiber bragg gratings interrogation systems under optical power variations," Presented at the 19th International Conference on Optical Fibre Sensors, Proc.SPIE, 2008.

[148] R. Zayani, R. Bouallegue, and D. Roviras, "Adaptive predistortions based on neural networks associated with Levenberg-Marquardt algorithm for satellite down links," *EURASIP Jornal on Wireless Communications and Networking,* vol. 20, pp. 1-15, 2008.

[149] S. Rajbhandari, Z. Ghassemlooy, and M. Angelova, "Performance of OOK with ANN equalization in indoor optical wireless communication system," *PGNET, Liverpool, UK,* pp. 86-89, 2007.

[150] B. Lu and B. L. Evans, "Channel equalization by feed forward neural networks circuits and systems," *Proceedings of the IEEE International Symposium, ISCAS apos,* vol. 5, pp. 587 - 590, 1999.

[151] G. Charalabopoulos, P. Stavroulakis, and A. H. Aghvami, "A frequency-domain neural network equalizer for OFDM," Presented at the *Global Telecommunications Conference. GLOBECOM. IEEE, vol.2*, pp. 571-575, 2003

[152] O. Simeone, Y. Bar-Ness, and U. Spagnolini, "Pilot-based channel estimation for OFDM systems by tracking the delay-subspace," *IEEE Transactions on Wireless Communications*, vol. 3, pp. 315-325, 2004.

[153] H. Jeehoon, S. Byoung-Joon, H. Yan, B. Jalali, and H. R. Fetterman, "Reduction of fiber chromatic dispersion effects in fiber-wireless and photonic time-stretching system using polymer modulators," *Journal of Lightwave Technology*, vol. 21, pp. 1504-1509, 2003.

[154] M. Riedmiller and H. Braun, "A direct adaptive method for faster backpropagation learning: the RPROP algorithm," Presented at the *IEEE International Conference on Neural Networks.*, pp. 586-591, 1993.

[155] E. Chen, R. Tao, and X. Zhao, "Channel equalization for OFDM system based on the BP neural network," in *The 8th International Conference on Signal Processing*, 2006.

[156] N. T., *Complex-valued neural networks: utilizing high-dimensional parameters*. Hershey, New York: Information science reference, 2009.

[157] R. Battiti, "First and second order methods for learning: Between steepest descent and Newton's method," *Neural Computation*, vol. 4, pp. 141-166, 1992.

[158] A. Li, W. Shieh, and R. S. Tucker, "Wavelet packet transform-based OFDM for optical communications," *Journal of Lightwave Technology*, vol. 28, pp. 3519-3528, 2010.